DE MONTFORT UNIVERSITY LEICESTER

Through Vial Impedance Spectroscopy (TVIS)

A new PAT for freeze-drying cycle development

Smi Pharmaceutical Freeze Drying Technology

13th - 14th June 2018

Holiday Inn Kensington Forum, London, United Kingdom

Prof. Geoff Smith

Leicester School of Pharmacy, De Montfort University, United Kingdom

Thanks to GEA Pharma Systems for financial support to attend the conference

Outline

- Introduction
  - Description of Measurement System
  - Theory (Dielectric loss mechanisms)
- TVIS Applications
  - Ice Formation and phase separation in freezing
  - Temperature calibration and prediction
  - Drying rate estimation
  - Heat transfer coefficient calculation
  - End-point determination
  - Dry Layer resistance and collapse (time permitting)
- Acknowledgements

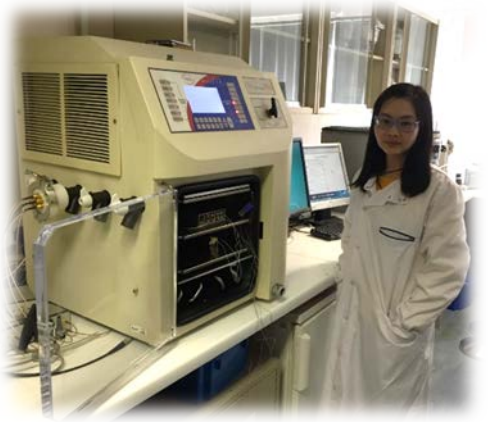

Yowwares Jeeraruangrattana
GPO Thailand

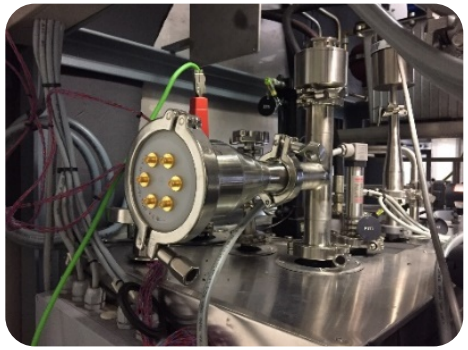

TVIS pass through on
GEA Lyophil dryer, Hurth, Cologne

Introduction to the TVIS System

- Impedance spectroscopy characterizes the ability of materials to conduct electricity under an applied an oscillating voltage (of varying frequency)
- Impedance measurements across a vial rather than within the vial
- Hence **"Through Vial Impedance Spectroscopy"**

- Features
  - Single vial "non-product invasive"
  - Both freezing and drying characterised in a single technique
  - Non-perturbing to the packing of vials
  - Stopper mechanism unaffected

Through Vial Impedance Spectroscopy (TVIS)

Description of Measurement System

Freeze drying chamber

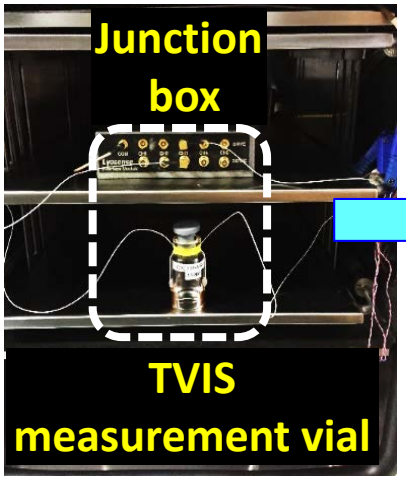

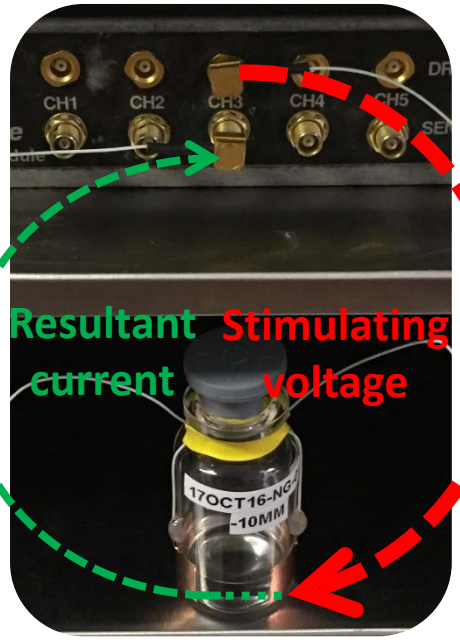

Pass-through

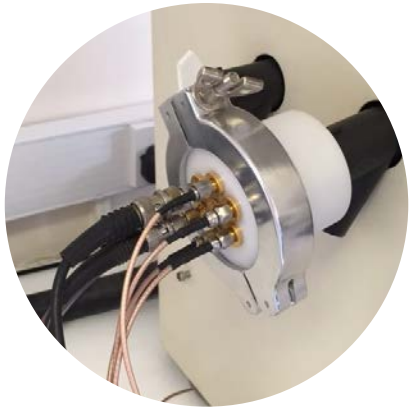

LyoView™ analysis software

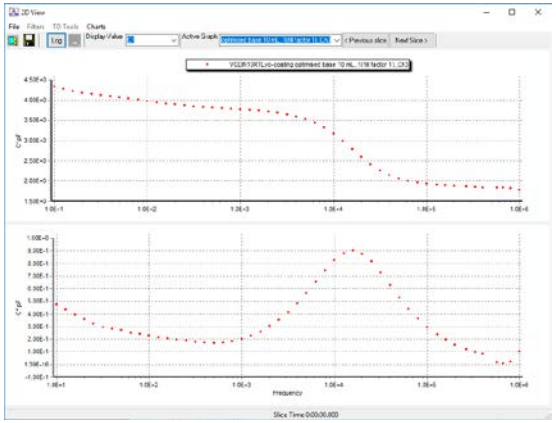

LyoDEA™ measurement software

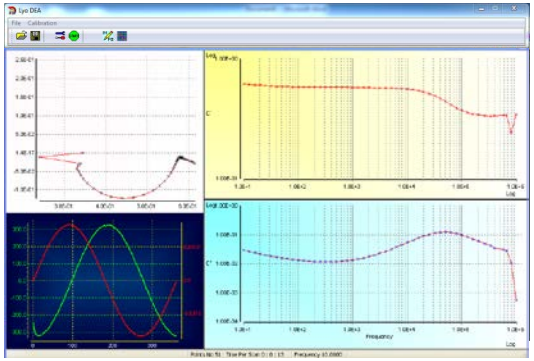

TVIS system (I to V convertor)

TVIS Measurement System

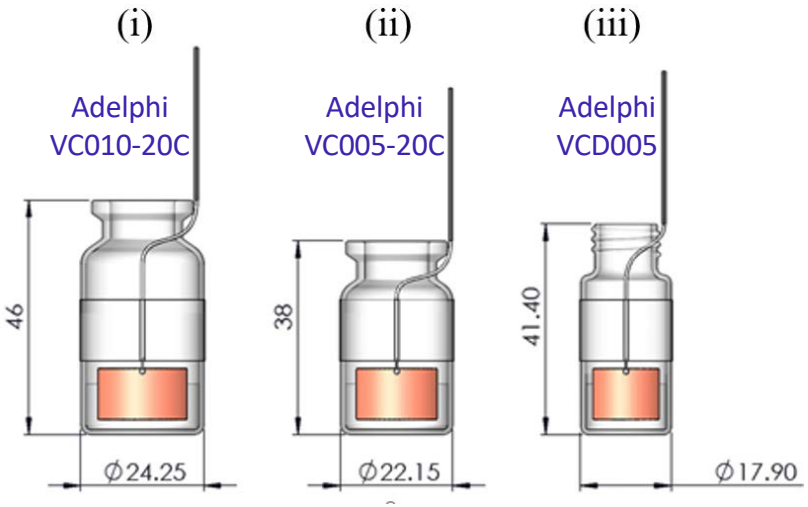

- The designs of various vials that have been modified with copper foil electrodes (10 mm in height and 3 mm from the base of each container

  i. 20 mm crimp-neck vial with 10 ml nominal capacity
  ii. 20 mm crimp-neck vial with 5 ml nominal capacity
  iii. screw-neck vial with 5 ml nominal capacity

- The different styles of a bespoke pass-through for TVIS systems

  A. Connected via the manifold hose on the outside of the dryer
  B. Connected via the port on top left side of the door on the dryer
  C. Connected to a port on the top of the drying chamber

A

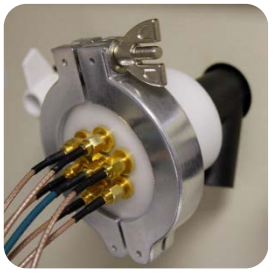

B

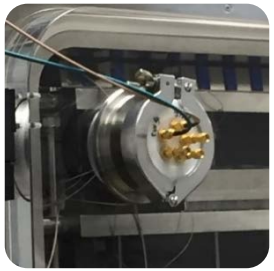

C

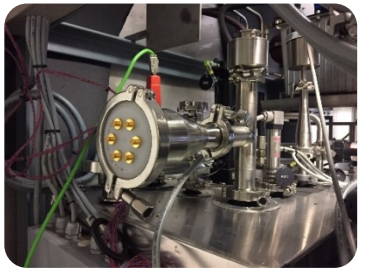

Through Vial Impedance Spectroscopy (TVIS)

Dielectric Loss Mechanisms

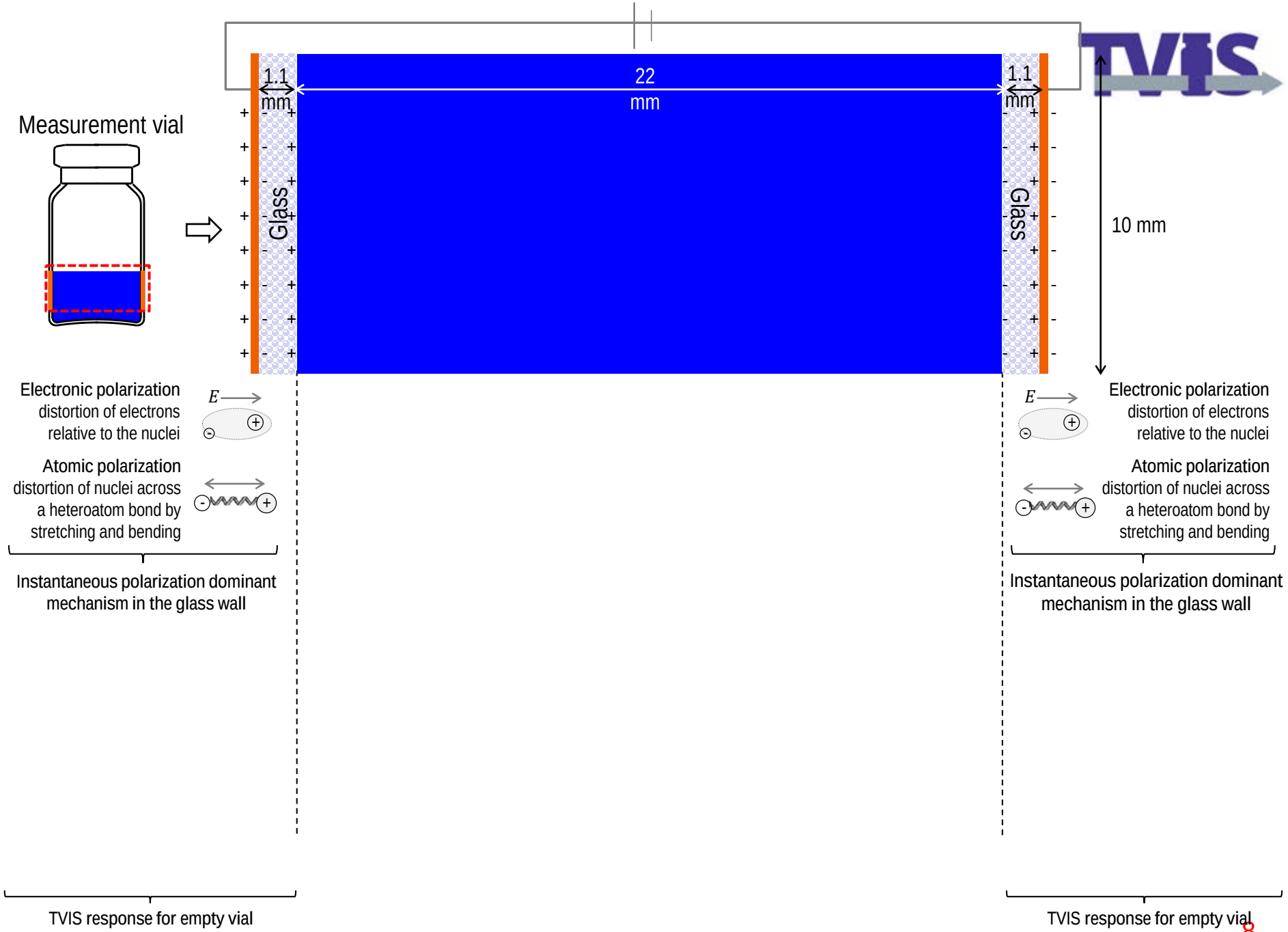
Measurement vial
1.1 mm
22 mm
1.1 mm
Glass
Glass
10 mm
Electronic polarization
distortion of electrons relative to the nuclei
Atomic polarization
distortion of nuclei across a heteroatom bond by stretching and bending
Instantaneous polarization dominant mechanism in the glass wall
Electronic polarization
distortion of electrons relative to the nuclei
Atomic polarization
distortion of nuclei across a heteroatom bond by stretching and bending
Instantaneous polarization dominant mechanism in the glass wall
TVIS response for empty vial
TVIS response for empty vial

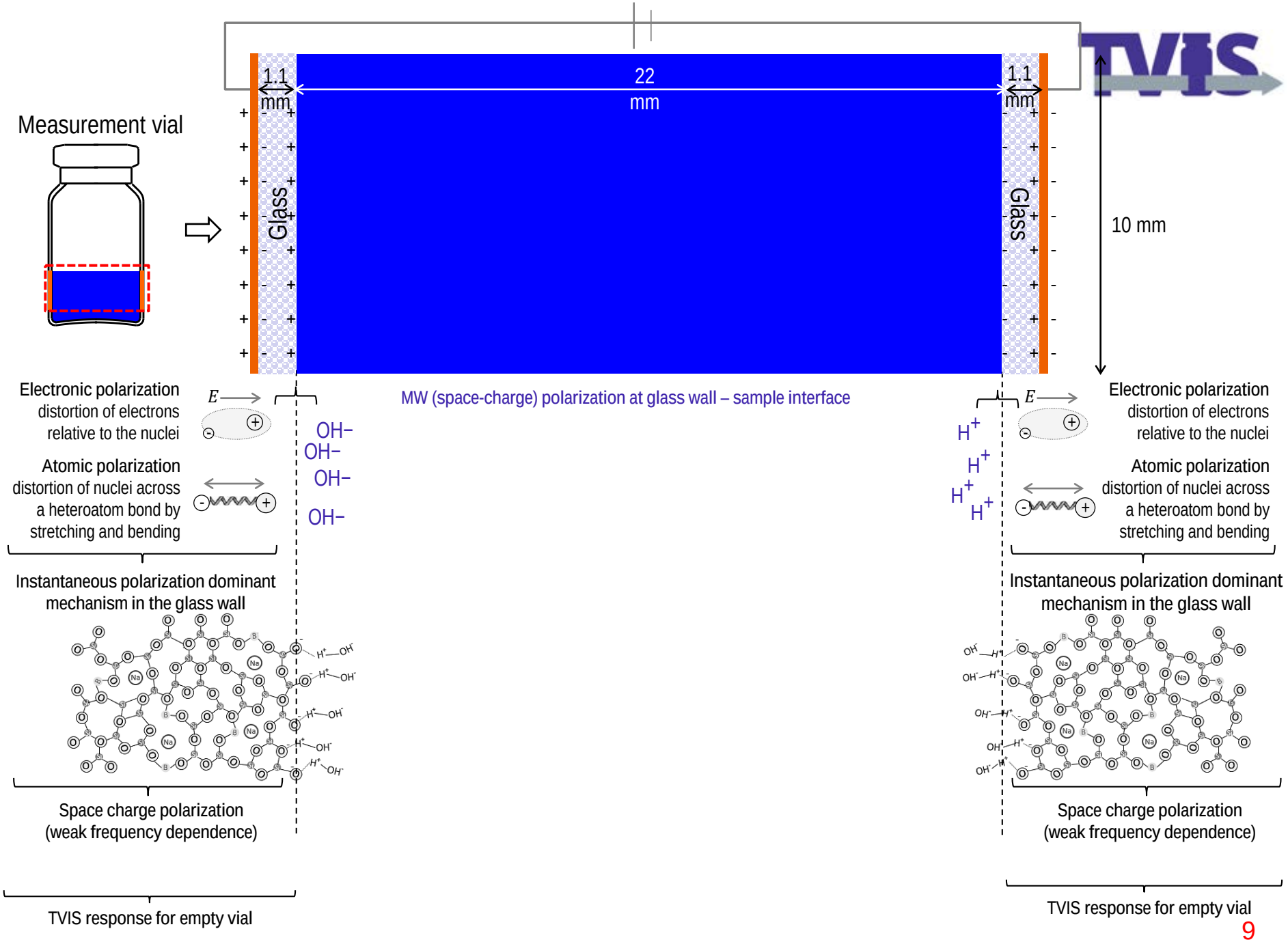
Measurement vial
1.1 mm
22 mm
1.1 mm
Glass
Glass
10 mm
Electronic polarization
distortion of electrons
relative to the nuclei
Atomic polarization
distortion of nuclei across
a heteroatom bond by
stretching and bending
E
OH−
OH−
OH−
OH−
MW (space-charge) polarization at glass wall – sample interface
H+
H+
H+
H+
E
Electronic polarization
distortion of electrons
relative to the nuclei
Atomic polarization
distortion of nuclei across
a heteroatom bond by
stretching and bending
Instantaneous polarization dominant
mechanism in the glass wall
Instantaneous polarization dominant
mechanism in the glass wall
Space charge polarization
(weak frequency dependence)
Space charge polarization
(weak frequency dependence)
TVIS response for empty vial
TVIS response for empty vial

Measurement vial

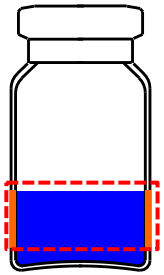

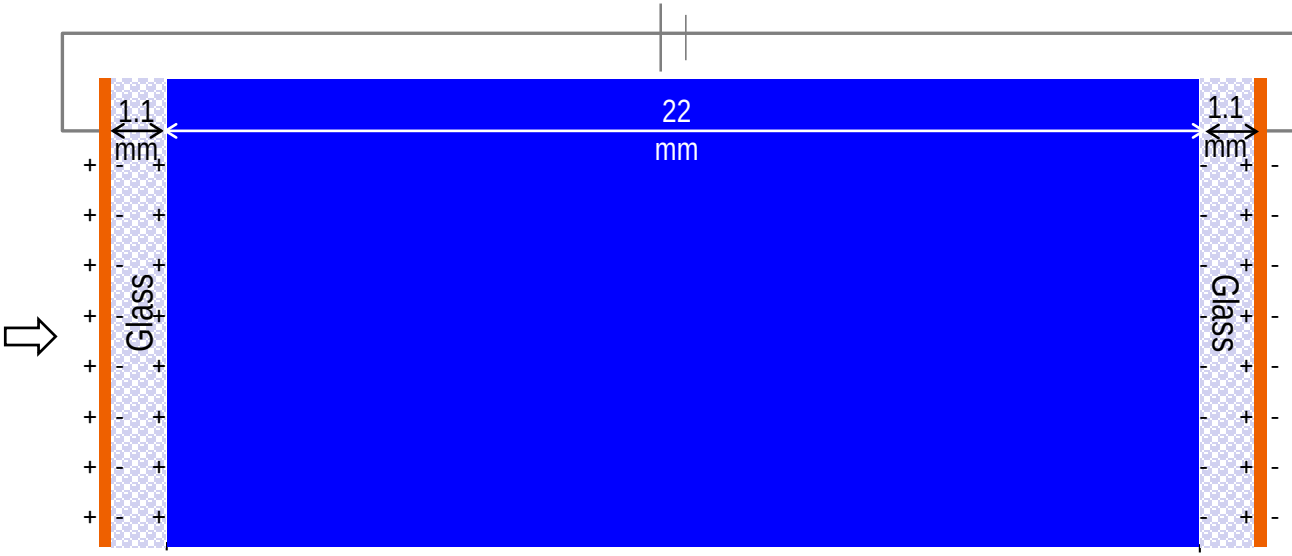

Electronic polarization
distortion of electrons relative to the nuclei

Atomic polarization
distortion of nuclei across a heteroatom bond by stretching and bending

Instantaneous polarization dominant mechanism in the glass wall

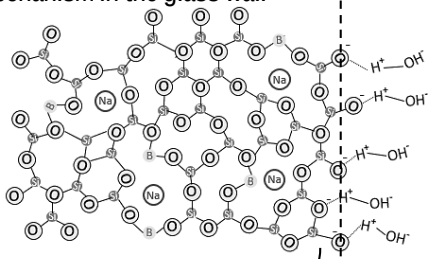

Space charge polarization
(weak frequency dependence)

MW (space-charge) polarization at glass wall – sample interface

TVIS response for empty vial

OH−
OH−
OH−
OH−

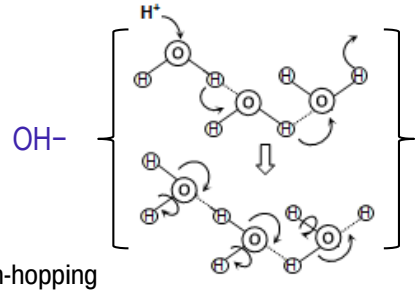

Proton-hopping
Conduction of protons in liquid water occurs through the Grotthuss "hop-turn" mechanism

Conductivity in pure water

Dipolar polarization
re-orientation/alignment of permanent dipoles in liquid water (Debye-like relaxation)

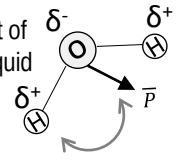

Polarization mechanisms in liquid water
(relaxation time, τ ~ 9 ps at 20°C)

TVIS response for liquid water

H+
H+
H+
H+

Electronic polarization
distortion of electrons relative to the nuclei

Atomic polarization
distortion of nuclei across a heteroatom bond by stretching and bending

Instantaneous polarization dominant mechanism in the glass wall

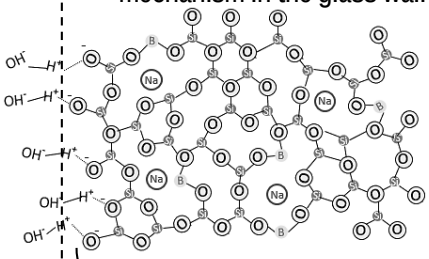

Space charge polarization
(weak frequency dependence)

MW (space-charge) polarization at glass wall – sample interface

TVIS response for empty vial

Measurement vial

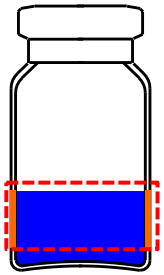

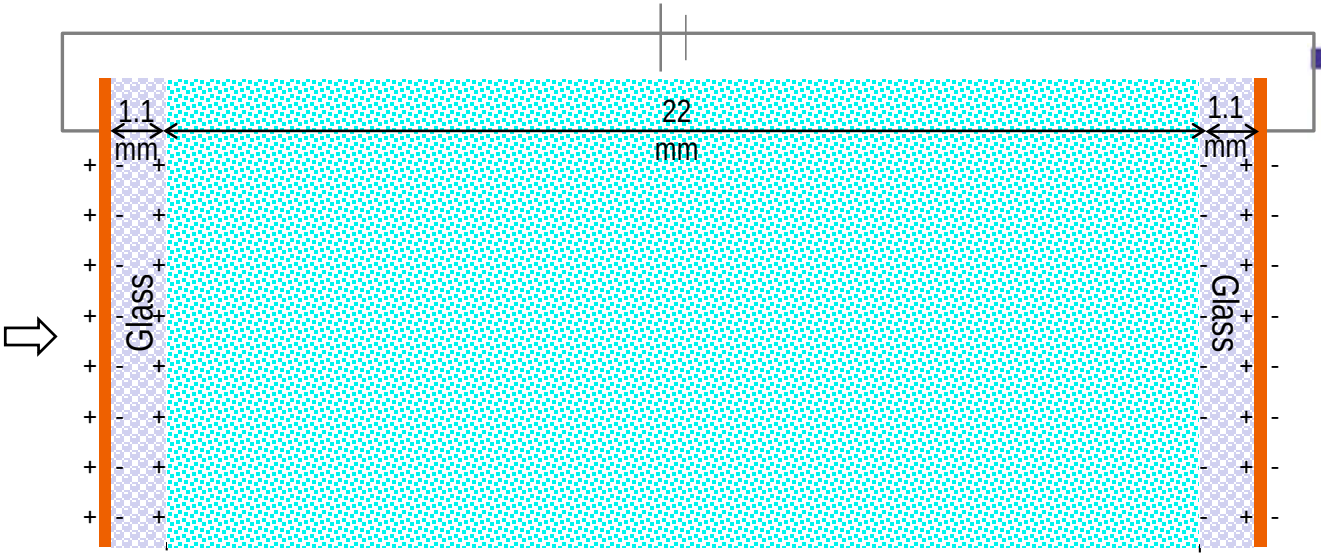

Electronic polarization
distortion of electrons relative to the nuclei

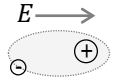

Atomic polarization
distortion of nuclei across a heteroatom bond by stretching and bending

Instantaneous polarization dominant mechanism in the glass wall

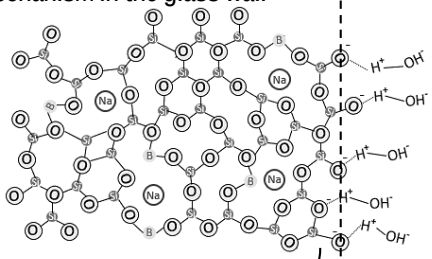

Space charge polarization
(weak frequency dependence)

MW (space-charge) polarization at glass wall – sample interface

TVIS response for empty vial

Dominant at T > 235 K (approx. −40 ºC)
Generation/migration of L- and D- orientation defects in ice Ih

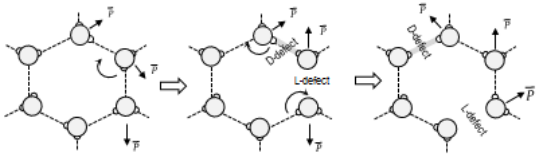

Dominant at T < 235 K (approx. −40 ºC)
Generation/migration of H3O+/OH− ion pairs (ionic defects) in ice Ih (similar to the Grotthus mechanism)

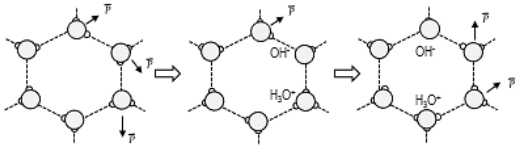

Polarization mechanism in ice

TVIS response for frozen water (ice)

Electronic polarization
distortion of electrons relative to the nuclei

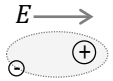

Atomic polarization
distortion of nuclei across a heteroatom bond by stretching and bending

Instantaneous polarization dominant mechanism in the glass wall

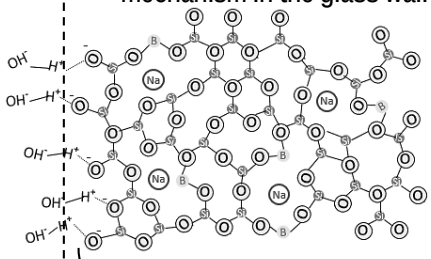

Space charge polarization
(weak frequency dependence)

MW (space-charge) polarization at glass wall – sample interface

TVIS response for empty vial

Frozen Water and Dielectric Relaxation of Ice

I. : The polarization of the water dipole in liquid water at 20 ˚C, with a dielectric loss peak frequency of ~ 18 GHz

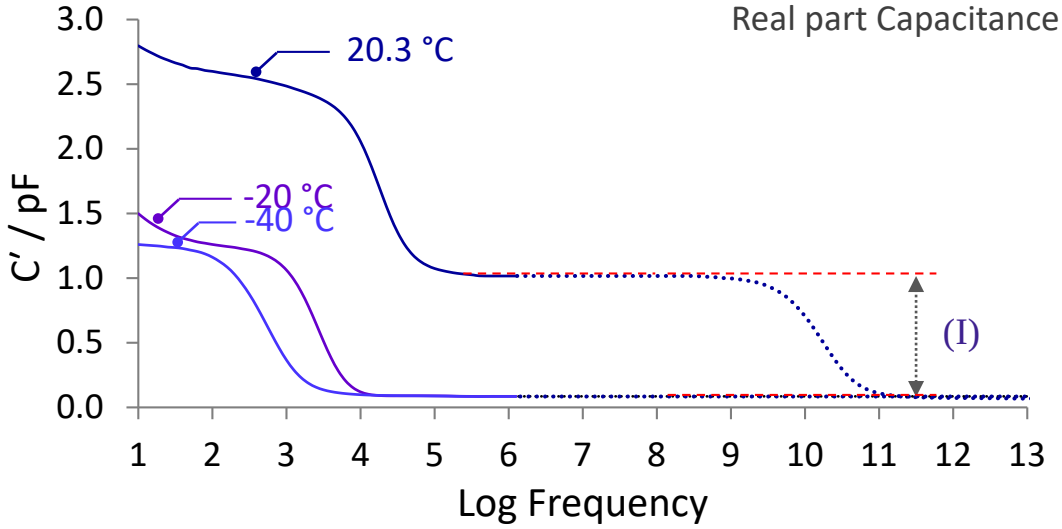

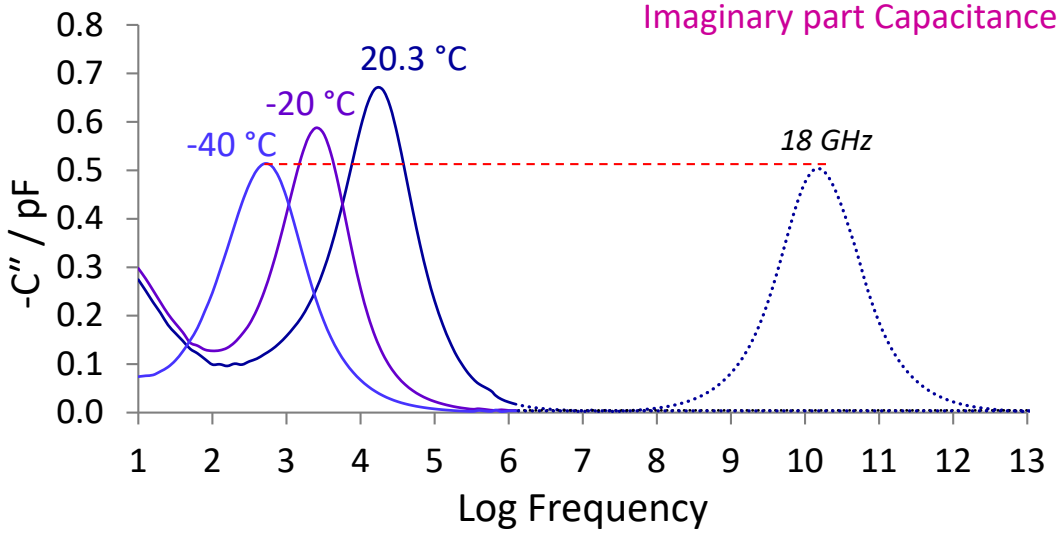

Frozen Water and Dielectric Relaxation of Ice

I. : The polarization of the water dipole in liquid water at 20 ˚C, with a dielectric loss peak frequency of ~ 18 GHz

II. : The Maxwell-Wagner (MW) polarization of the glass wall of the TVIS vial at 20 ˚C, with a dielectric loss peak frequency of 17.8 kHz

Real part Capacitance

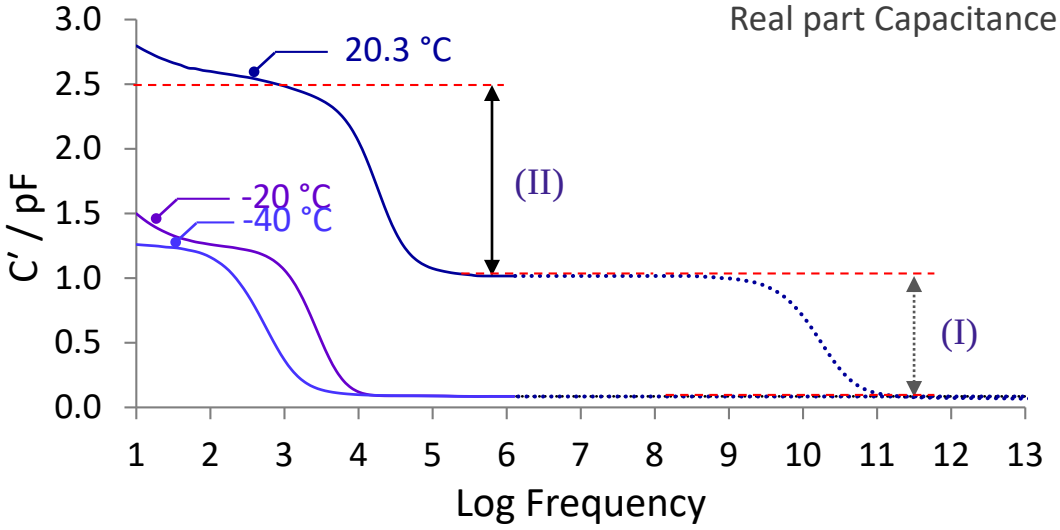

Imaginary part Capacitance

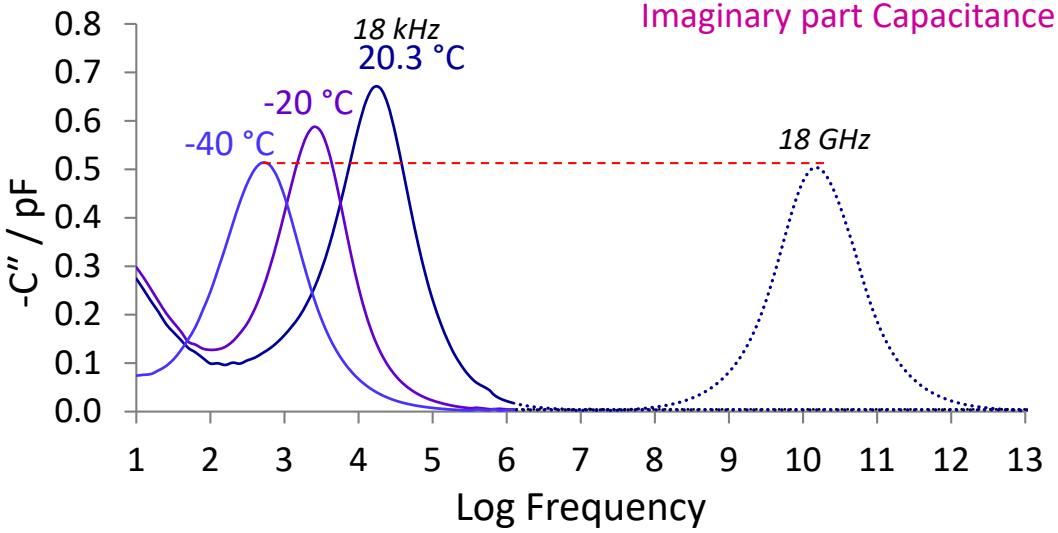

Frozen Water and Dielectric Relaxation of Ice

I. : The polarization of the water dipole in liquid water at 20 ˚C, with a dielectric loss peak frequency of ~ 18 GHz

II. : The Maxwell-Wagner (MW) polarization of the glass wall of the TVIS vial at 20 ˚C, with a dielectric loss peak frequency of 17.8 kHz

III. : The dielectric polarization of ice at −20 ˚C, with a dielectric loss peak frequencies of 2.57 kHz

Real part Capacitance

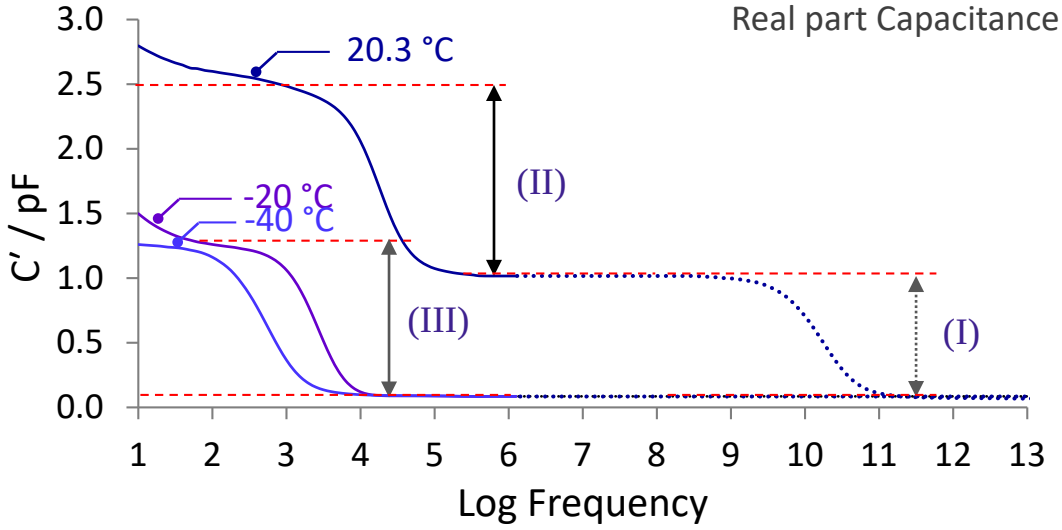

Imaginary part Capacitance

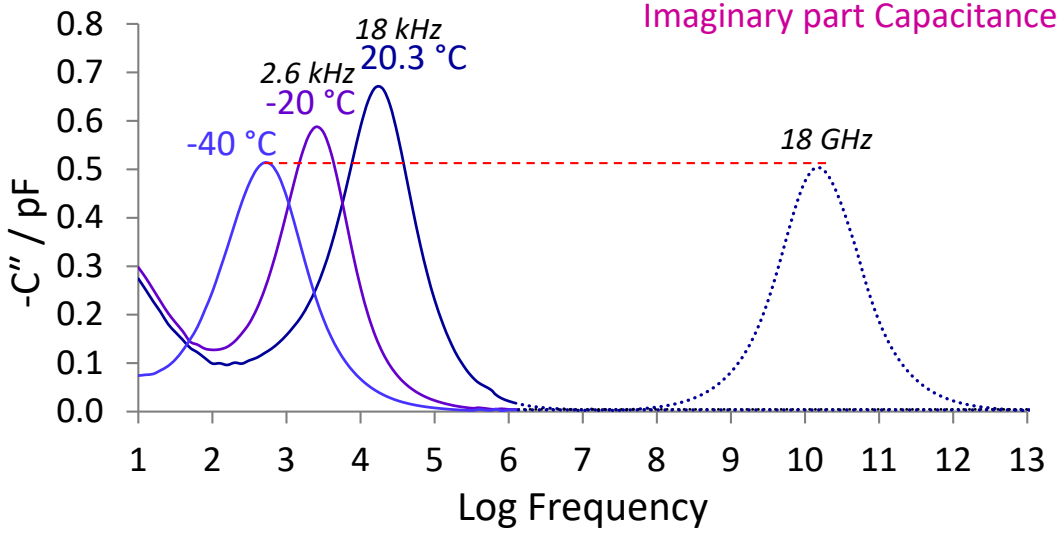

Frozen Water and Dielectric Relaxation of Ice

I. : The polarization of the water dipole in liquid water at 20 ˚C, with a dielectric loss peak frequency of ~ 18 GHz

II. : The Maxwell-Wagner (MW) polarization of the glass wall of the TVIS vial at 20 ˚C, with a dielectric loss peak frequency of 17.8 kHz

III. : The dielectric polarization of ice at −20 ˚C, with a dielectric loss peak frequencies of 2.57 kHz

IV. : The dielectric polarization of ice at −40 ˚C with a dielectric loss peak frequencies of 537 Hz.

Real part Capacitance

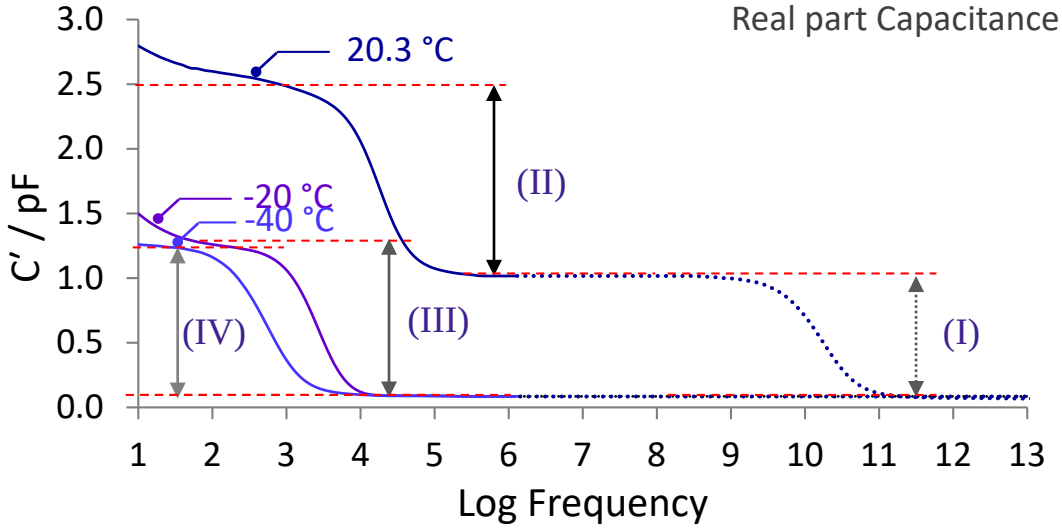

Imaginary part Capacitance

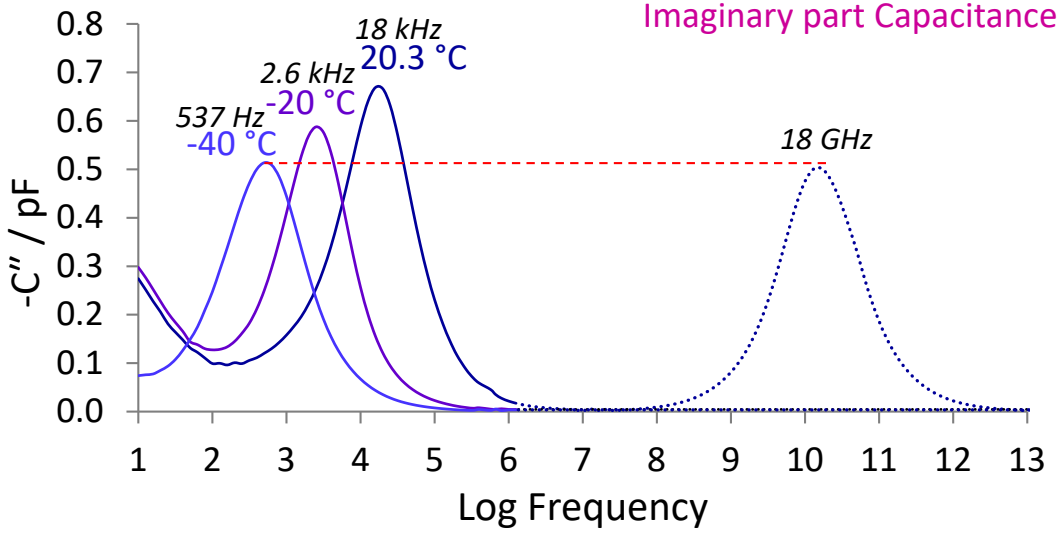

Through Vial Impedance Spectroscopy (TVIS)

Applications

Through Vial Impedance Spectroscopy (TVIS)

Monitoring **Phase Behaviour** (ice nucleation temperature and solidification end points by using F_{PEAK}

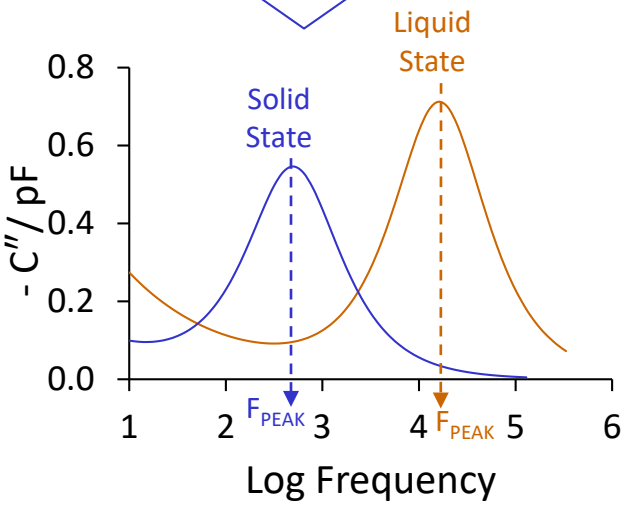

Through Vial Impedance Spectroscopy (TVIS)

Monitoring **Phase Behaviour** (ice nucleation temperature and solidification end points by using F_{PEAK}

F_{PEAK} temperature calibration for **predicting temperature** of the product in primary drying

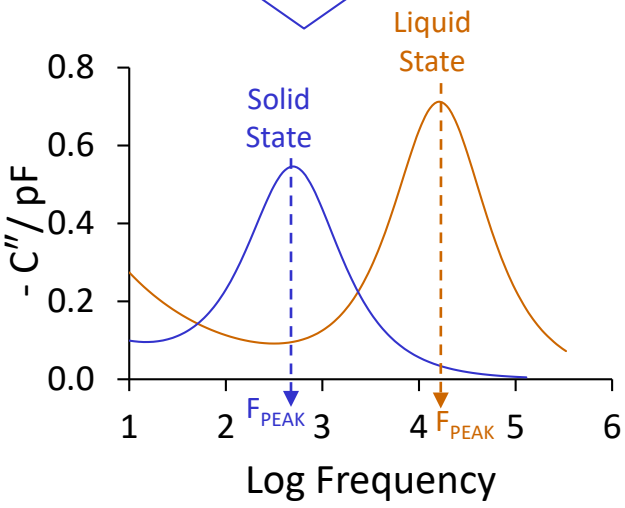

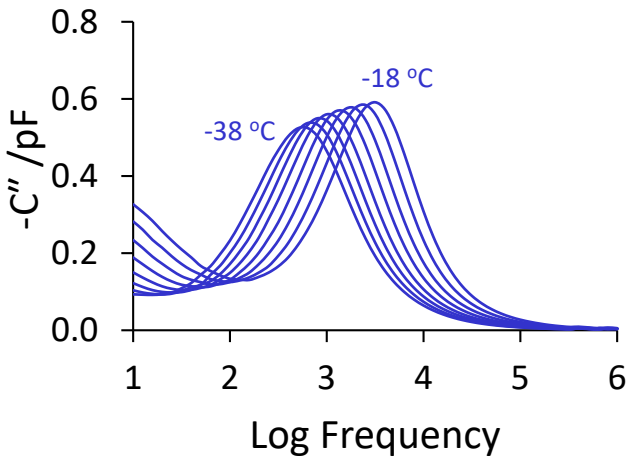

Through Vial Impedance Spectroscopy (TVIS)

Monitoring **Phase Behaviour** (ice nucleation temperature and solidification end points by using F_{PEAK}

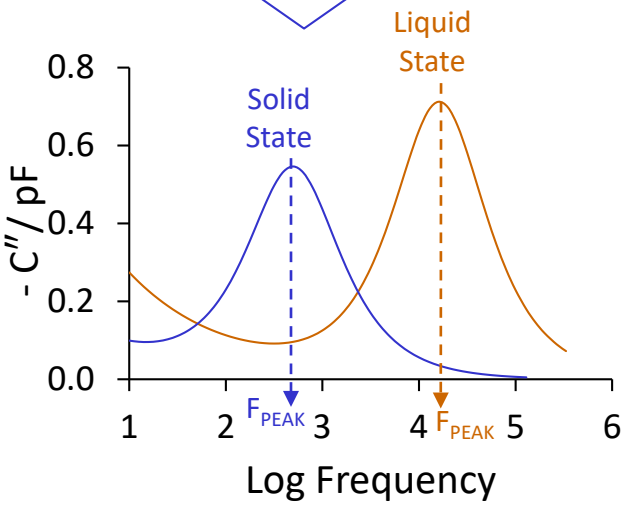

F_{PEAK} temperature calibration for **predicting temperature** of the product in primary drying

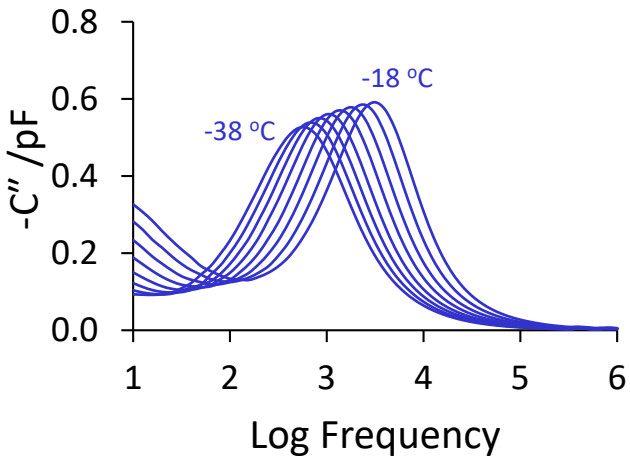

Surrogate **drying rate** (from $\frac{dC''_{PEAK}}{dt}$)

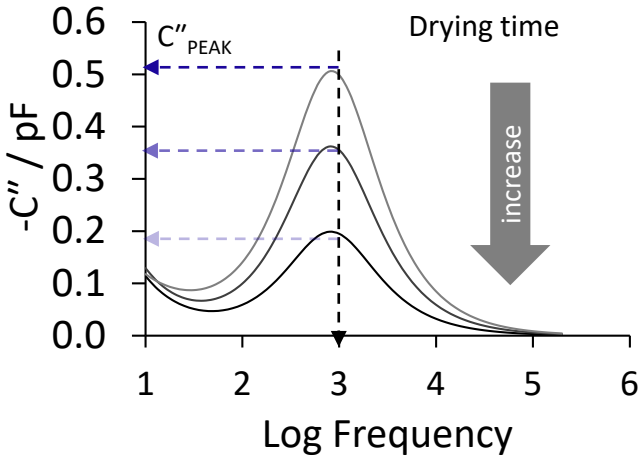

Through Vial Impedance Spectroscopy (TVIS)

Monitoring **Phase Behaviour** (ice nucleation temperature and solidification end points by using F_{PEAK}

F_{PEAK} temperature calibration for **predicting temperature** of the product in primary drying

Surrogate **drying rate** (from $\frac{dC''_{PEAK}}{dt}$)

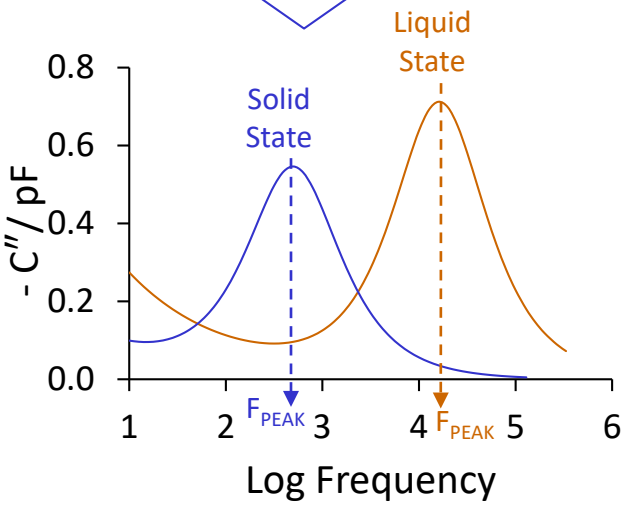

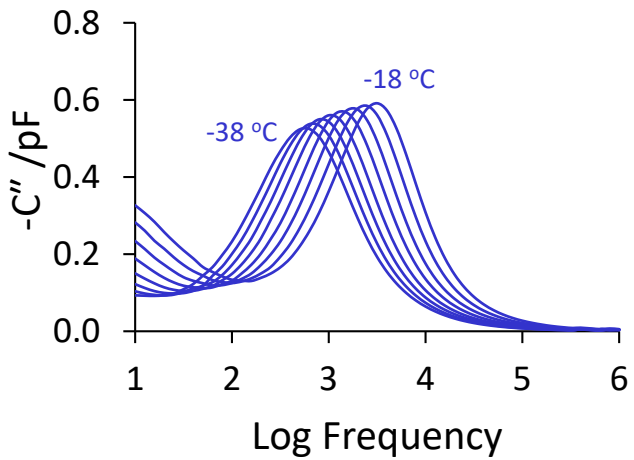

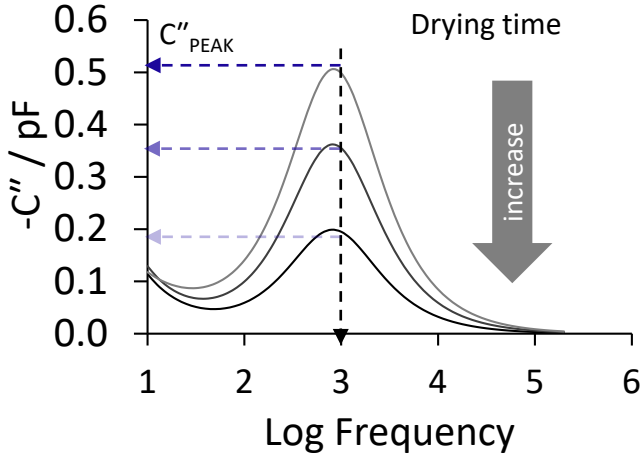

C'(~ 100 kHz) is highly sensitive to low ice volumes; therefore it could be used for determination **end point** of primary drying

TVIS Response Surface (3D-Plot)

Imaginary Part of Capacitance

Real Part of Capacitance

Annealing = Re-heating and Re-cooling

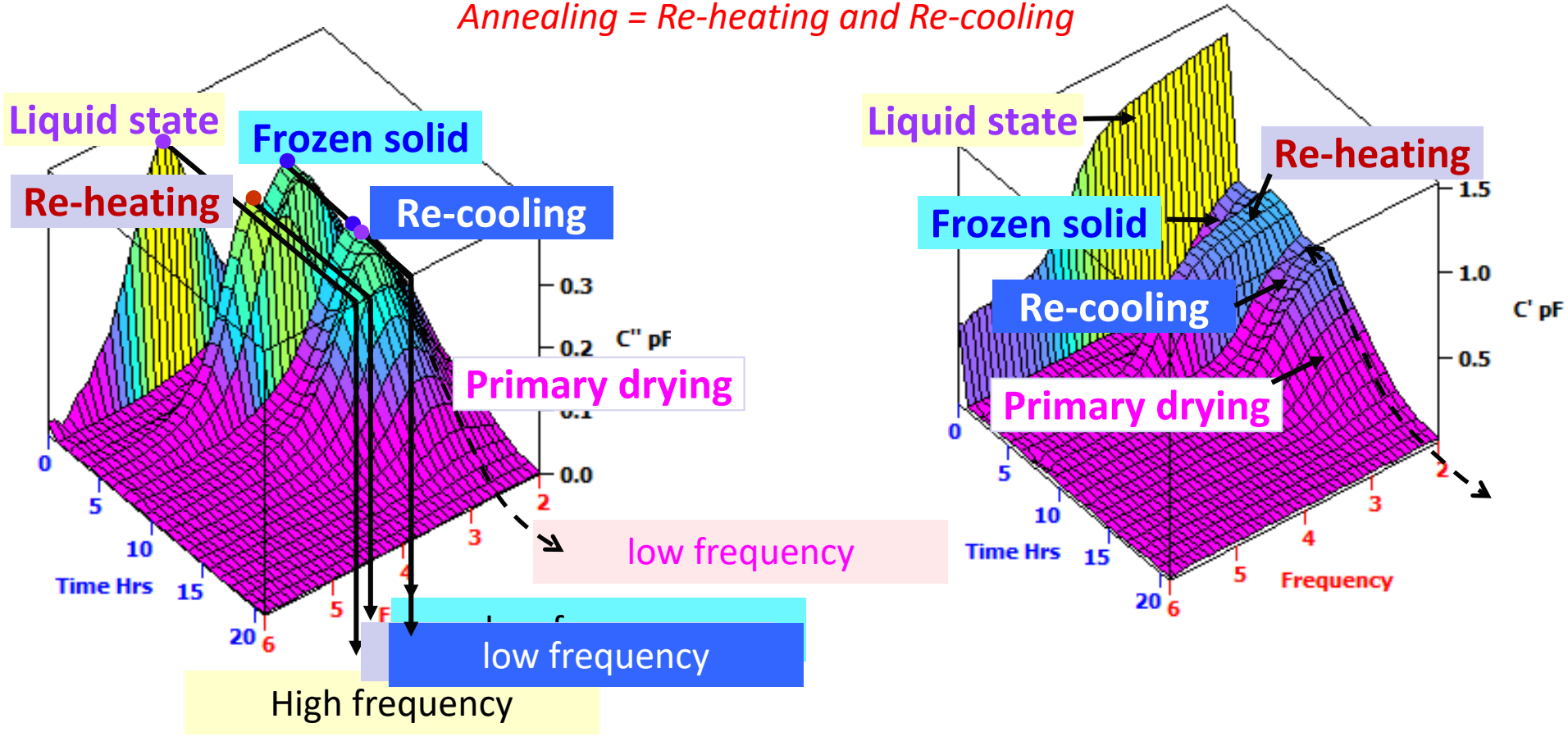

Phase Separation in Freezing Step

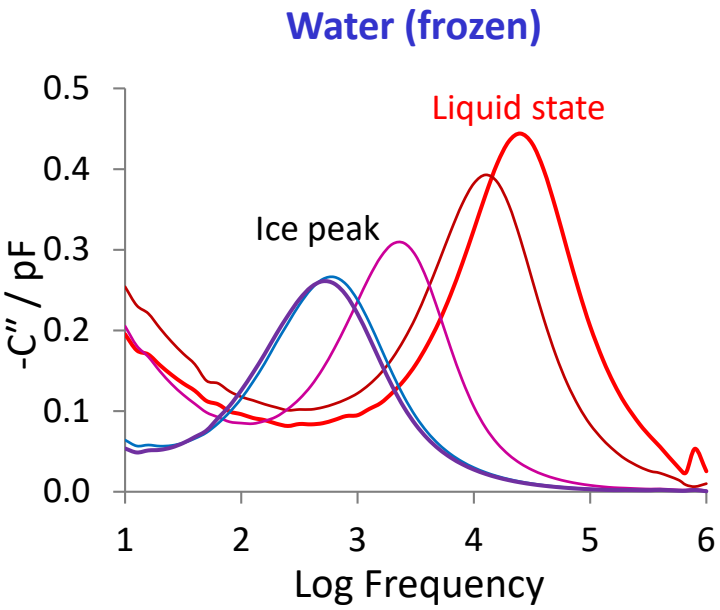

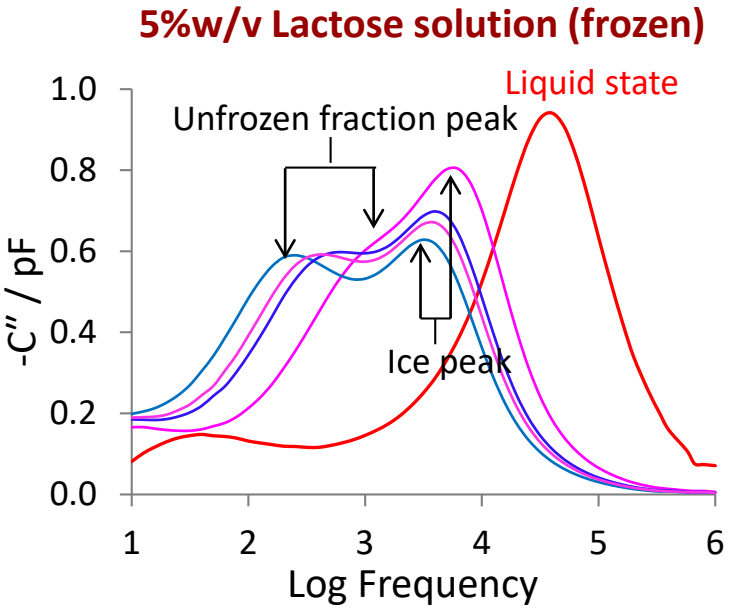

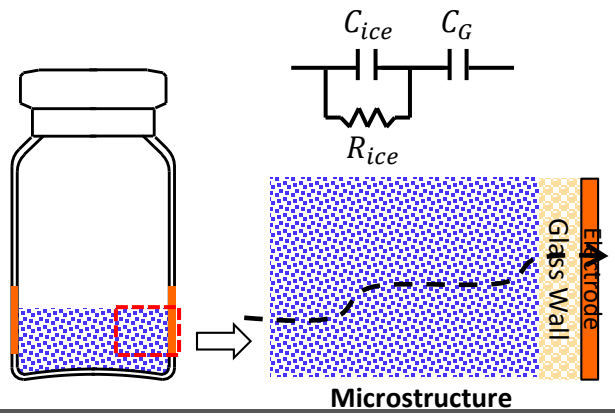

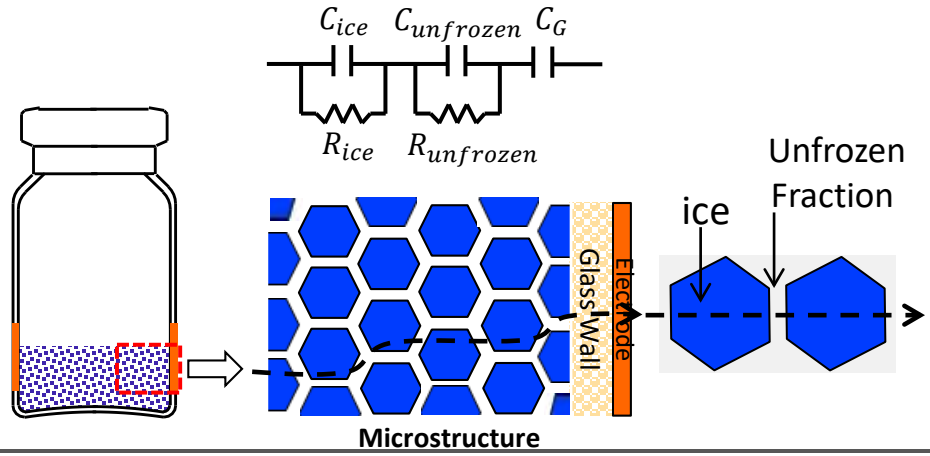

Dielectric loss spectrum

- *Data analysing software (LyoView ™) identifies the peak frequency (F_{PEAK}) and peak amplitude (C''_{PEAK}) in the imaginary part of the capacitance spectrum*

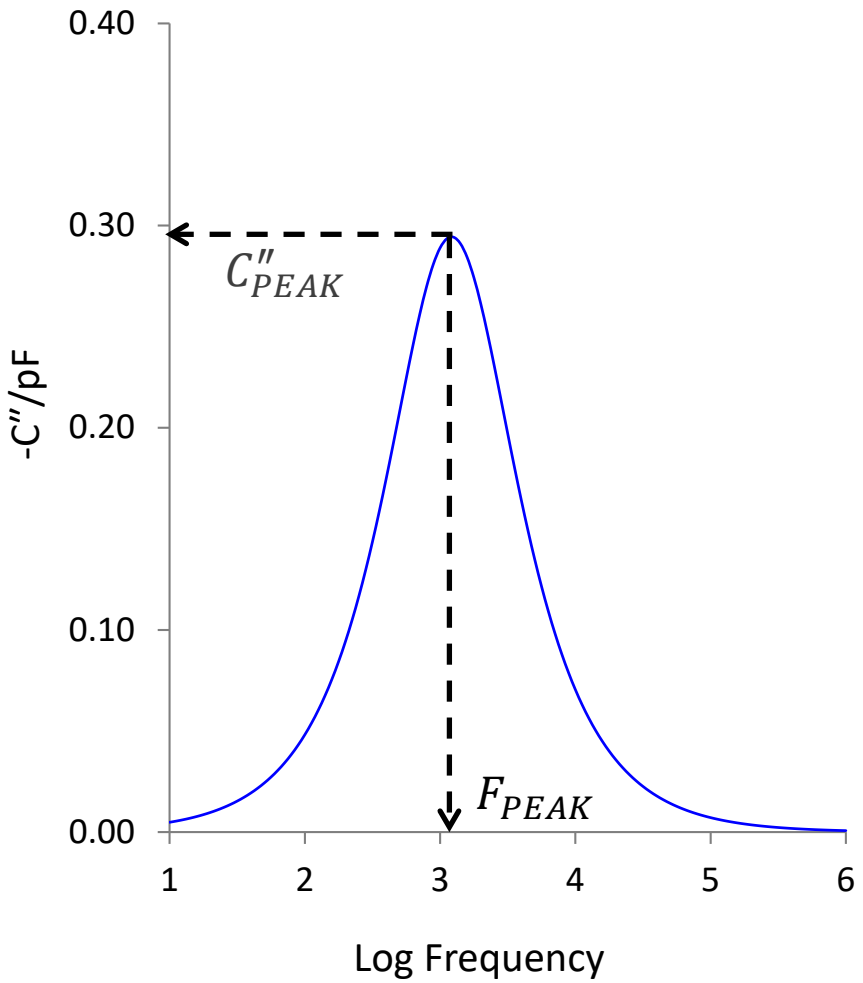

Through Vial Impedance Spectroscopy (TVIS)

Temperature calibration & Temperature prediction

Temperature Calibration

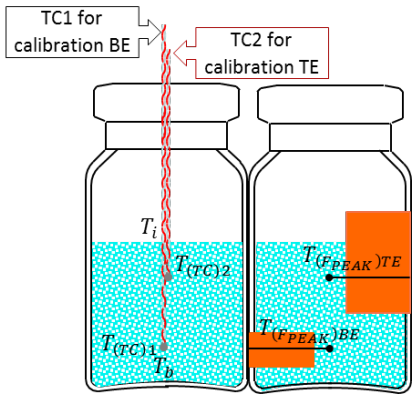

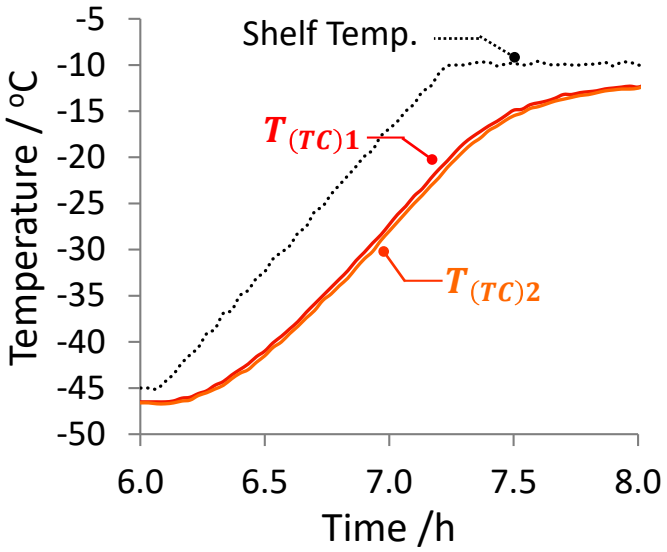

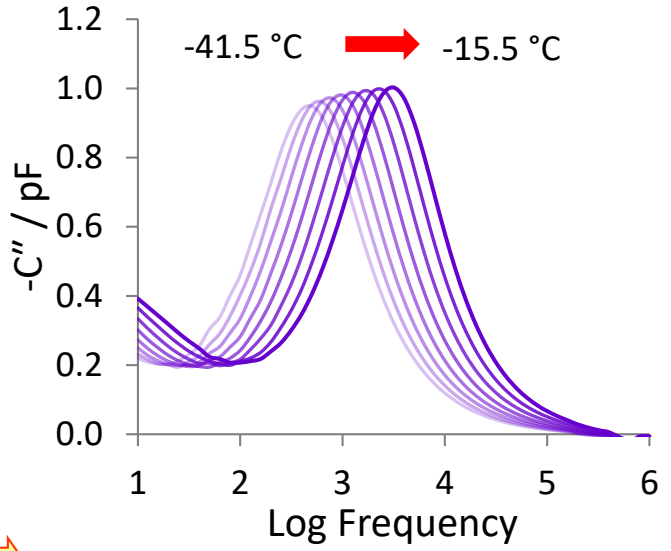

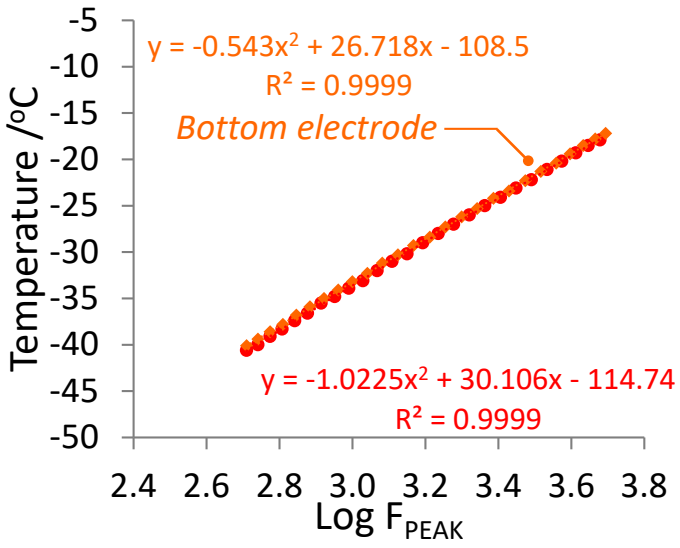

Polynomial coefficient from $Log\ F_{PEAK}$ – temperature calibration

	a	b	c
TE	*-1.02*	*30.1*	*-114*
BE	*-5.43 x 10^{-1}*	*26.7*	*-109*

Temperature Prediction

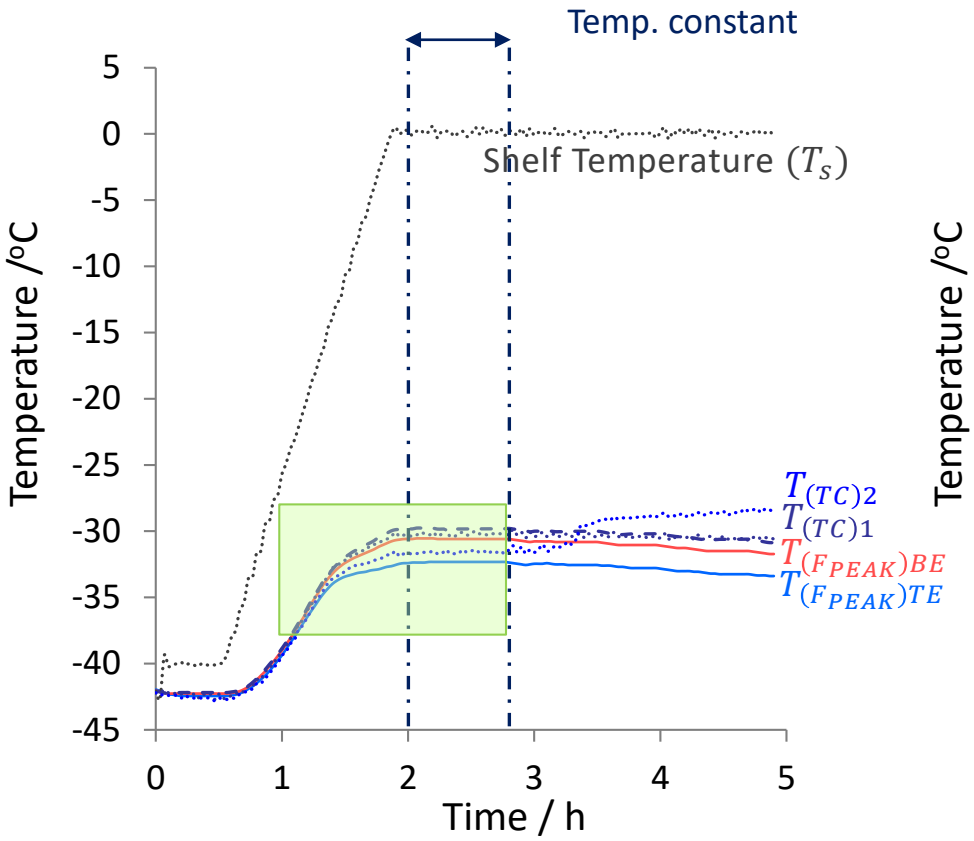

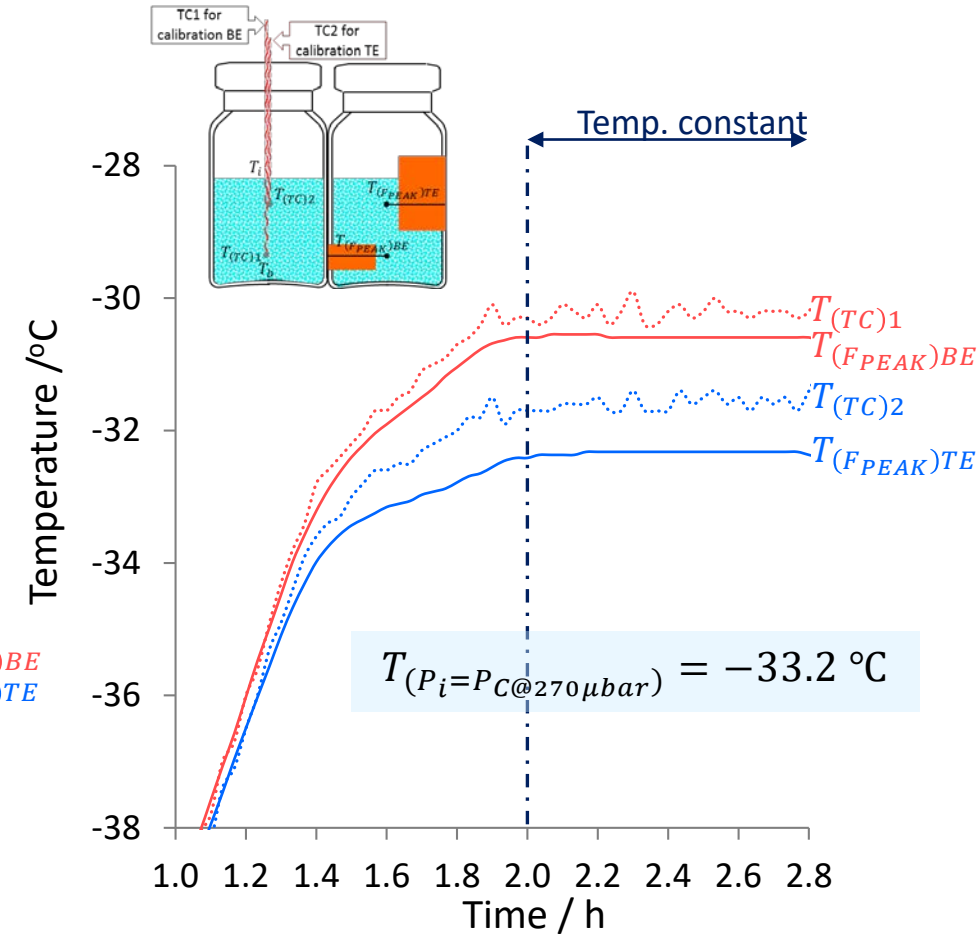

Through Vial Impedance Spectroscopy (TVIS)

Drying rate estimation

Drying Rate Estimation

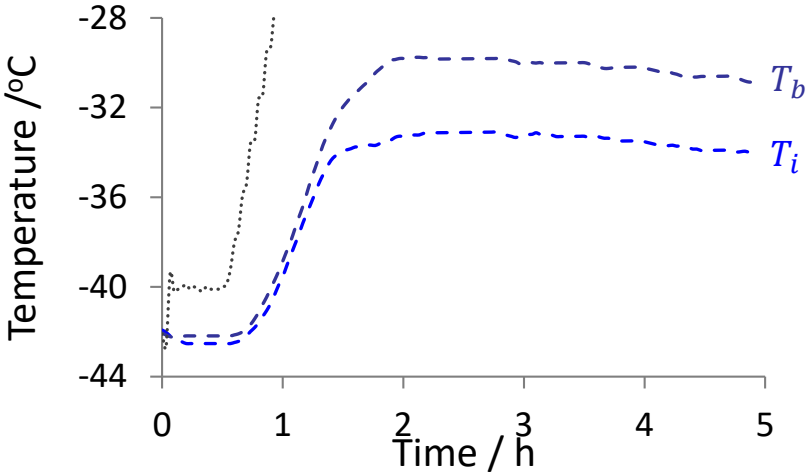

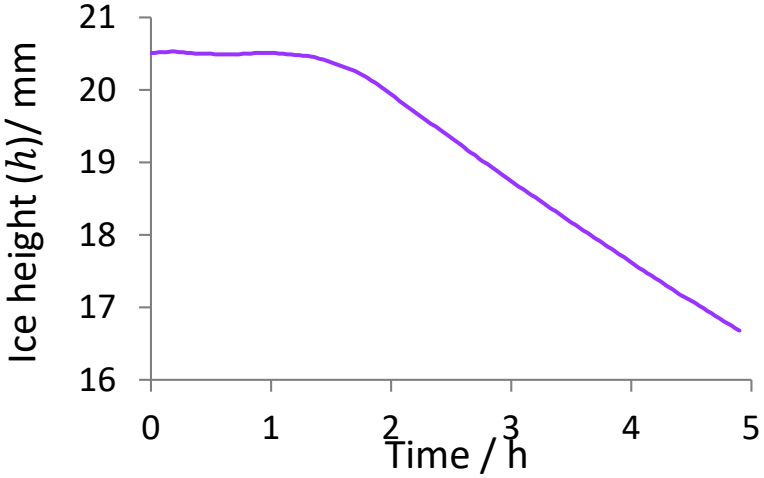

Drying Rate Estimation

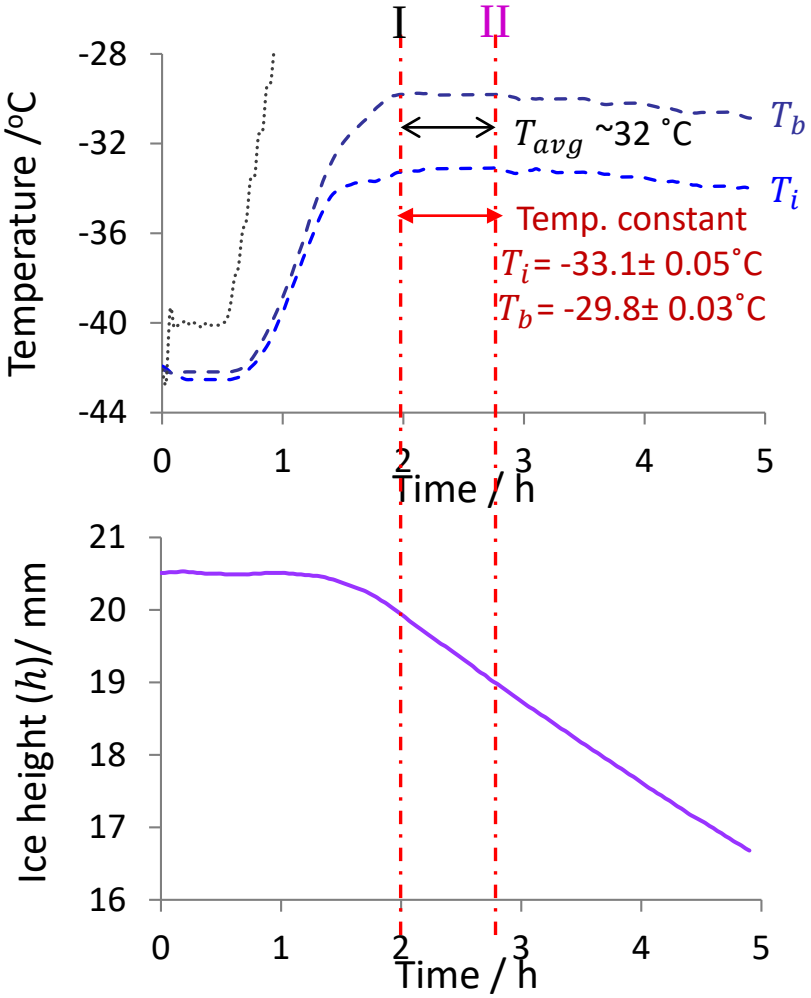

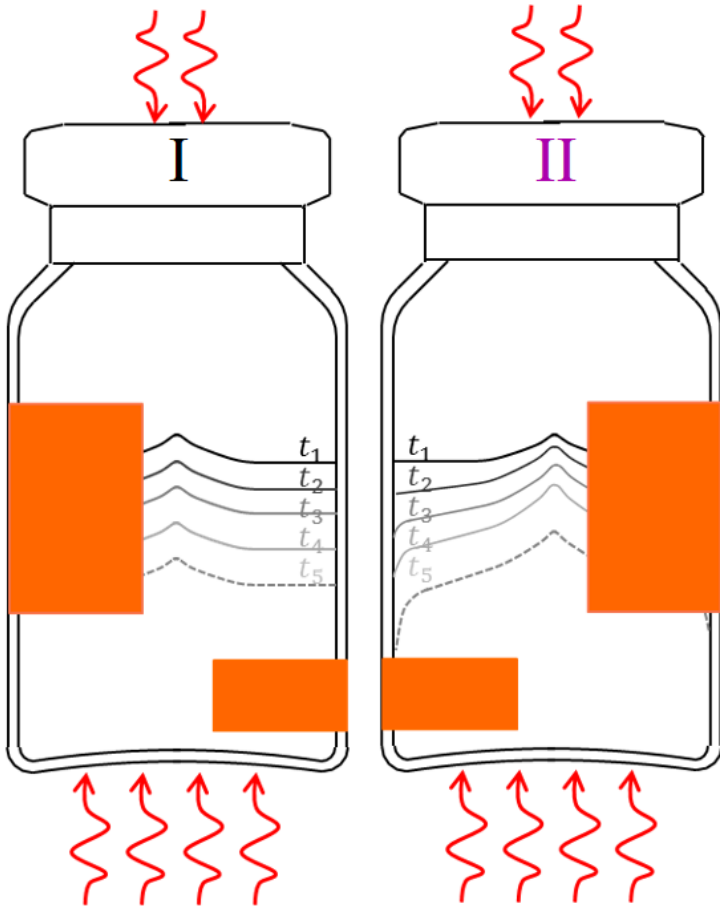

DE MONTFORT UNIVERSITY LEICESTER

Drying Rate Estimation

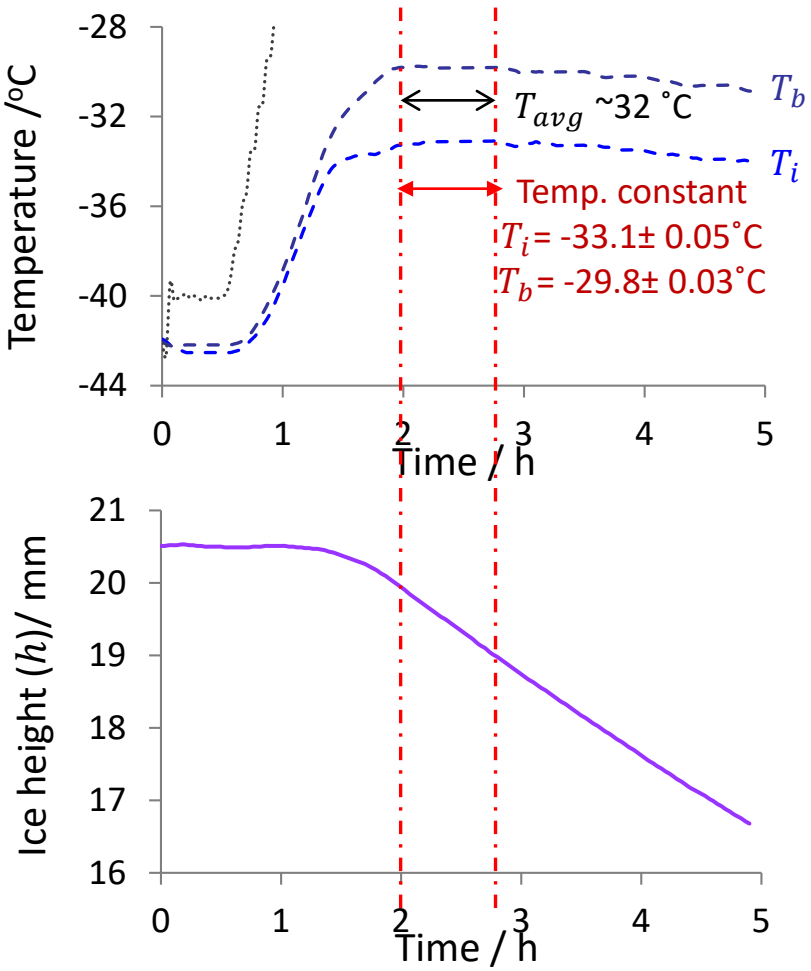

- Drying rate during the steady state

$$Drying\ rate\ (\frac{\Delta m}{\Delta t}) = \rho_i \cdot A \cdot \frac{h_{(t1)} - h_{(t2)}}{t_2 - t_1}$$

DE MONTFORT UNIVERSITY LEICESTER

Drying Rate Estimation

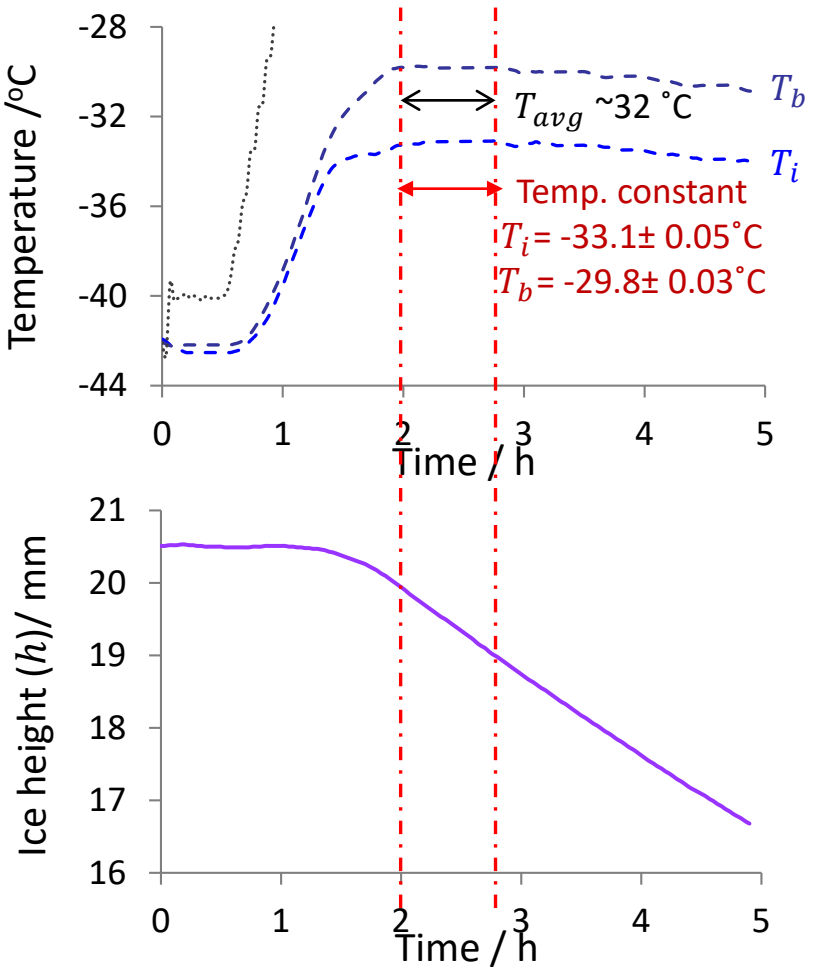

- Drying rate during the steady state

$$Drying\ rate\ (\frac{\Delta m}{\Delta t}) = \rho_i \cdot A \cdot \frac{h_{(t1)} - h_{(t2)}}{t_2 - t_1}$$

Ice density (ρ_i) at -32˚C = 0.920 g·cm^{-3}

(Calculated ice temperature between T_i & T_b)

Drying Rate Estimation

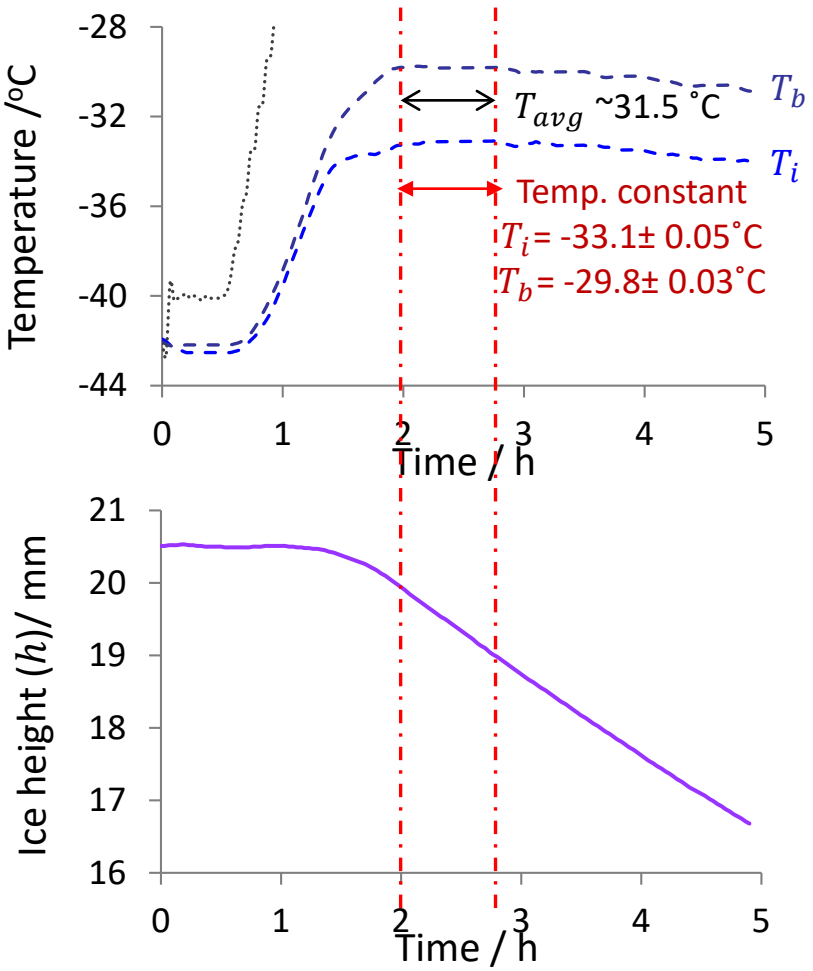

- Drying rate during the steady state

$$Drying\ rate\ (\frac{\Delta m}{\Delta t}) = \rho_i \cdot A \cdot \frac{h_{(t1)} - h_{(t2)}}{t_2 - t_1}$$

Ice density (ρ_i) at -32˚C = 0.920 g·cm^{-3}

(Calculated ice temperature between T_i & T_b)

Internal vial diameter (VC010-20C) = 2.21 cm

DE MONTFORT UNIVERSITY LEICESTER

Drying Rate Estimation

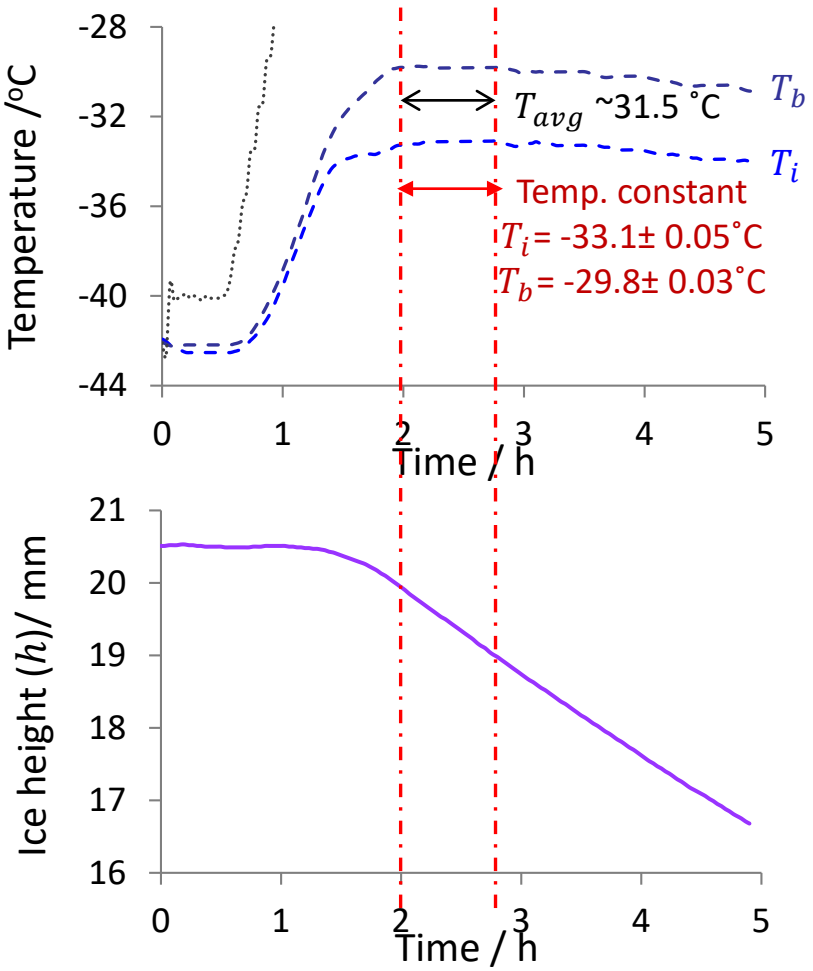

- Drying rate during the steady state

$$Drying\ rate\ (\frac{\Delta m}{\Delta t}) = \rho_i \cdot A \cdot \frac{h_{(t1)} - h_{(t2)}}{t_2 - t_1}$$

Ice density (ρ_i) at -32˚C = 0.920 g·cm^{-3}

(Calculated ice temperature between T_i & T_b)

Internal vial diameter (VC010-20C) = 2.21 cm

Cross-section area (A) = 3.80 cm^2

DE MONTFORT UNIVERSITY LEICESTER

Drying Rate Estimation

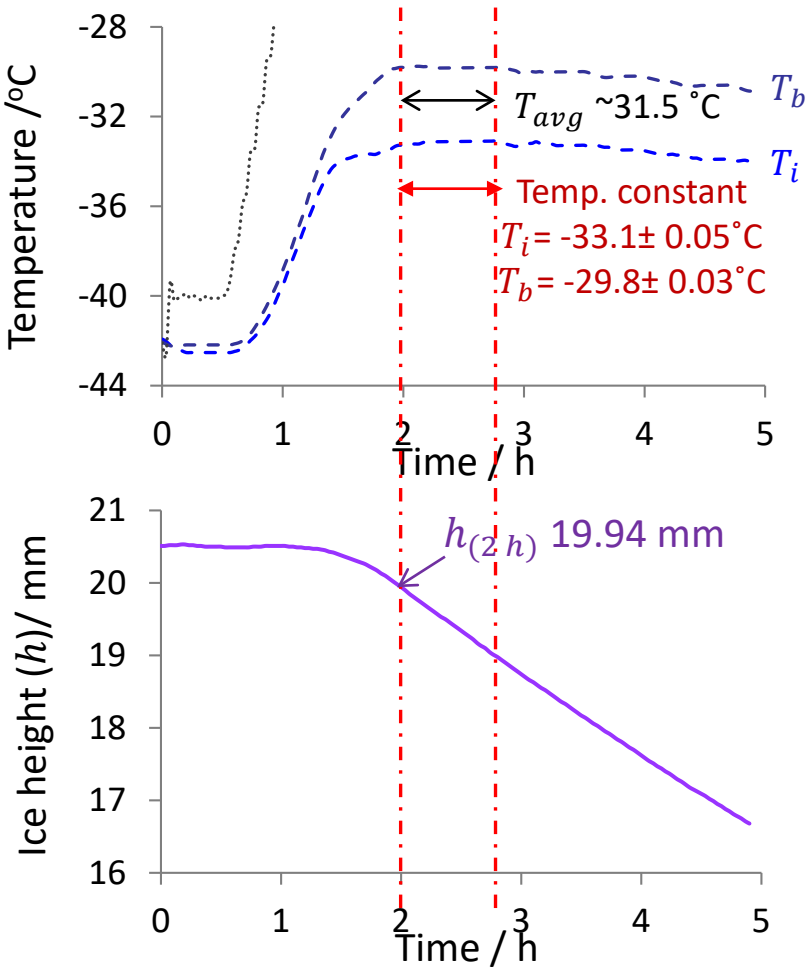

- Drying rate during the steady state

$$Drying\ rate\ (\frac{\Delta m}{\Delta t}) = \rho_i \cdot A \cdot \frac{h_{(t1)} - h_{(t2)}}{t_2 - t_1}$$

Ice density (ρ_i) at -32˚C = 0.920 g·cm^{-3}

(Calculated ice temperature between T_i & T_b)

Internal vial diameter (VC010-20C) = 2.21 cm

Cross-section area (A) = 3.80 cm^2

Ice height at 2 h ($h_{(2\,h)}$) = 19.94 mm

DE MONTFORT UNIVERSITY LEICESTER

Drying Rate Estimation

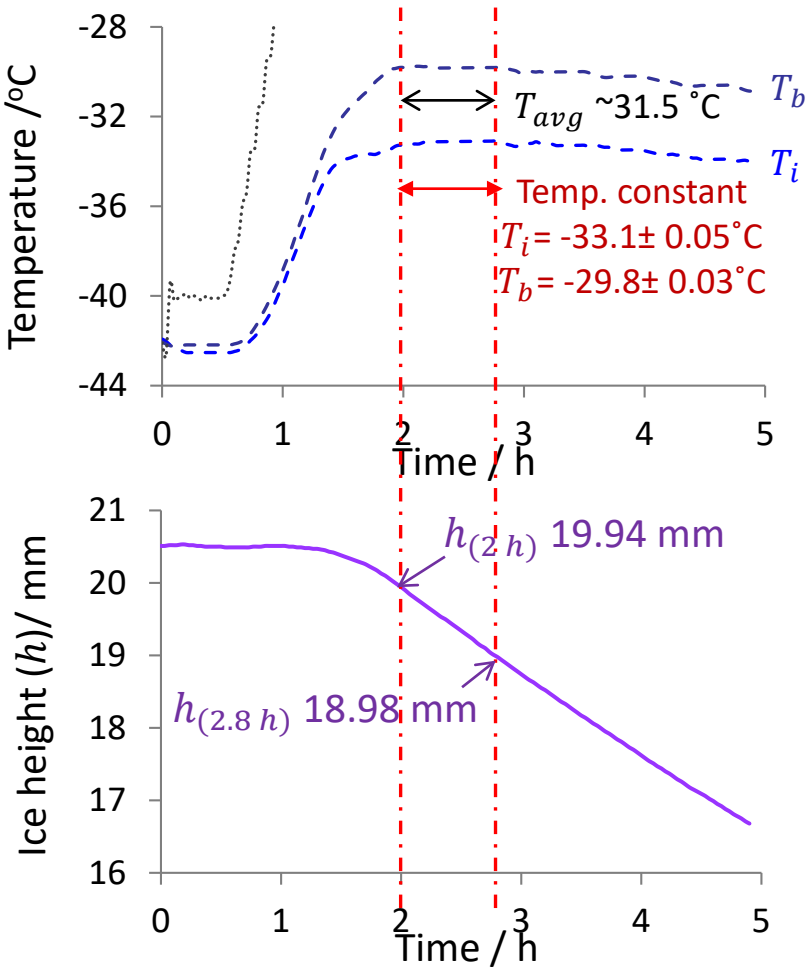

- Drying rate during the steady state

$$Drying\ rate\ (\frac{\Delta m}{\Delta t}) = \rho_i \cdot A \cdot \frac{h_{(t1)} - h_{(t2)}}{t_2 - t_1}$$

Ice density (ρ_i) at -32˚C = 0.920 g·cm^{-3}

(Calculated ice temperature between T_i & T_b)

Internal vial diameter (VC010-20C) = 2.21 cm

Cross-section area (A) = 3.80 cm^2

Ice height at 2 h ($h_{(2\,h)}$) = 19.94 mm

Ice height at 2.8 h ($h_{(2.8\,h)}$) = 18.98 mm

DE MONTFORT UNIVERSITY LEICESTER

Drying Rate Estimation

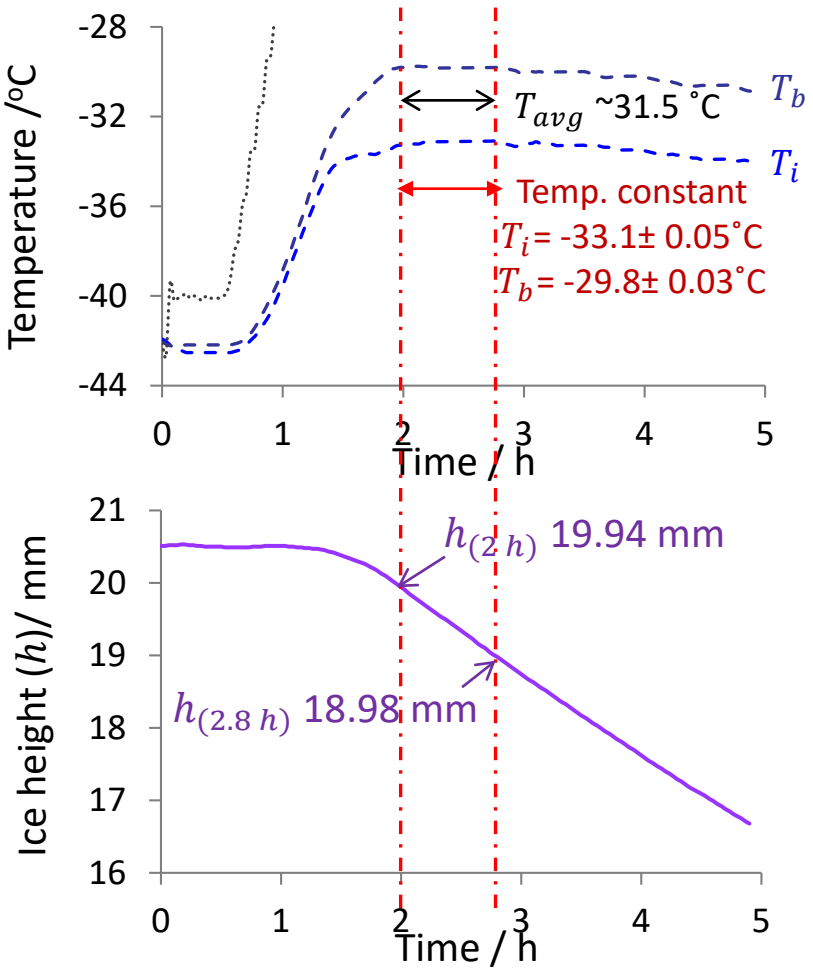

- Drying rate during the steady state

$$Drying\ rate\ (\frac{\Delta m}{\Delta t}) = \rho_i \cdot A \cdot \frac{h_{(t1)} - h_{(t2)}}{t_2 - t_1}$$

Ice density (ρ_i) at -32˚C = 0.920 g·cm^{-3}

(Calculated ice temperature between T_i & T_b)

Internal vial diameter (VC010-20C) = 2.21 cm

Cross-section area (A) = 3.80 cm^2

Ice height at 2 h ($h_{(2\,h)}$) = 19.94 mm

Ice height at 2.8 h ($h_{(2.8\,h)}$) = 18.98 mm

$$Drying\ rate\ = 0.920\ g \cdot cm^{-3} \times 3.80\ cm^2 \times \frac{(19.94 - 18.98) \times 10^{-1} cm}{(2.8 - 2.0)\ h}$$

$$= \mathbf{0.42\ g \cdot h^{-1}}$$

DE MONTFORT UNIVERSITY LEICESTER

Drying Rate Estimation

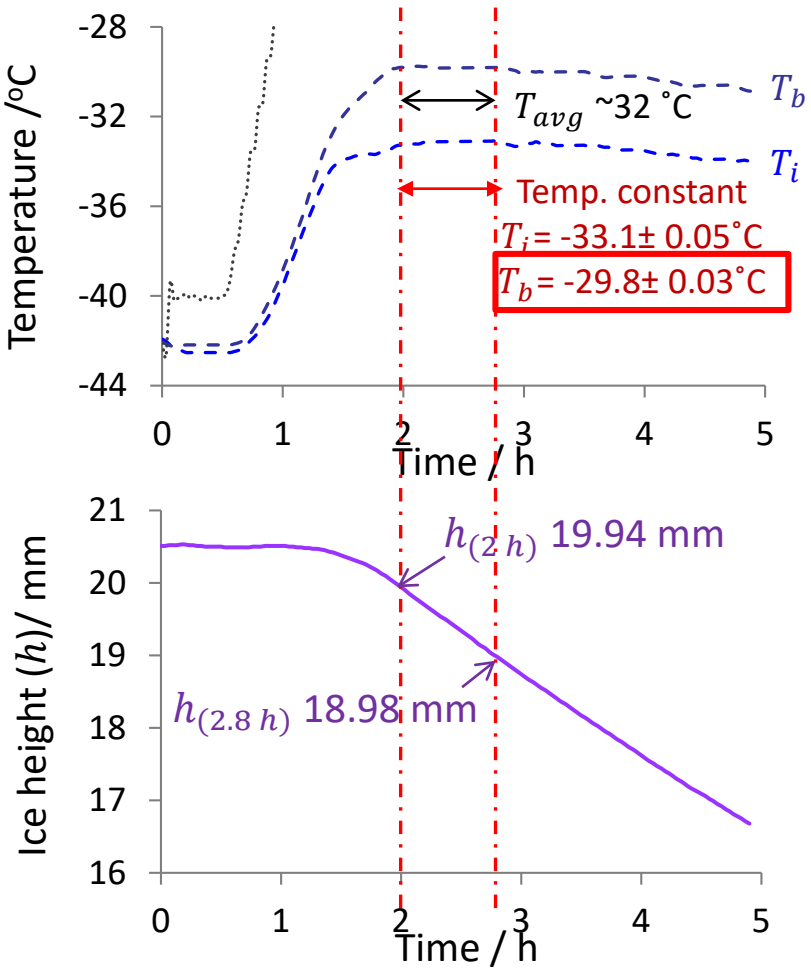

- Drying rate during the steady state

$$Drying\ rate\ (\frac{\Delta m}{\Delta t}) = \rho_i \cdot A \cdot \frac{h_{(t1)} - h_{(t2)}}{t_2 - t_1}$$

Ice density (ρ_i) at -32˚C = 0.920 g·cm^{-3}

(Calculated ice temperature between T_i & T_b)

Internal vial diameter (VC010-20C) = 2.21 cm

Cross-section area (A) = 3.80 cm^2

Ice height at 2 h ($h_{(2\,h)}$) = 19.94 mm

Ice height at 2.8 h ($h_{(2.8\,h)}$) = 18.98 mm

TVIS parameters used for determination:

$\frac{\Delta m}{\Delta t}$ = 0.42 g·h^{-1}

T_b = -29.8˚C

$$Drying\ rate\ = 0.920\ g \cdot cm^{-3} \times 3.80\ cm^2 \times \frac{(19.94 - 18.98) \times 10^{-1} cm}{(2.8 - 2.0)\ h}$$

$$= \mathbf{0.42\ g \cdot h^{-1}}$$

DE MONTFORT UNIVERSITY LEICESTER

Through Vial Impedance Spectroscopy (TVIS)

Heat Transfer Coefficient Determination

DE MONTFORT UNIVERSITY LEICESTER

Heat Transfer Coefficient (K_v)Determination

Parameters	TVIS
Drying rate at steady state (g/h) (2-2.8 h into primary drying)	0.42
Shelf Temperature, T_s (K)	273.3
Vial's base Temperature, T_b(K)	243.3

Heat Transfer Coefficient (K_v)Determination

Parameters	TVIS
Drying rate at steady state (g/h) (2-2.8 h into primary drying)	0.42
Shelf Temperature, T_s (K)	273.3
Vial's base Temperature, T_b(K)	243.3

$$L\frac{\Delta m}{\Delta t} = A_e K_v (T_s - T_b) \Rightarrow K_v = \frac{L\frac{\Delta m}{\Delta t}}{A_e(T_s - T_b)}$$

L is the latent heat of sublimation of ice (2844 J·g^{-1} or 679.7 cal ·g^{-1}) and A_e is external cross-sectional area of the base of the TVIS vial (4.62 cm^2)

Heat Transfer Coefficient (K_v)Determination

Parameters	TVIS
Drying rate at steady state (g/h) (2-2.8 h into primary drying)	0.42
Shelf Temperature, T_s (K)	273.3
Vial's base Temperature, T_b(K)	243.3

$$L\frac{\Delta m}{\Delta t} = A_e K_v (T_s - T_b) \Rightarrow K_v = \frac{L\frac{\Delta m}{\Delta t}}{A_e(T_s - T_b)}$$

L is the latent heat of sublimation of ice (2844 J·g^{-1} or 679.7 cal ·g^{-1}) and A_e is external cross-sectional area of the base of the TVIS vial (4.62 cm^2)

$$K_v(270\ \mu bar) = \frac{L\frac{\Delta m}{\Delta t}}{A_e(T_s - T_b)}$$

$$= \frac{679.7\ cal \cdot g^{-1} \times 0.42\ g \cdot h^{-1}}{4.62\ cm^2 \times (273.3 - 243.3)K}$$

$$= 2.06\ cal \cdot h^{-1} \cdot cm^{-2} \cdot K^{-1}$$

$$= 5.73 \times 10^{-4} cal \cdot s^{-1} \cdot cm^{-2} \cdot K^{-1}$$

$$K_v(270\ \mu bar) = 5.73 \times 10^{-4} cal \cdot s^{-1} \cdot cm^{-2} \cdot K^{-1}$$

Heat Transfer Coefficient (K_v)Determination

Parameters	TVIS
Drying rate at steady state (g/h) (2-2.8 h into primary drying)	0.42
Shelf Temperature, T_s (K)	273.3
Vial's base Temperature, T_b(K)	243.3

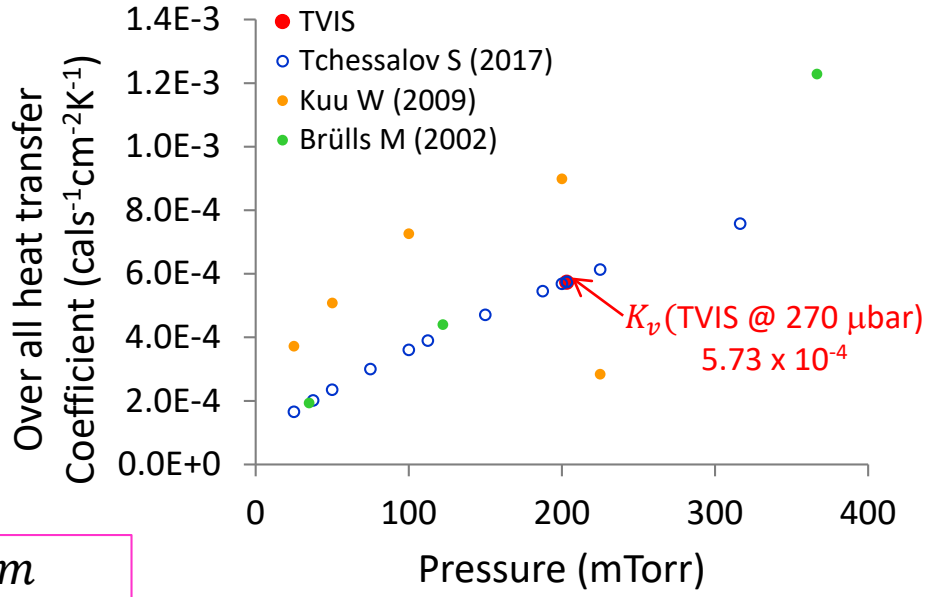

$$L\frac{\Delta m}{\Delta t} = A_e K_v (T_s - T_b) \Rightarrow K_v = \frac{L\frac{\Delta m}{\Delta t}}{A_e(T_s - T_b)}$$

$$K_v(270\ \mu bar) = \frac{L\frac{\Delta m}{\Delta t}}{A_e(T_s - T_b)}$$

L is the latent heat of sublimation of ice (2844 J·g^{-1} or 679.7 cal ·g^{-1}) and A_e is external cross-sectional area of the base of the TVIS vial (4.62 cm^2)

$$= \frac{679.7\ cal \cdot g^{-1} \times 0.42\ g \cdot h^{-1}}{4.62\ cm^2 \times (273.3 - 243.3)K}$$

$$= 2.06\ cal \cdot h^{-1} \cdot cm^{-2} \cdot K^{-1}$$

$$= 5.73 \times 10^{-4} cal \cdot s^{-1} \cdot cm^{-2} \cdot K^{-1}$$

$$K_v(270\ \mu bar) = 5.73 \times 10^{-4} cal \cdot s^{-1} \cdot cm^{-2} \cdot K^{-1}$$

Through Vial Impedance Spectroscopy (TVIS)

End-point Determination

End–Point Determination (T_s-15 °C and P_c 400 µbar)

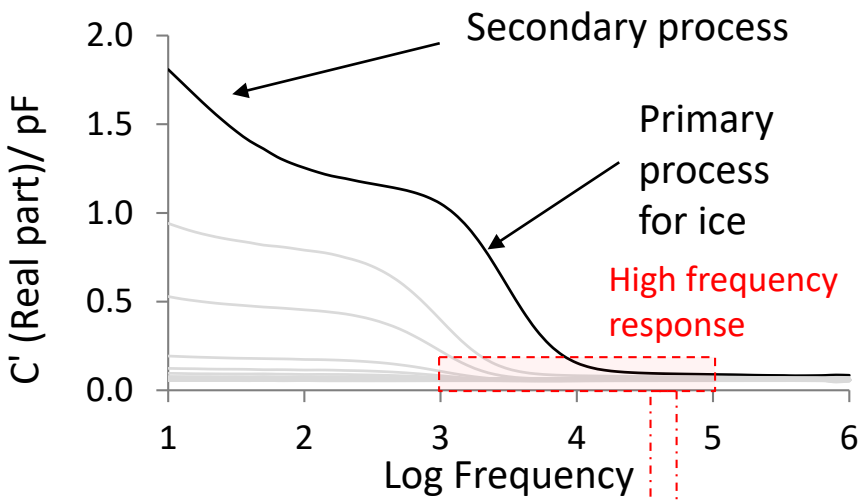

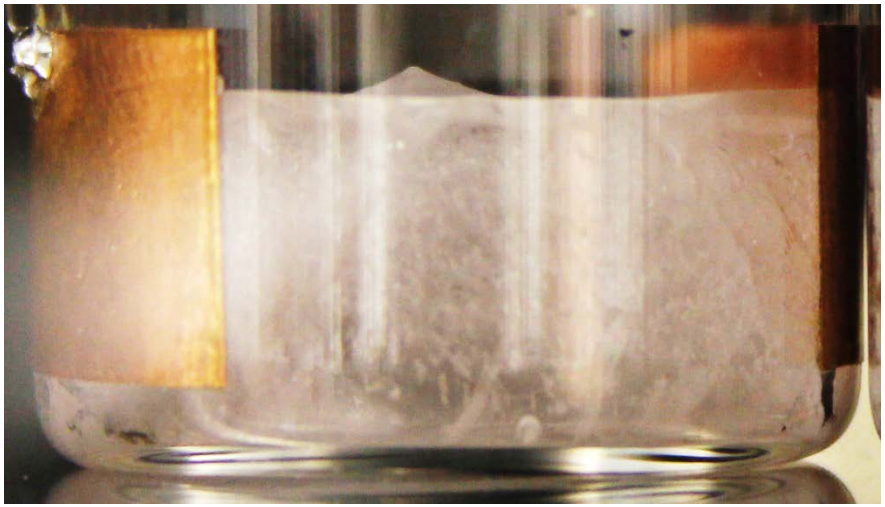

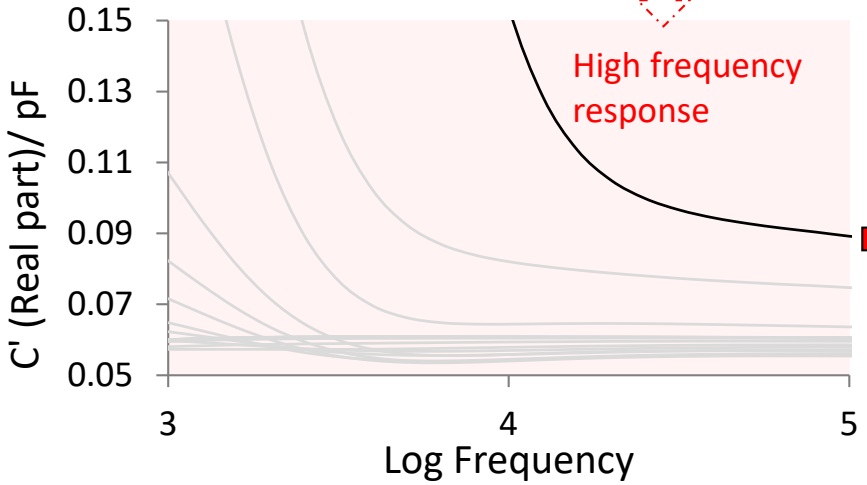

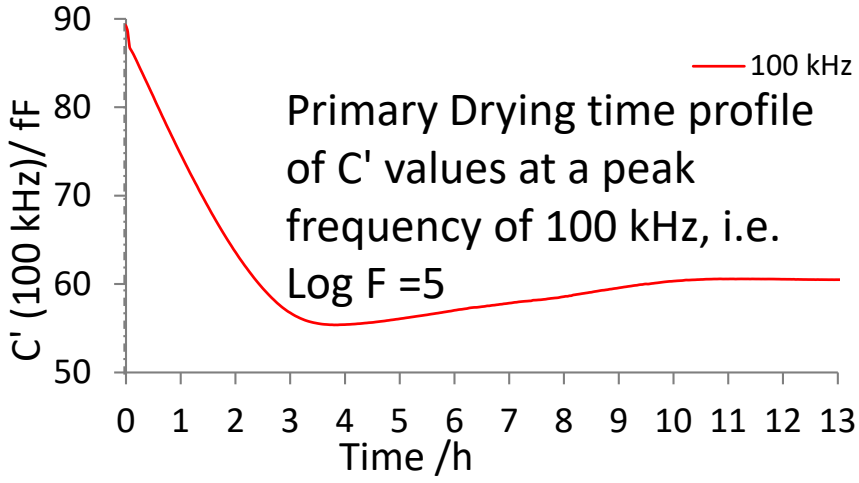

End–Point Determination (T_s-15 °C and P_c 400 µbar)

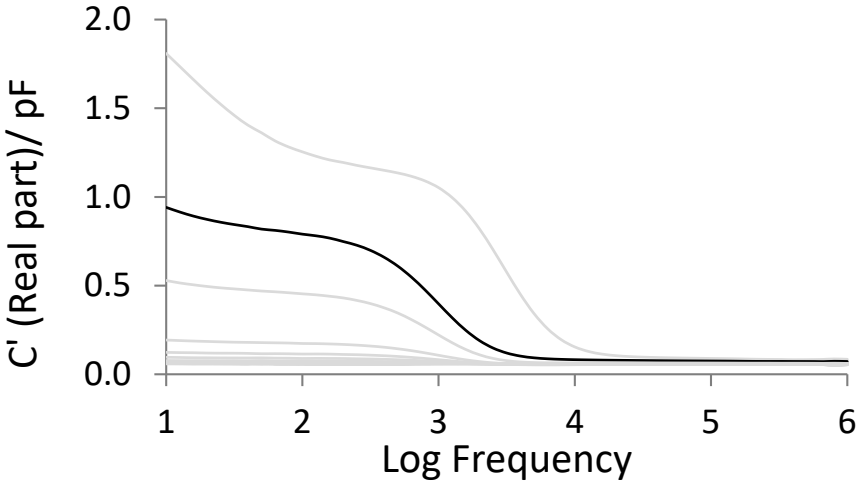

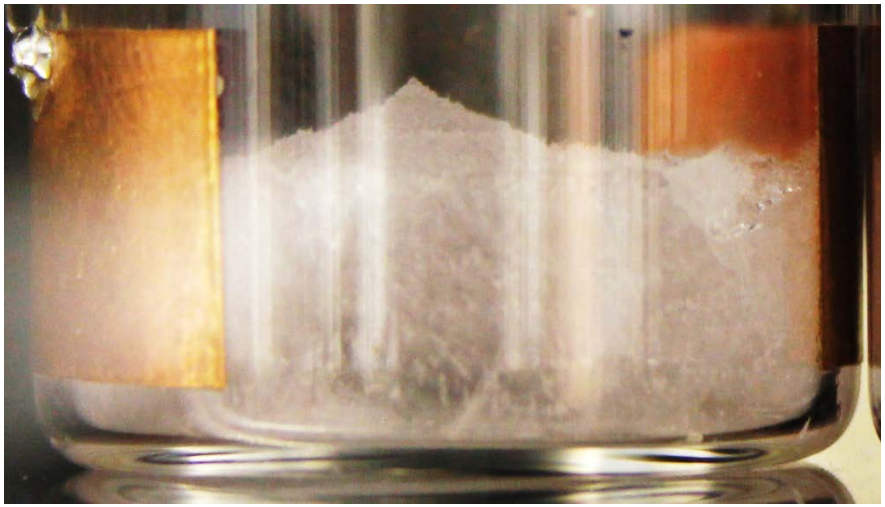

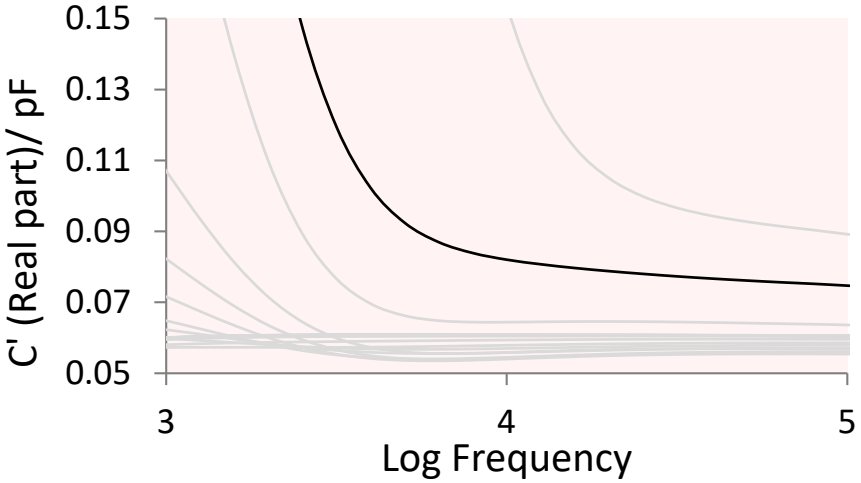

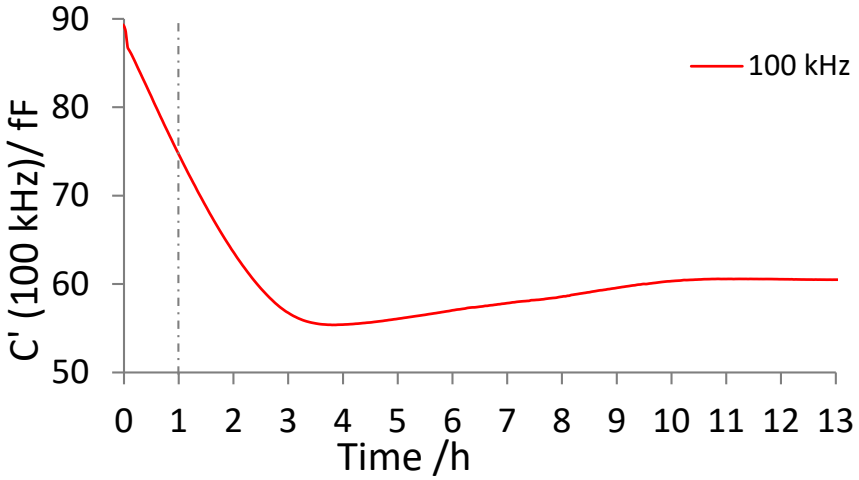

End–Point Determination (T_s-15 °C and P_c 400 µbar)

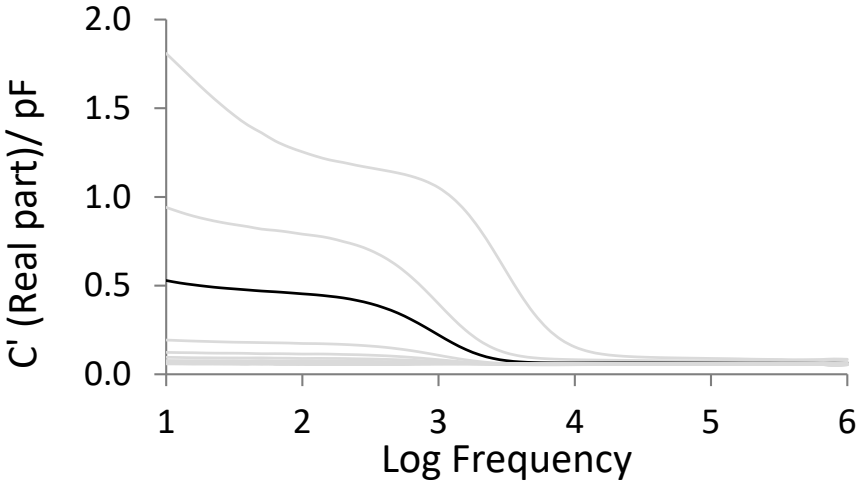

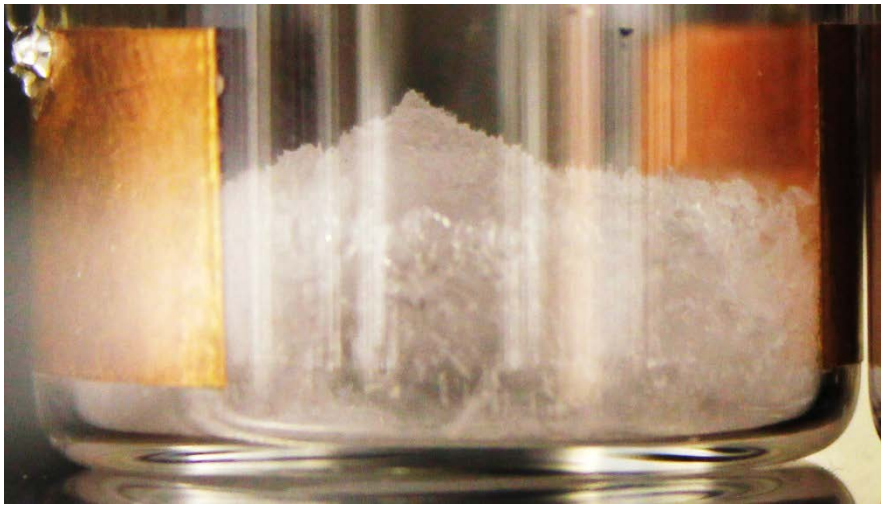

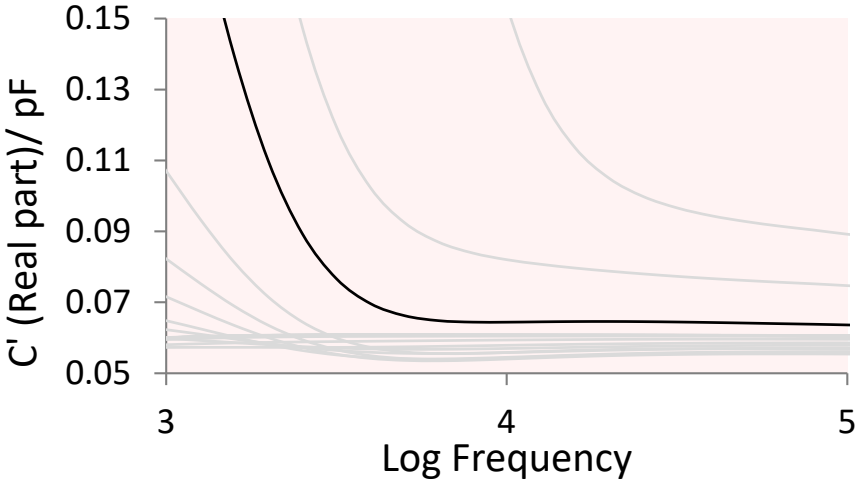

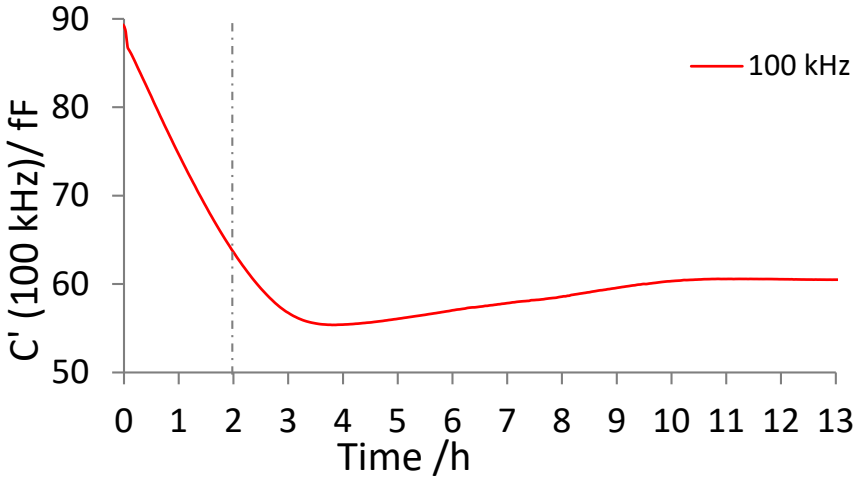

End–Point Determination (T_s-15 °C and P_c 400 µbar)

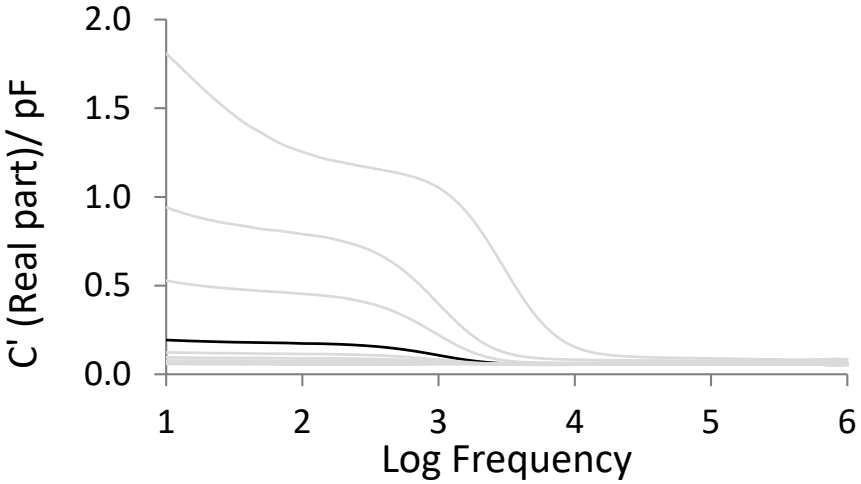

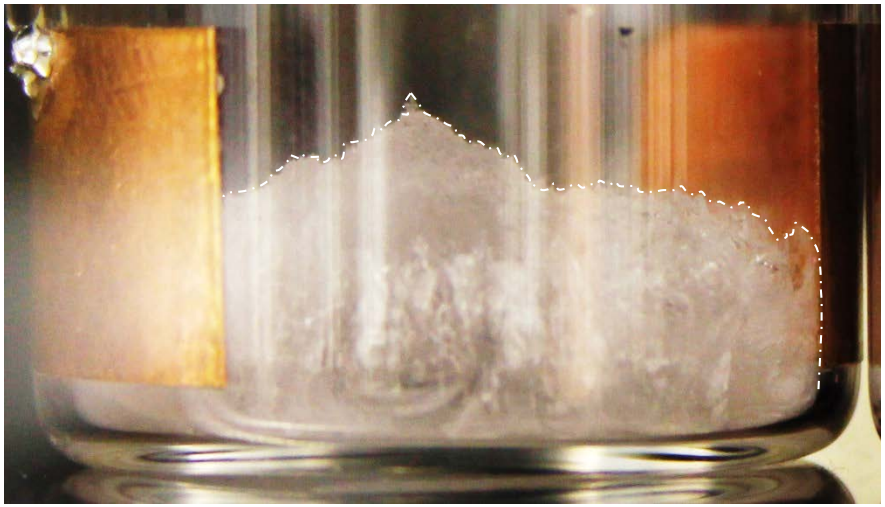

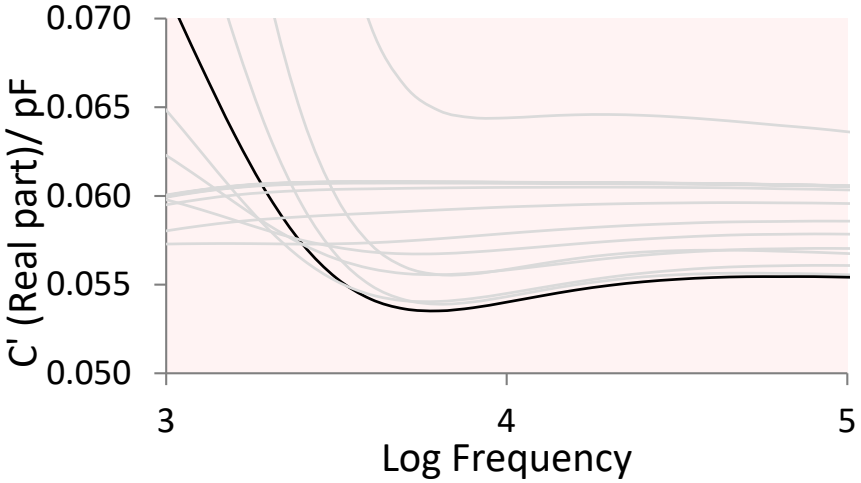

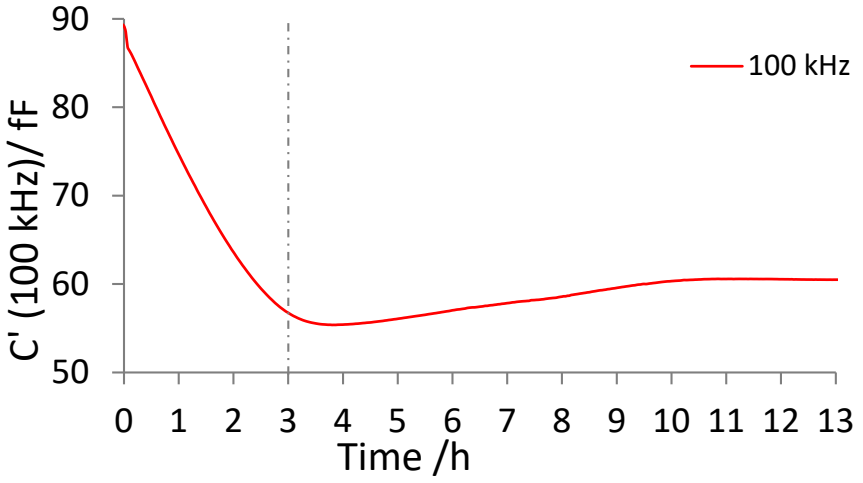

End–Point Determination (T_s-15 °C and P_c 400 µbar)

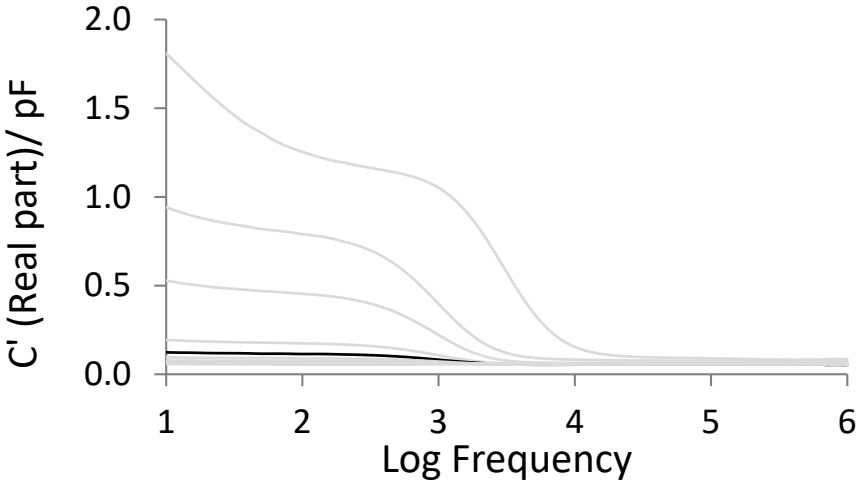

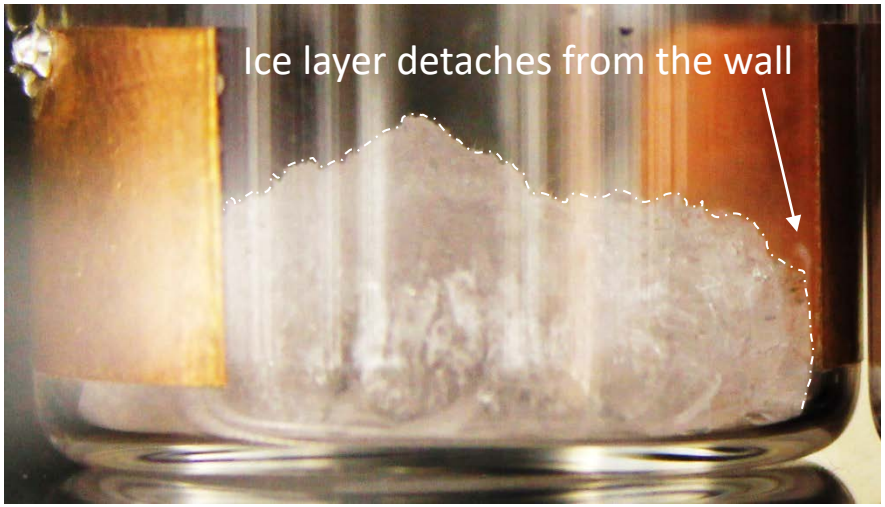

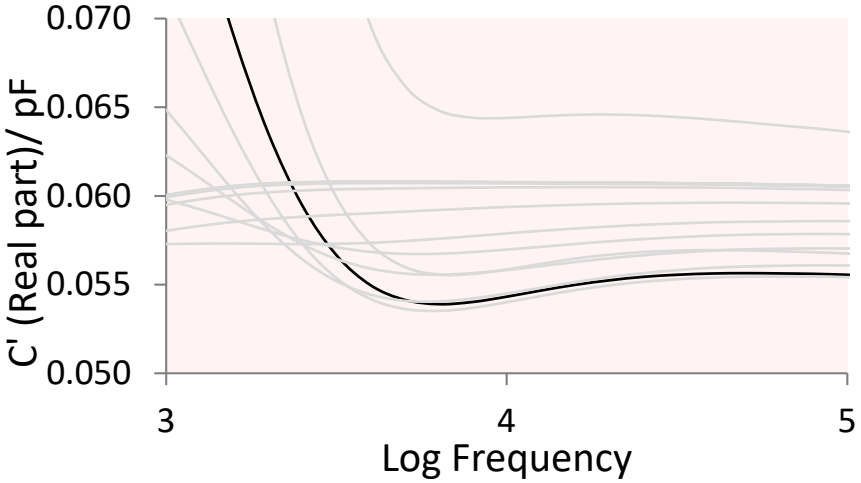

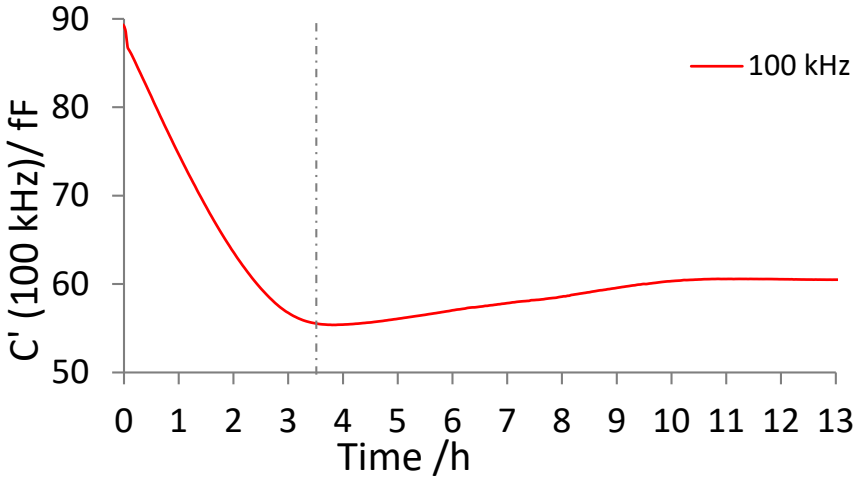

End–Point Determination (T_s-15 °C and P_c 400 µbar)

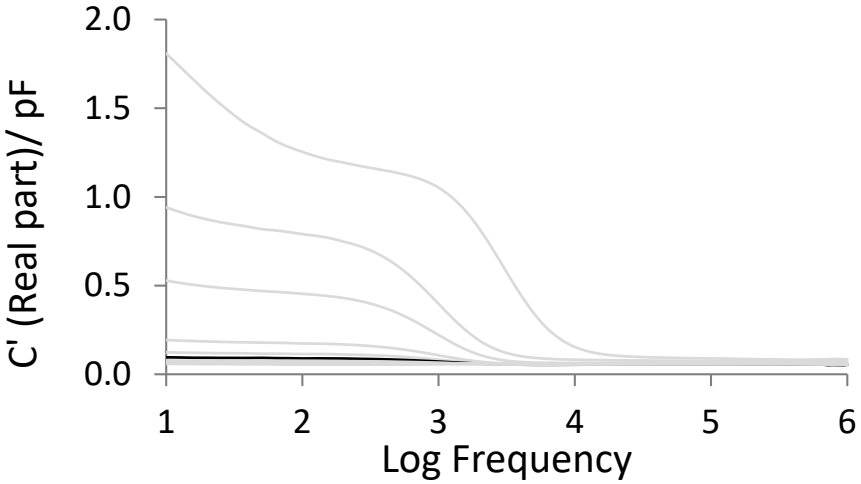

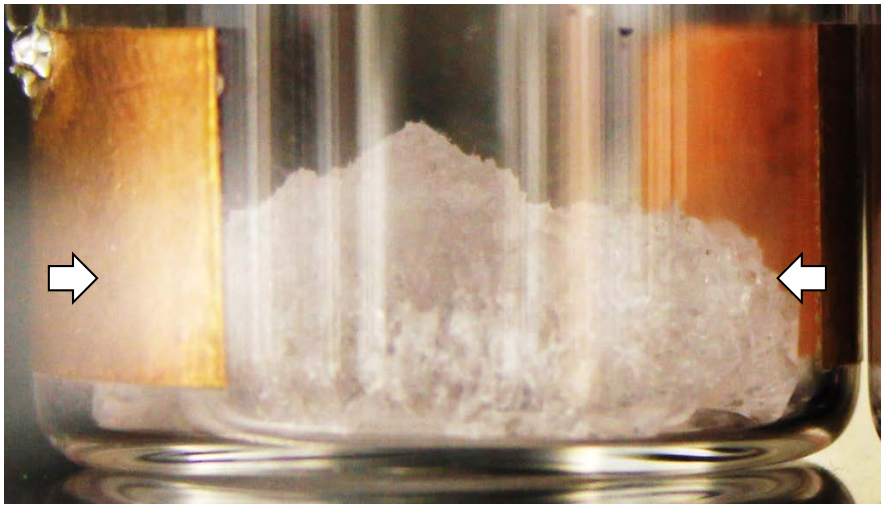

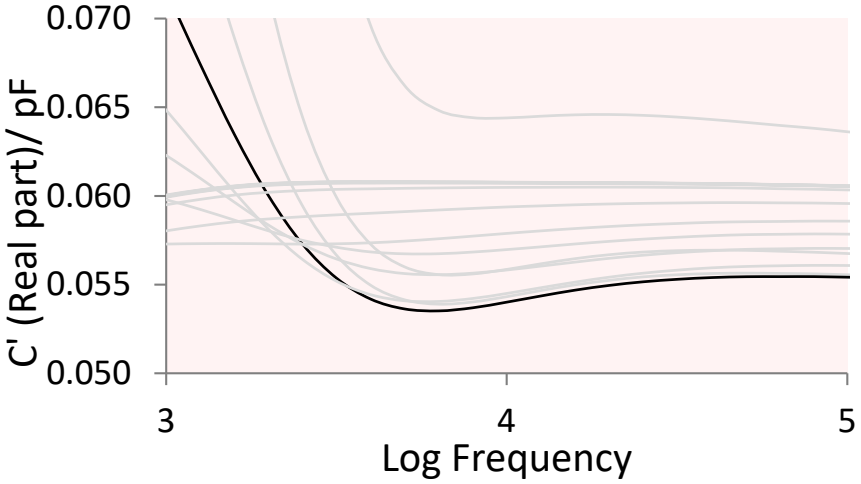

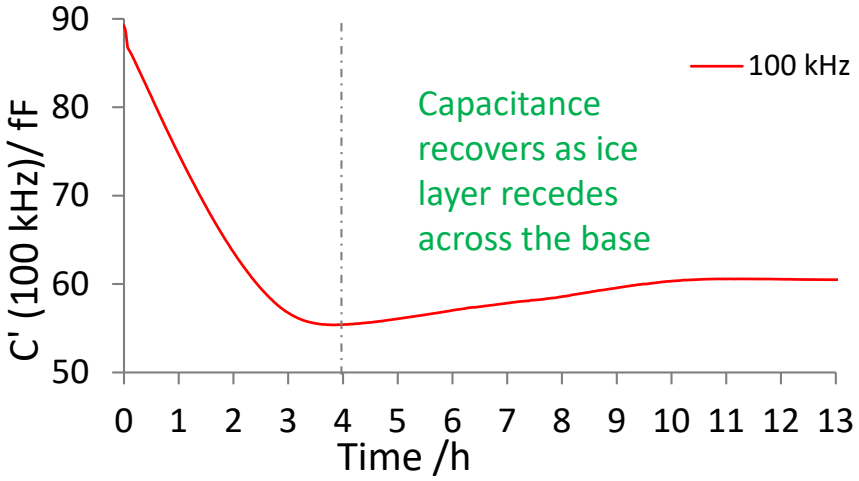

End–Point Determination (T_s-15 °C and P_c 400 µbar)

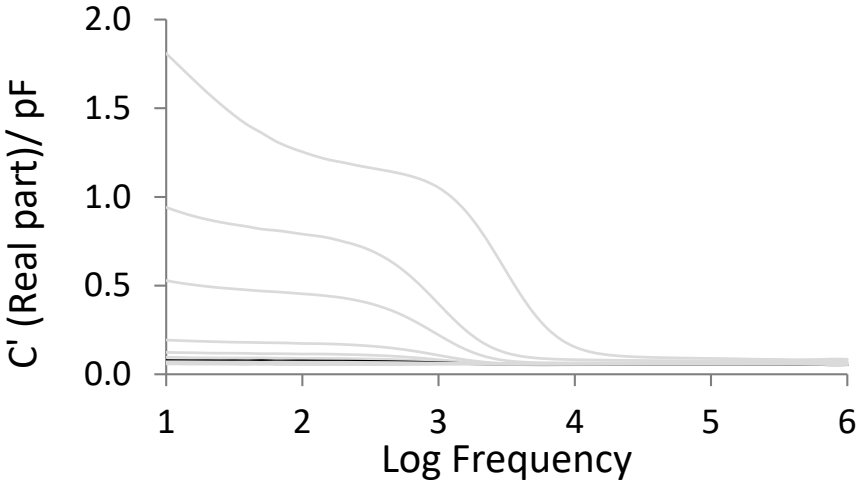

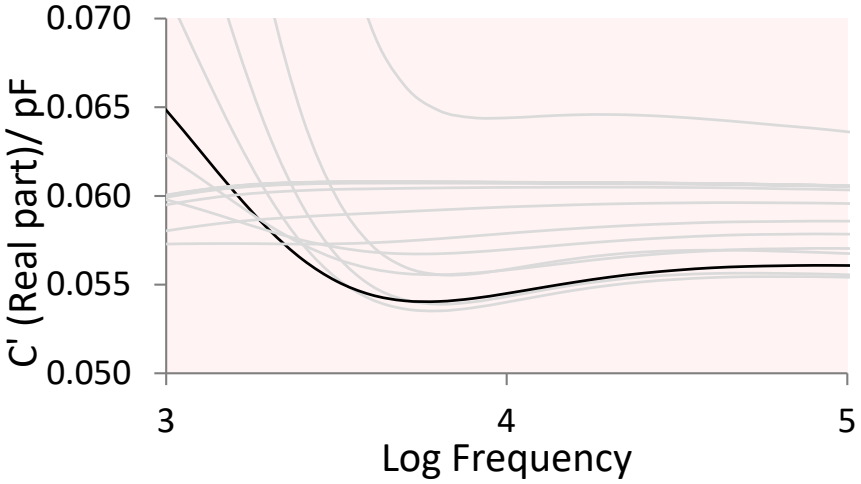

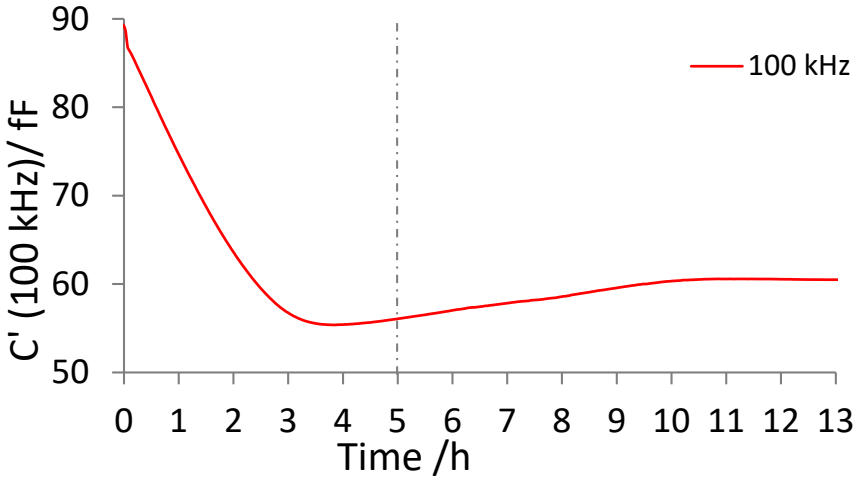

End–Point Determination (T_s-15 °C and P_c 400 µbar)

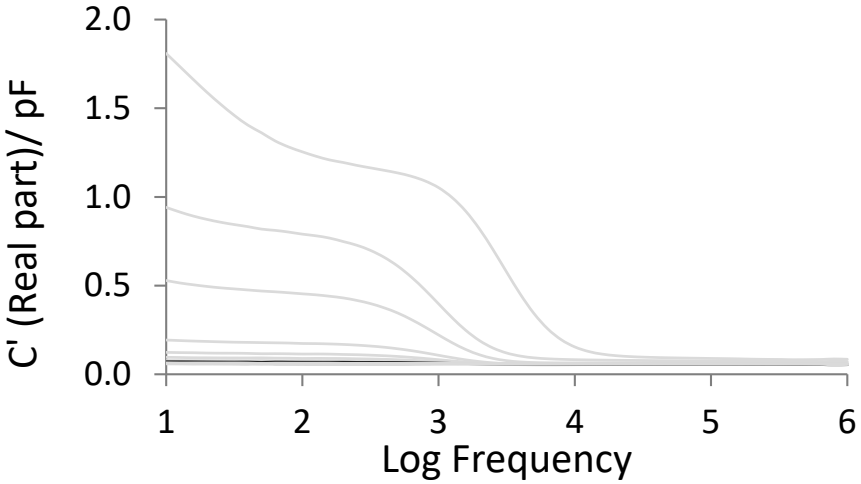

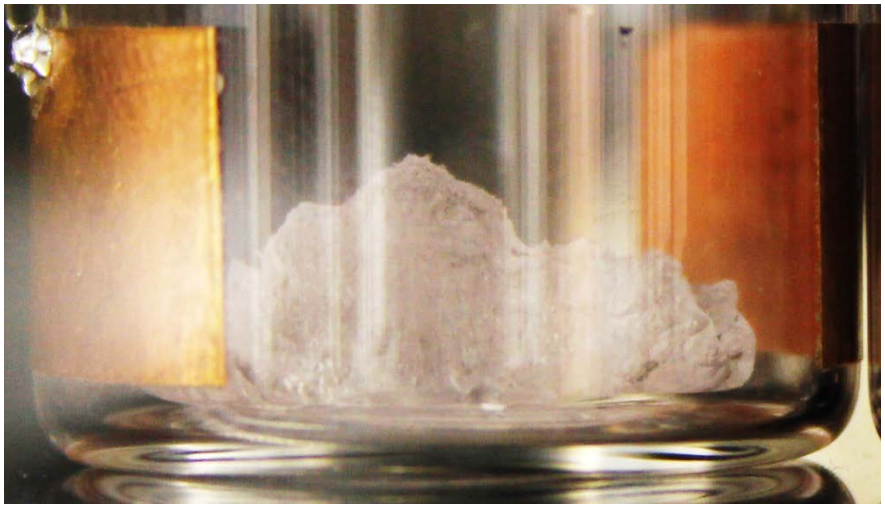

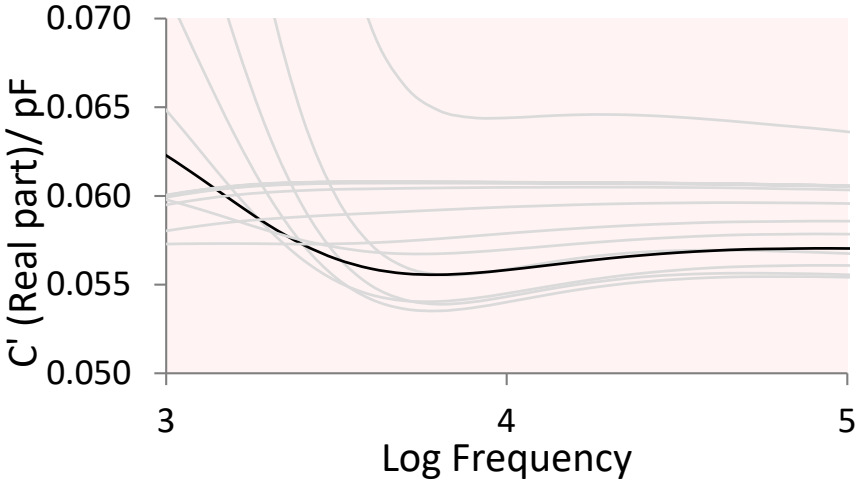

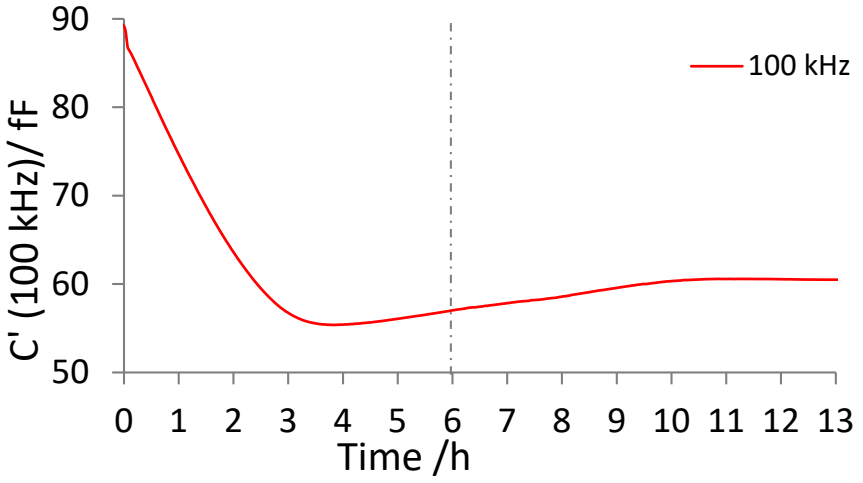

End–Point Determination (T_s-15 °C and P_c 400 µbar)

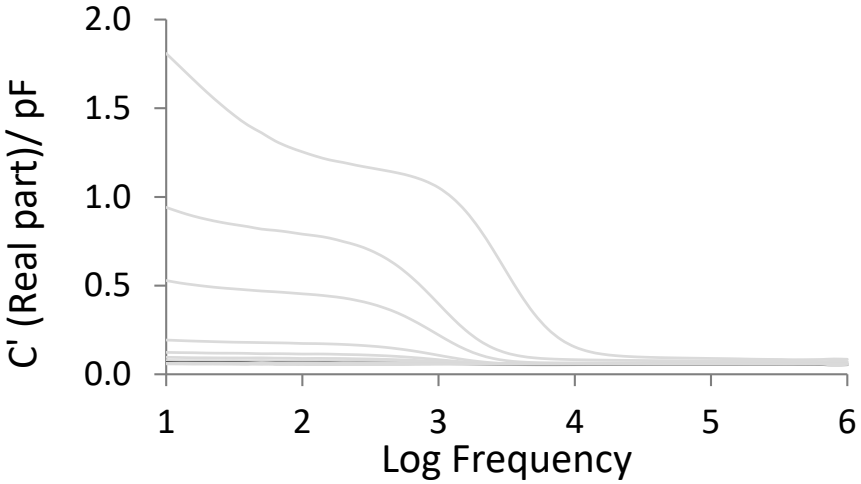

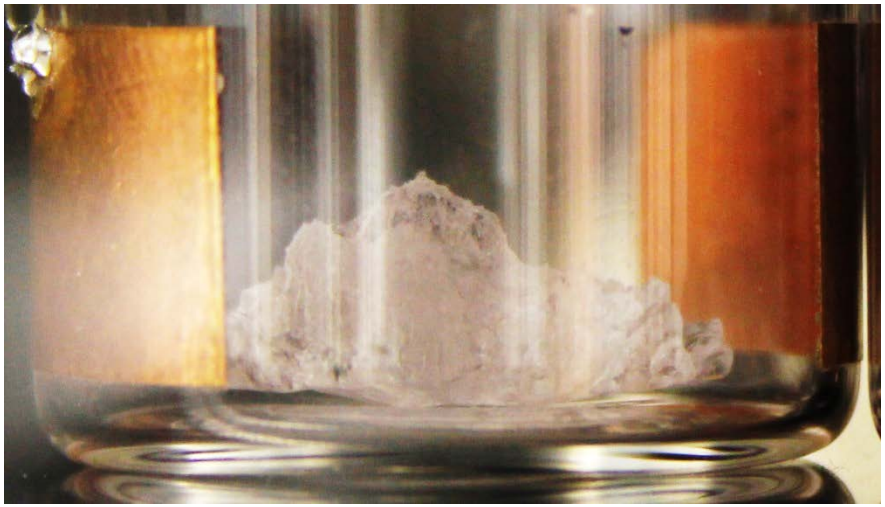

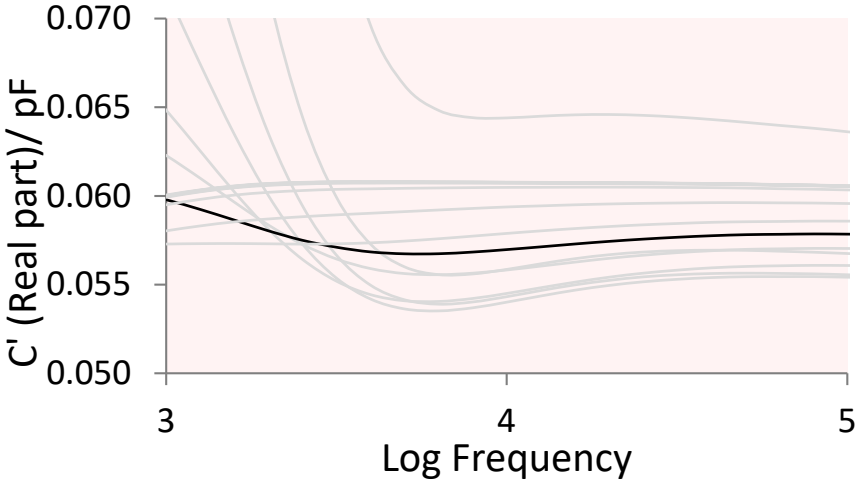

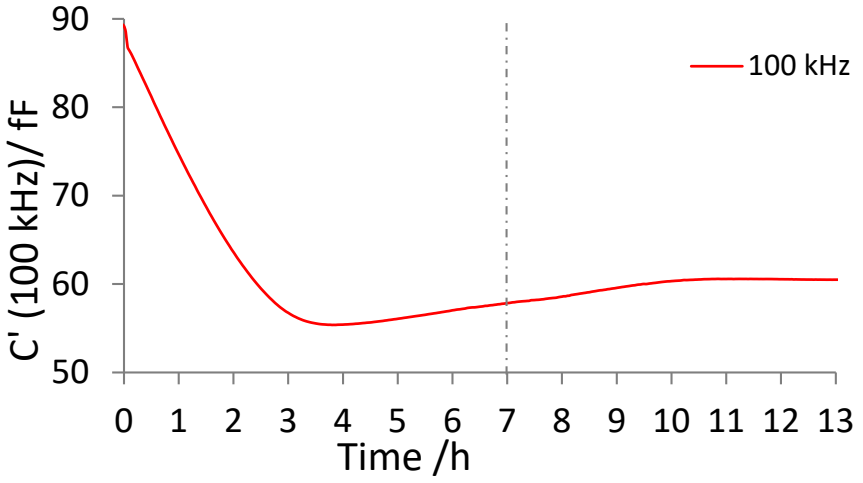

End–Point Determination (T_s-15 °C and P_c 400 µbar)

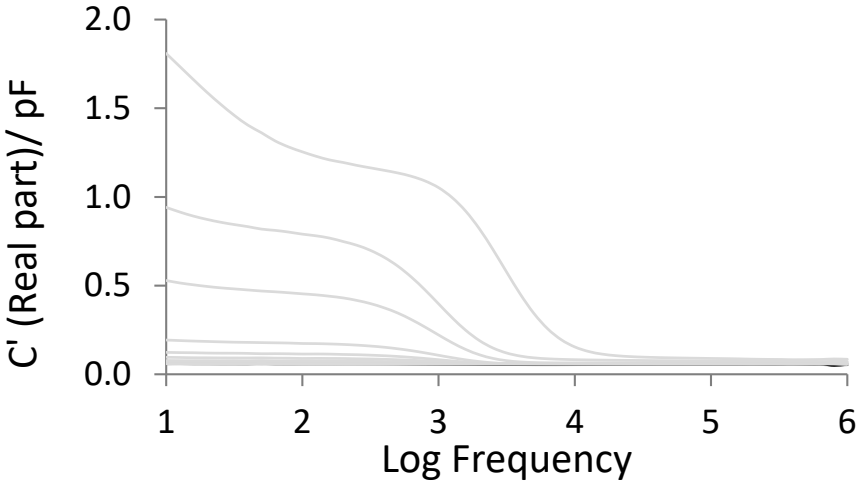

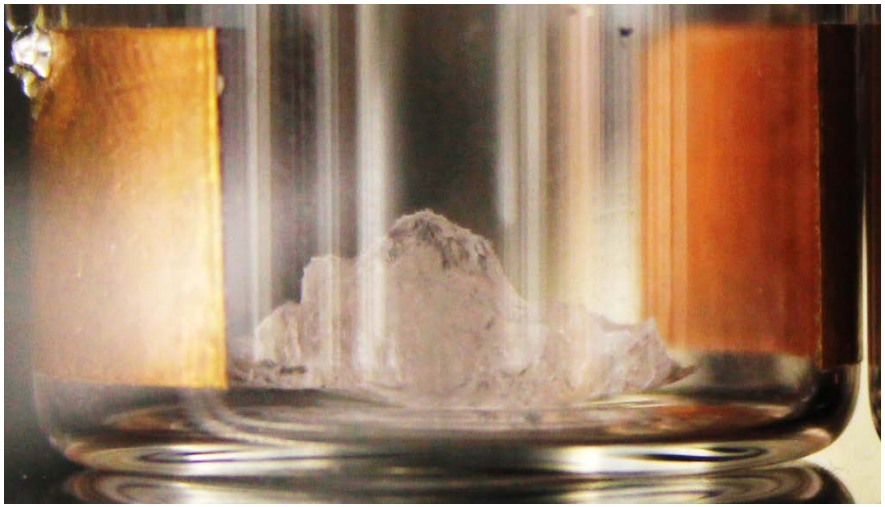

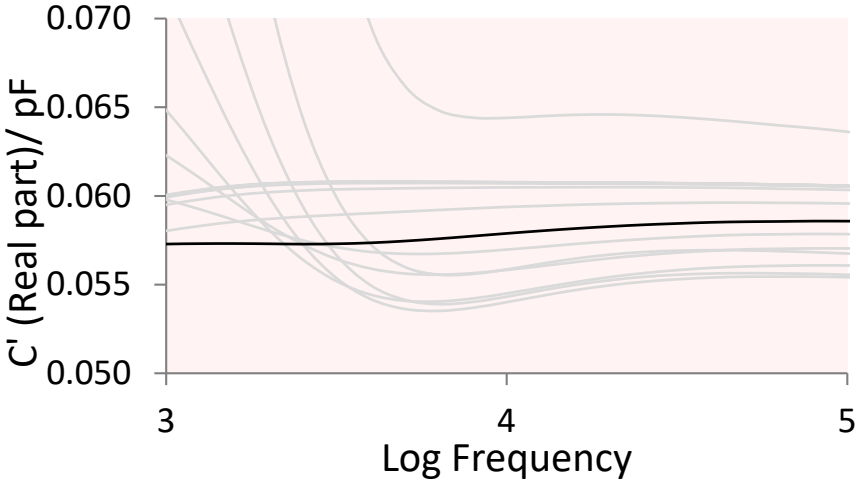

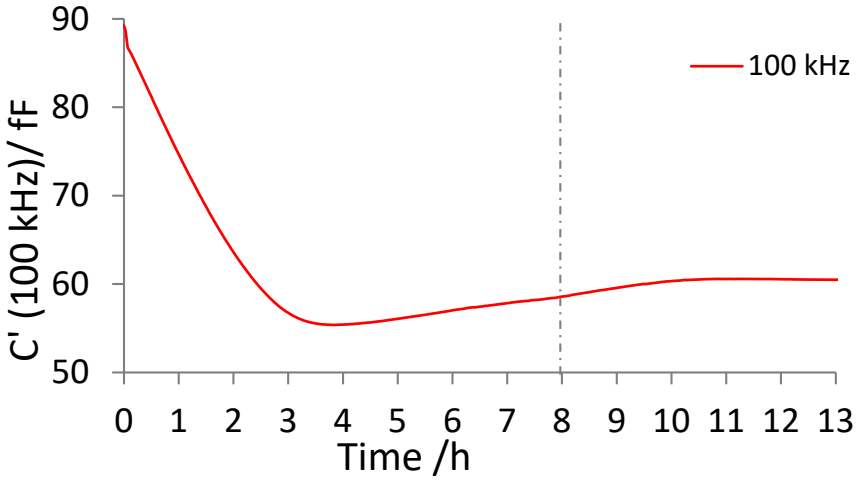

End–Point Determination (T_s-15 °C and P_c 400 µbar)

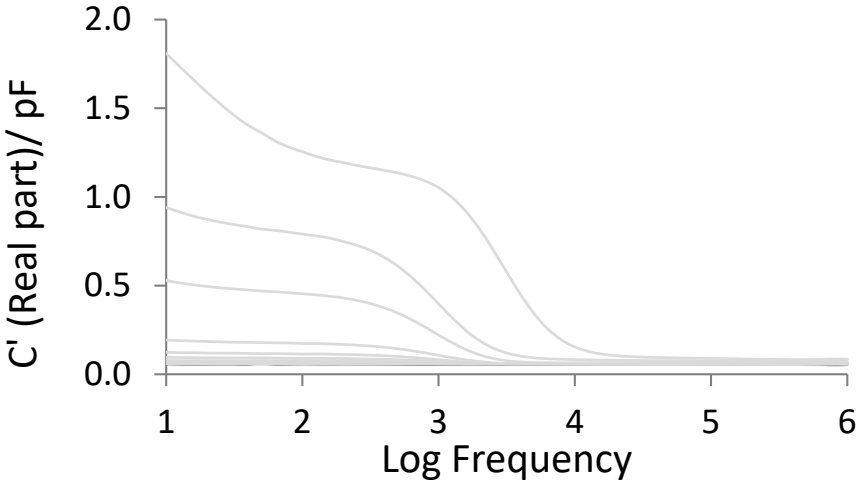

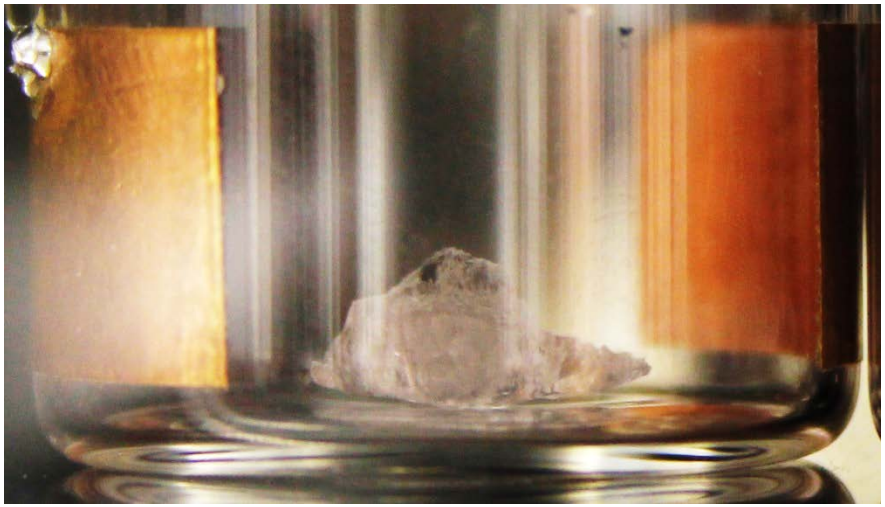

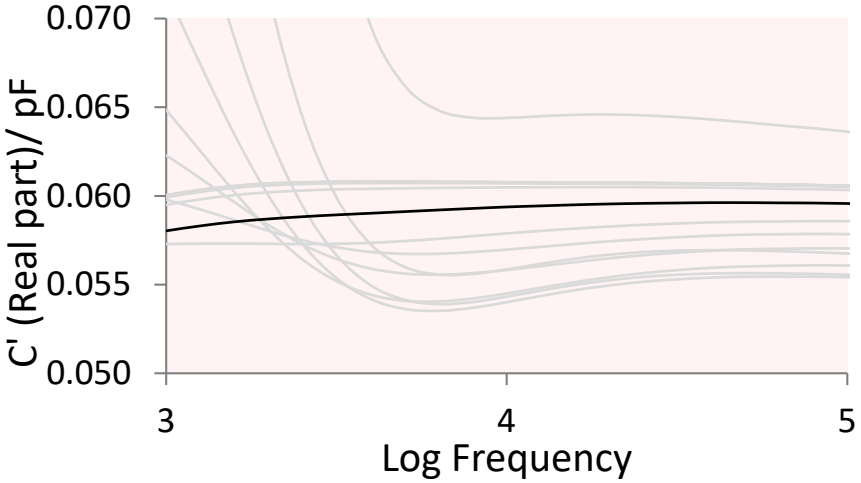

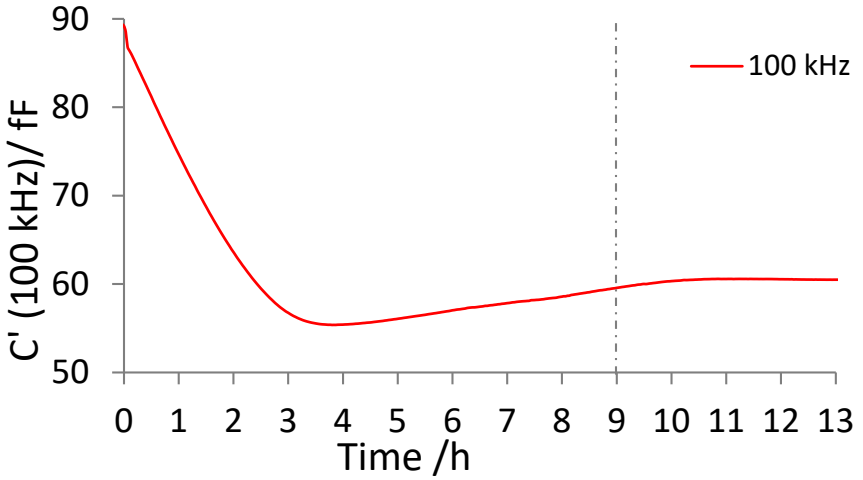

End–Point Determination (T_s-15 °C and P_c 400 µbar)

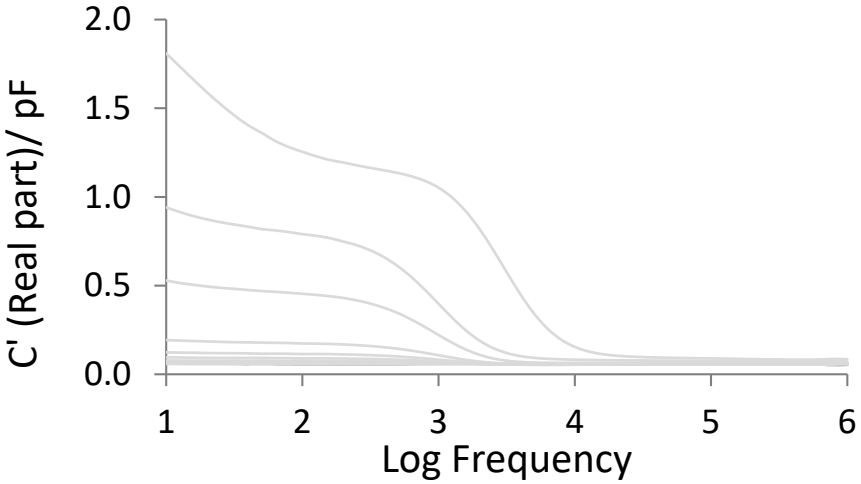

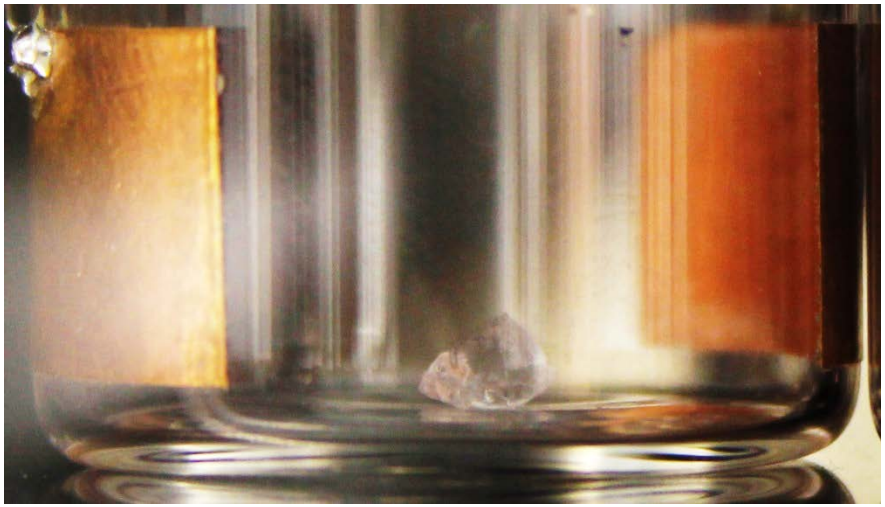

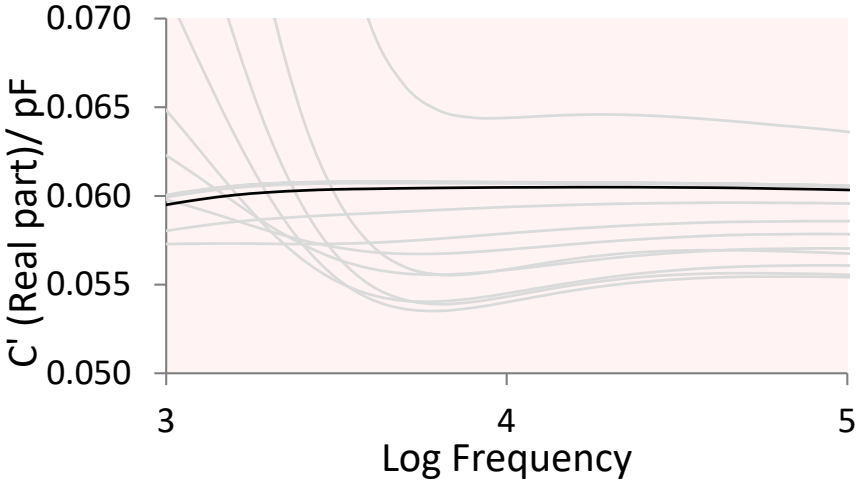

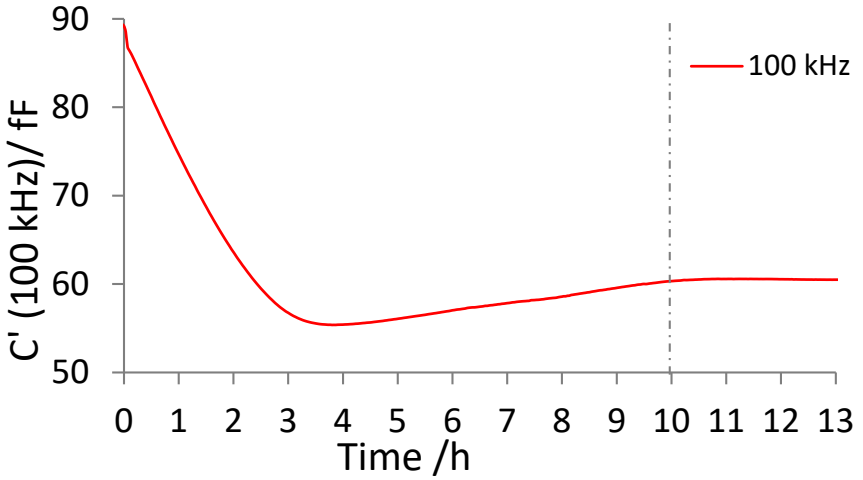

End–Point Determination (T_s-15 °C and P_c 400 µbar)

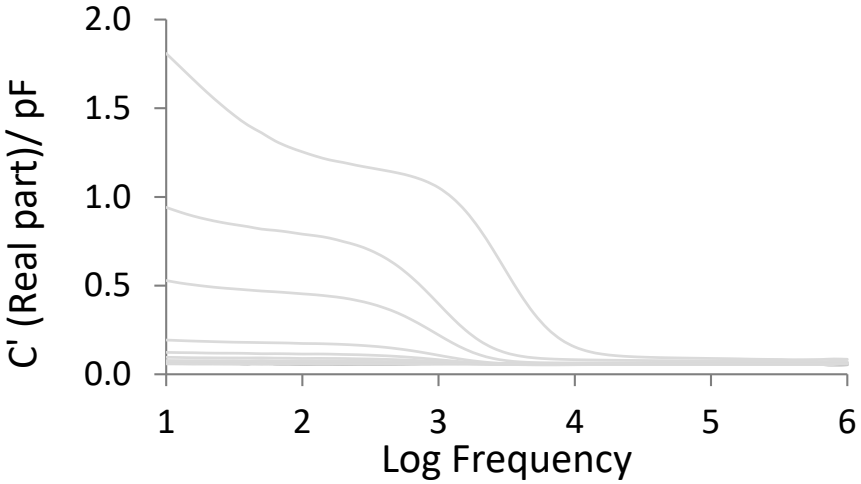

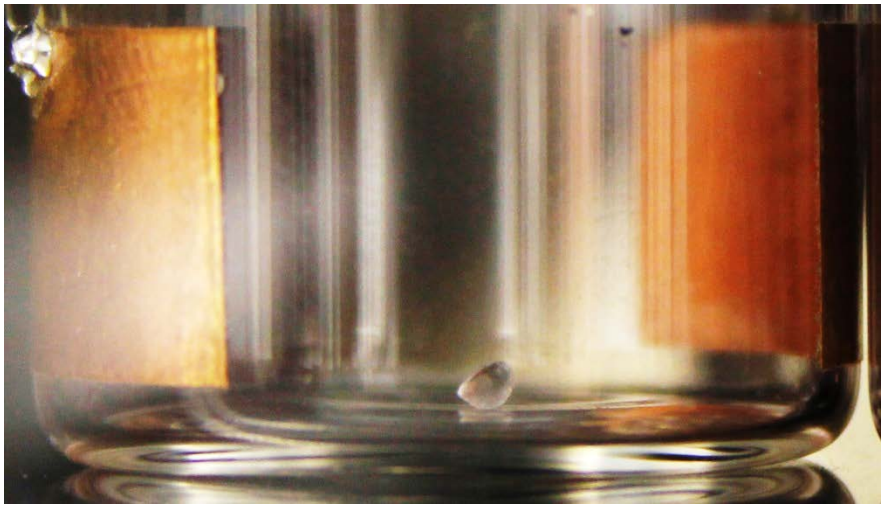

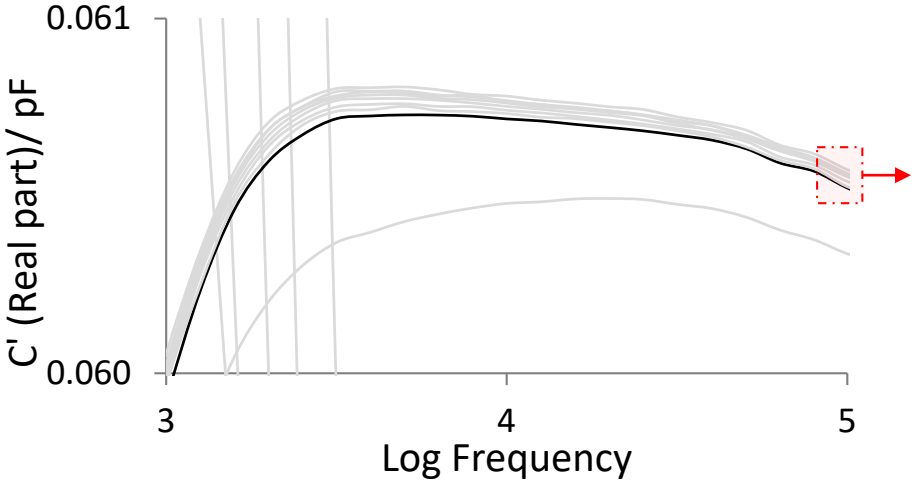

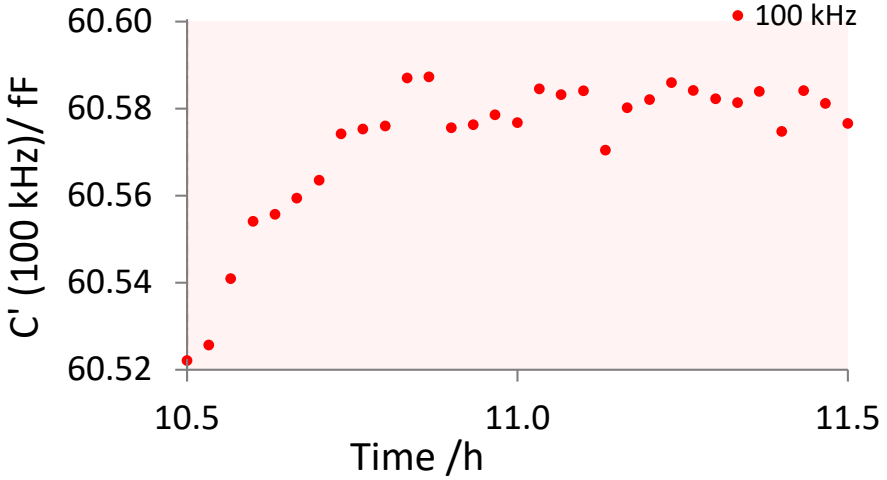

End–Point Determination (T_s-15 °C and P_c 400 µbar)

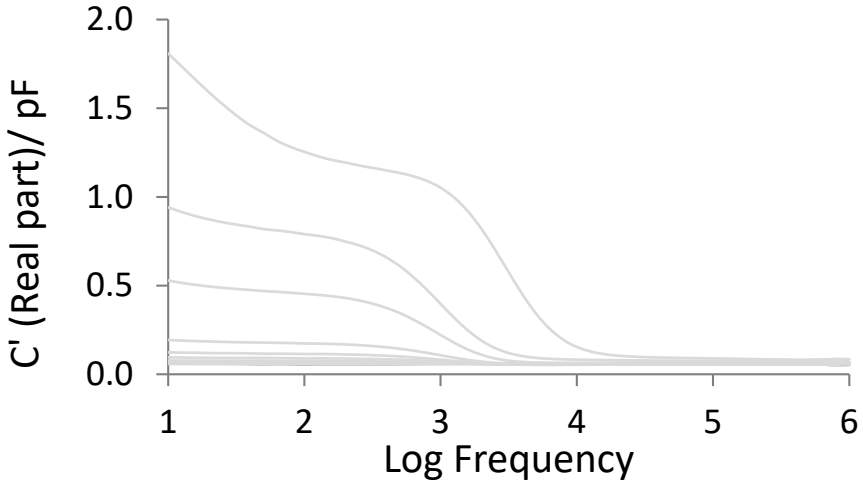

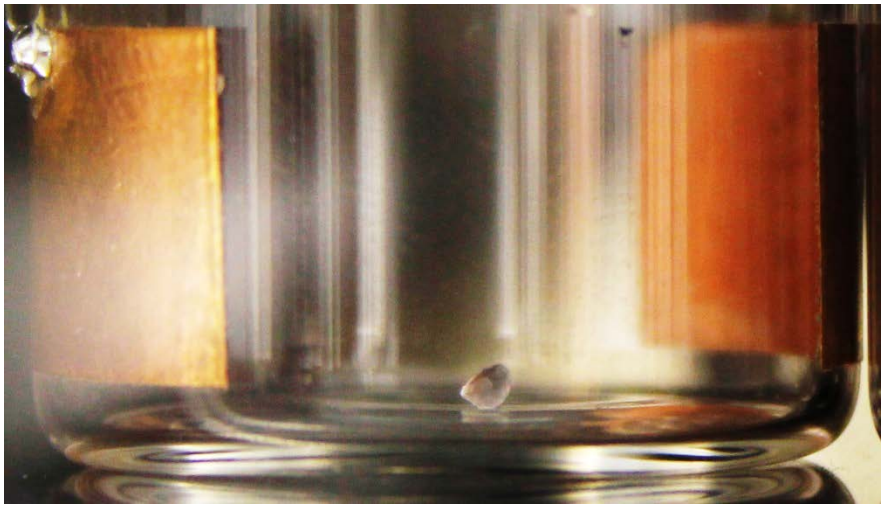

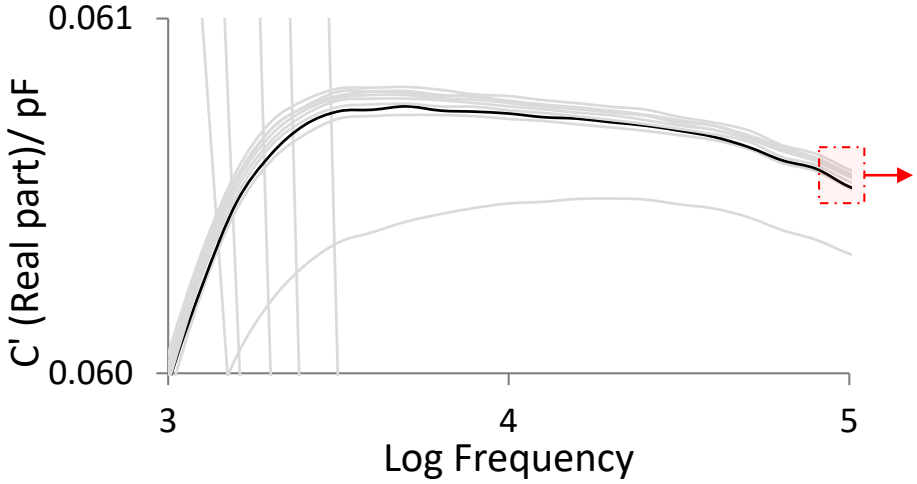

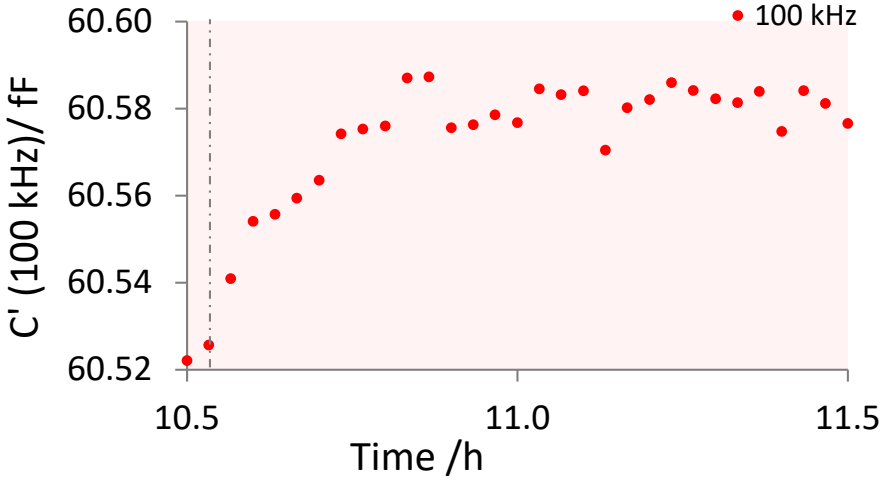

End–Point Determination (T_s-15 °C and P_c 400 µbar)

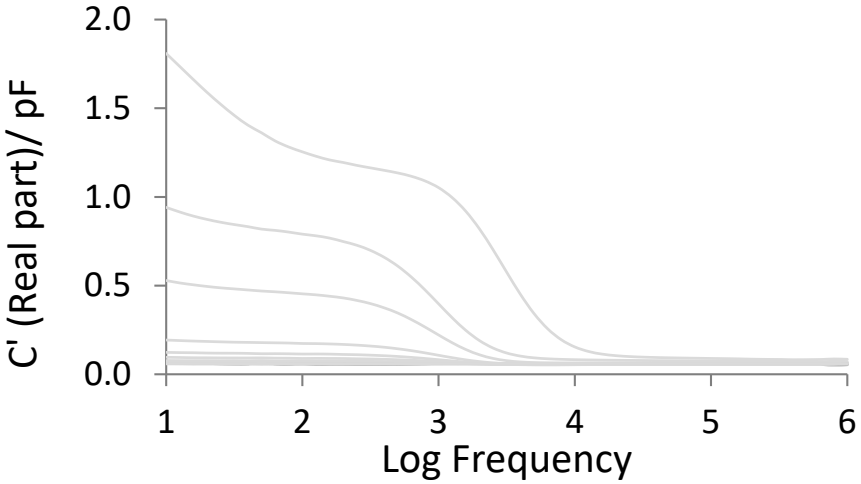

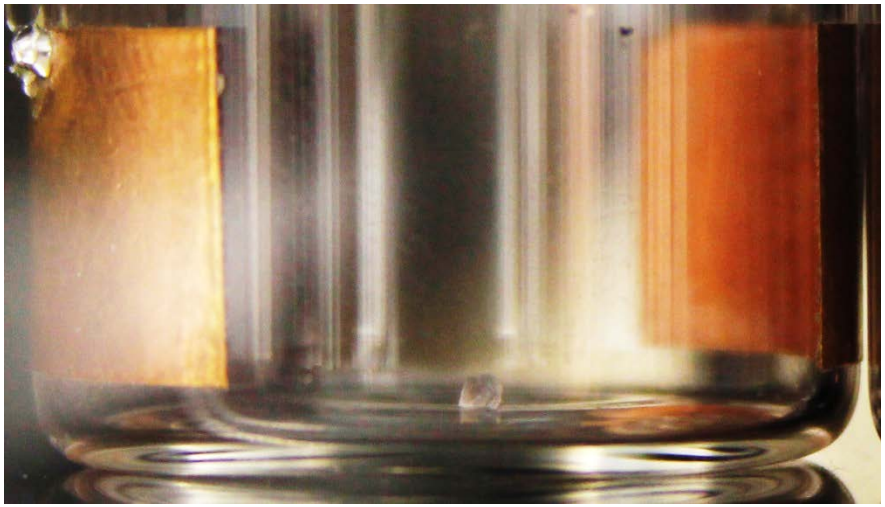

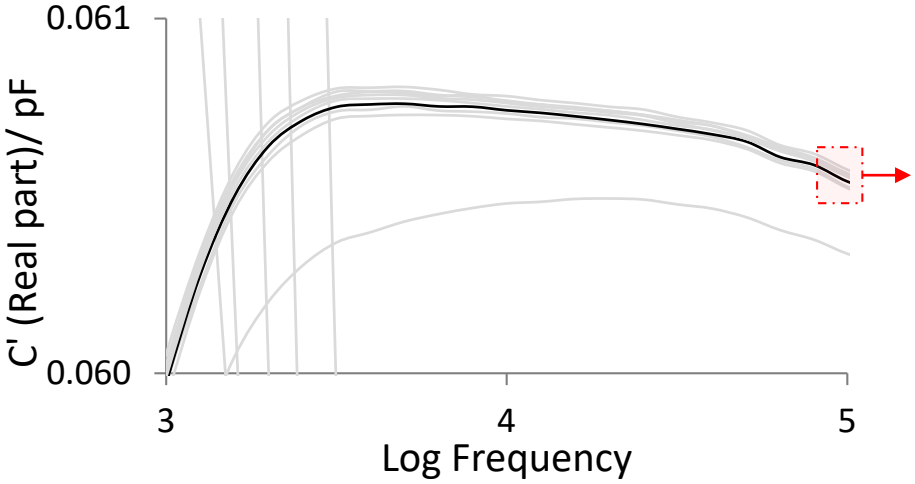

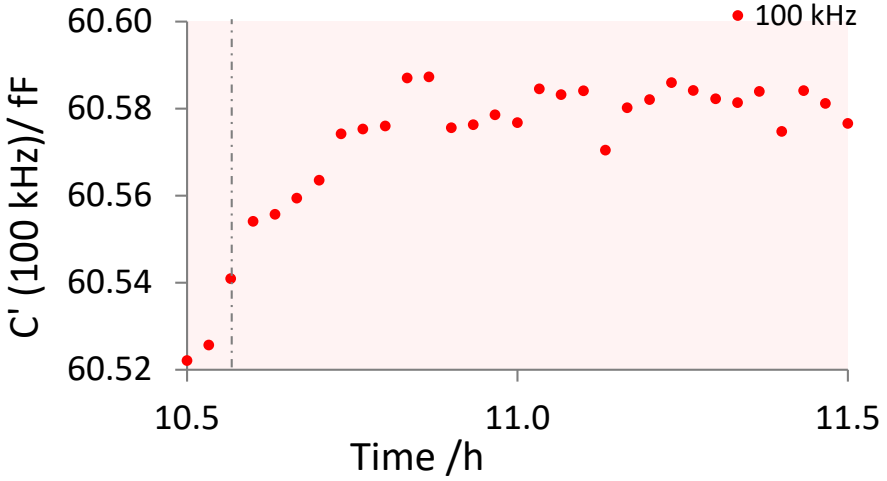

End–Point Determination (T_s-15 °C and P_c 400 µbar)

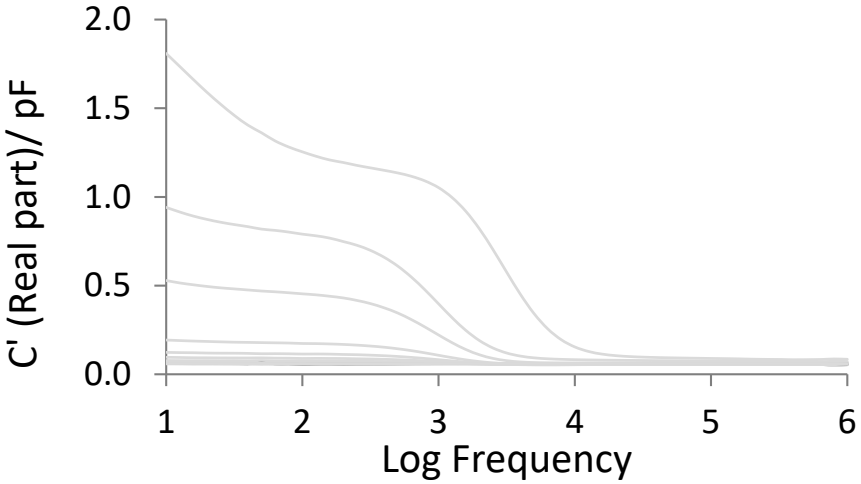

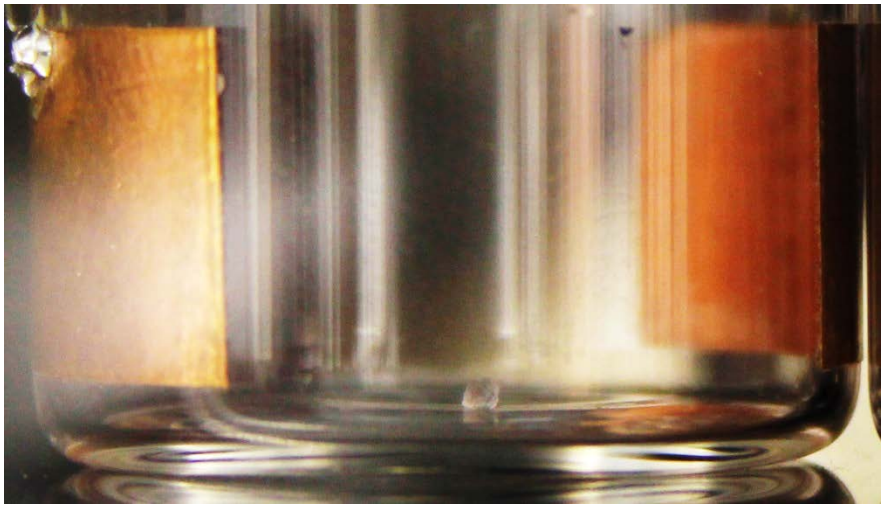

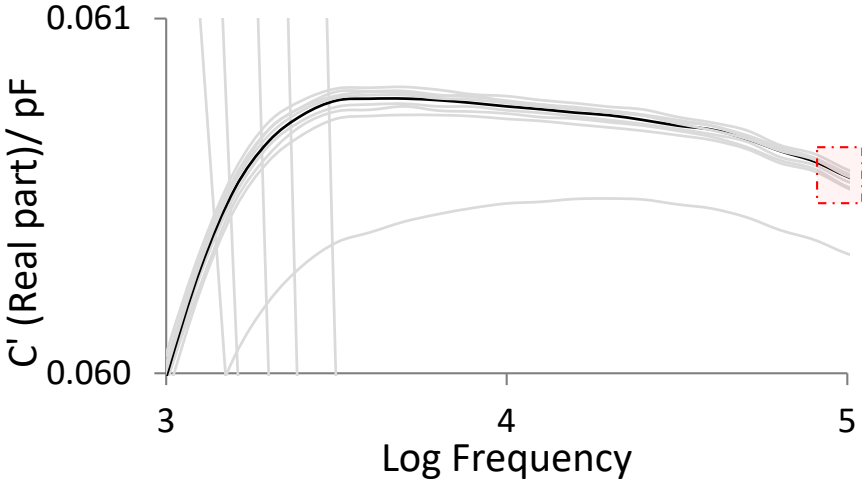

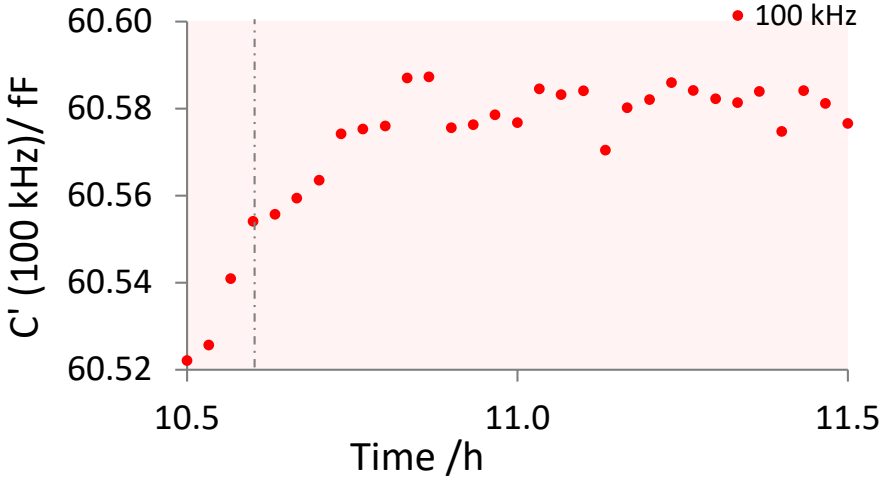

End–Point Determination (T_s-15 °C and P_c 400 µbar)

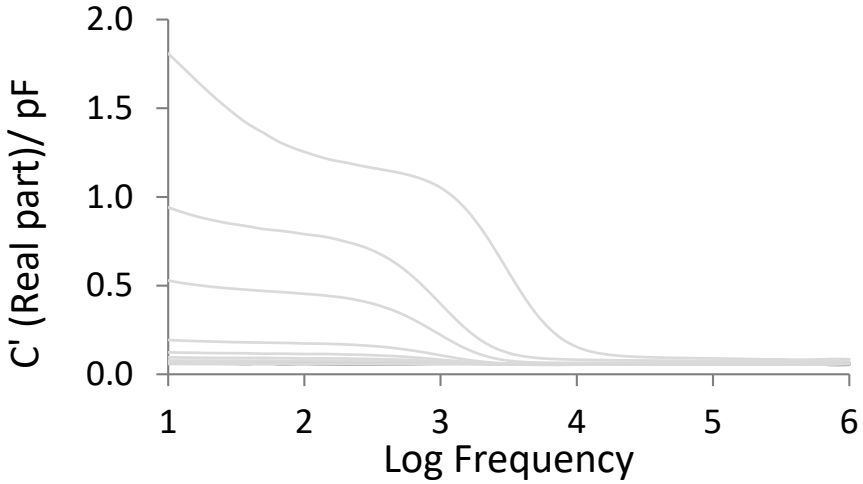

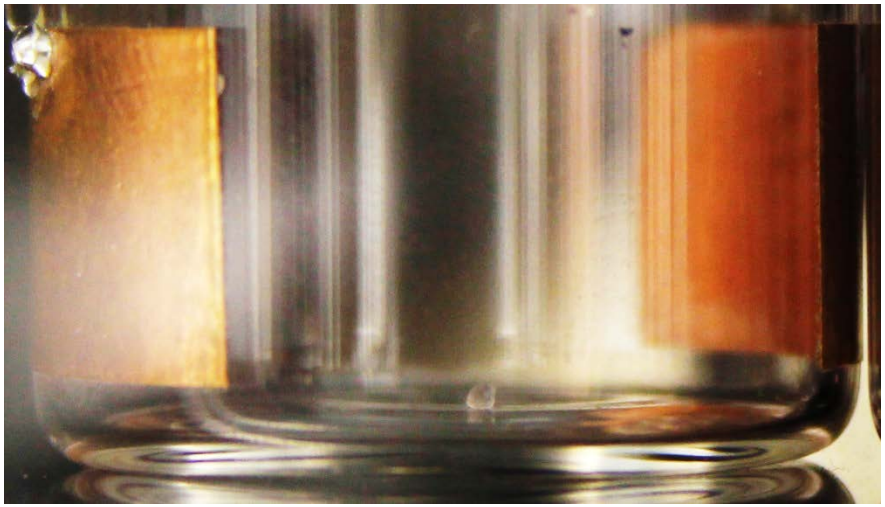

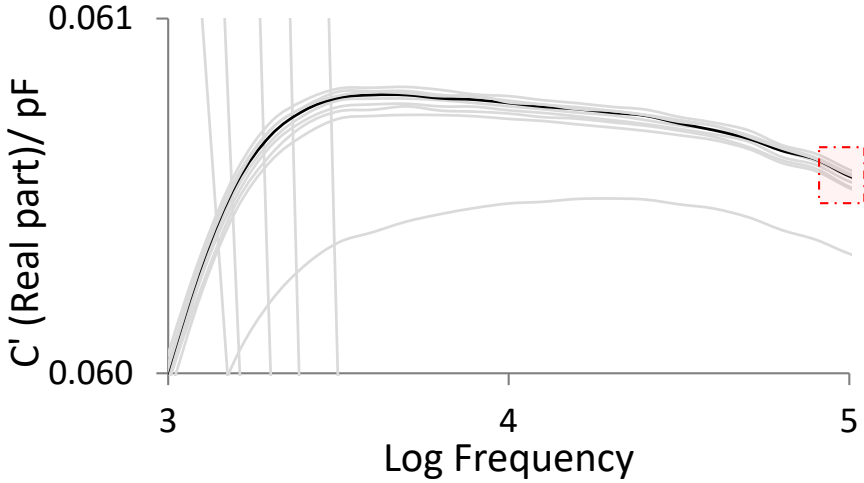

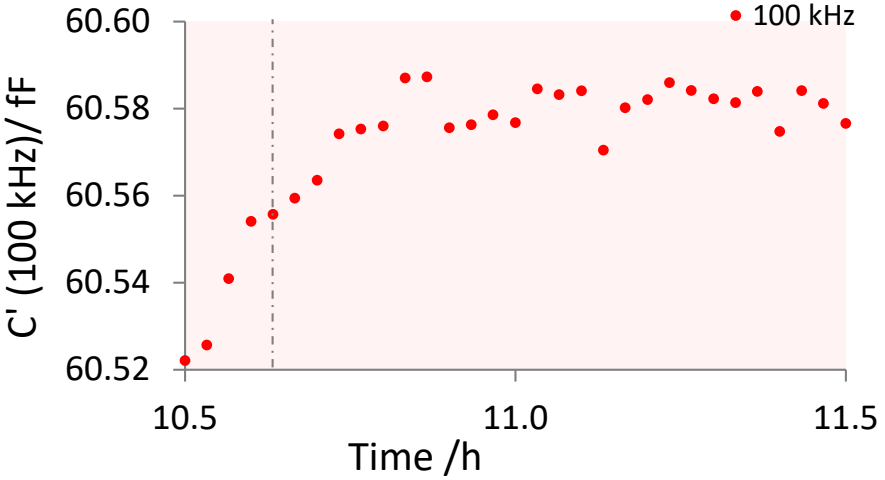

End–Point Determination (T_s-15 °C and P_c 400 µbar)

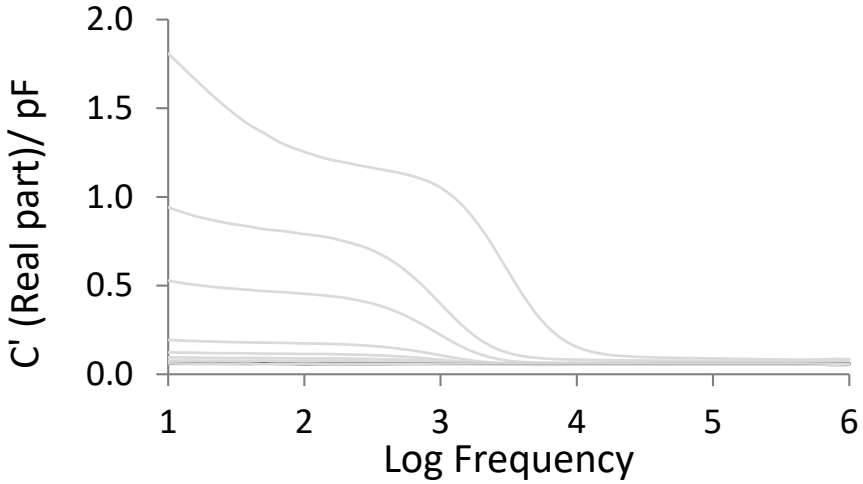

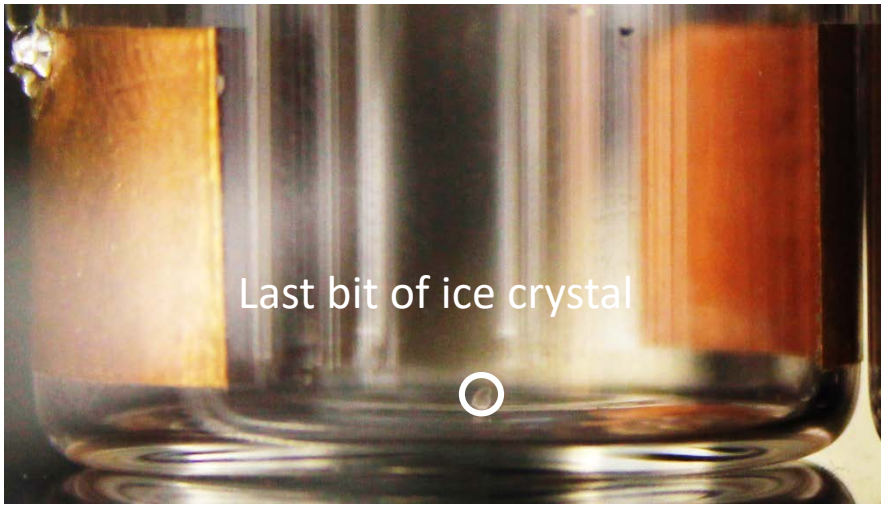

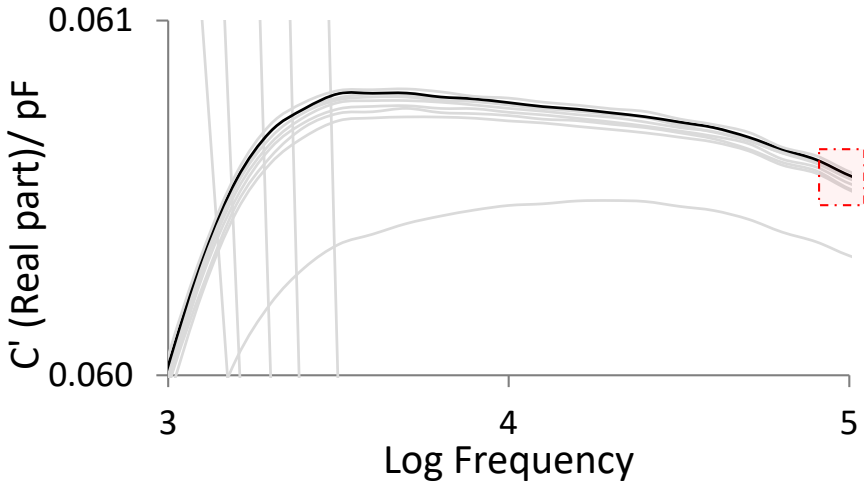

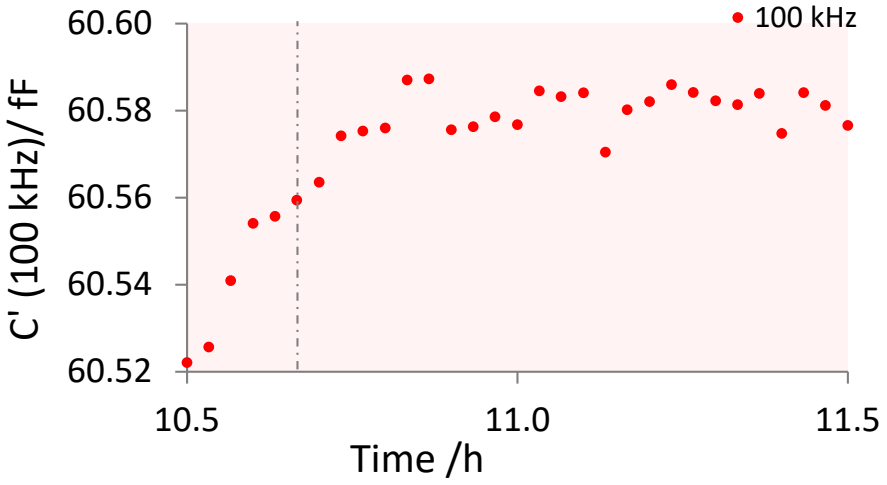

End–Point Determination (T_s-15 °C and P_c 400 µbar)

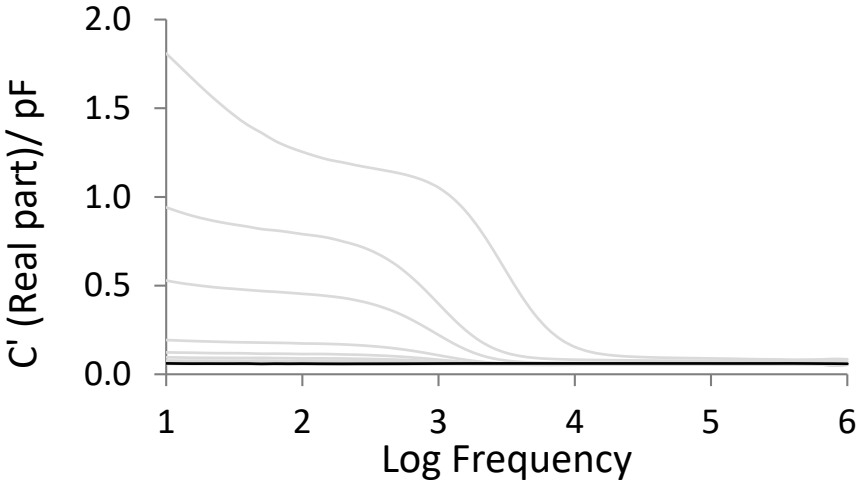

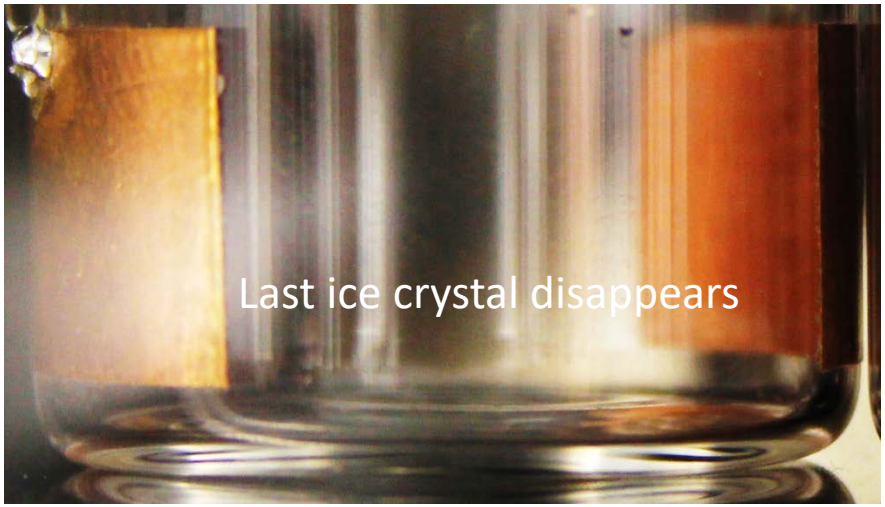

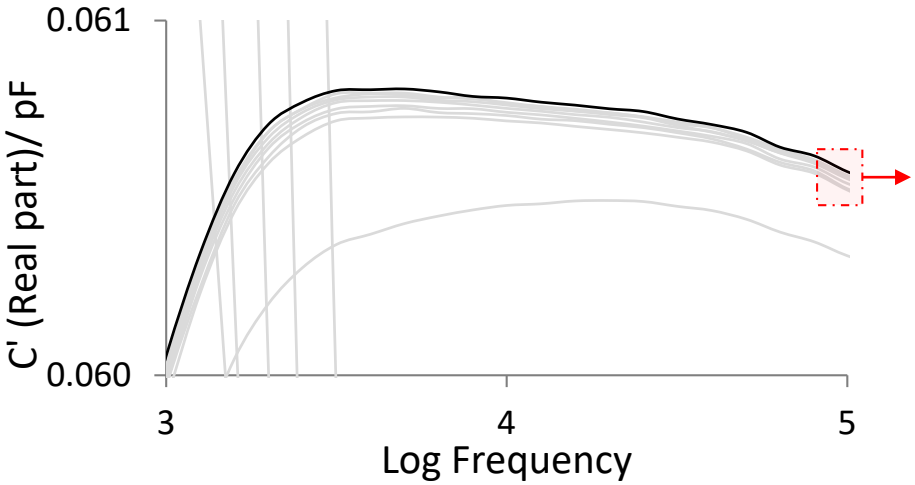

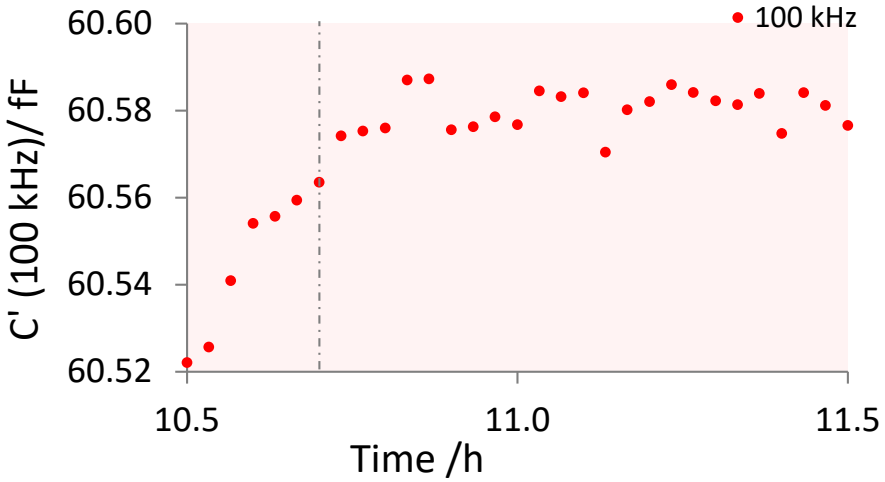

End–Point Determination (T_s-15 °C and P_c 400 µbar)

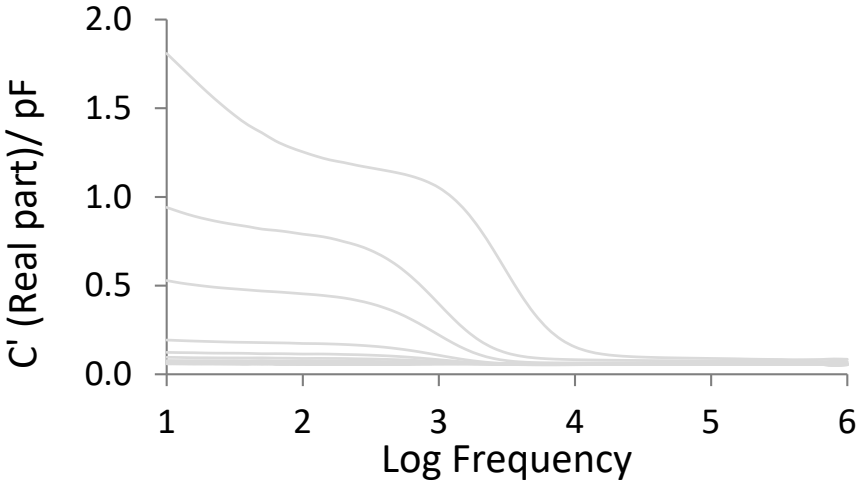

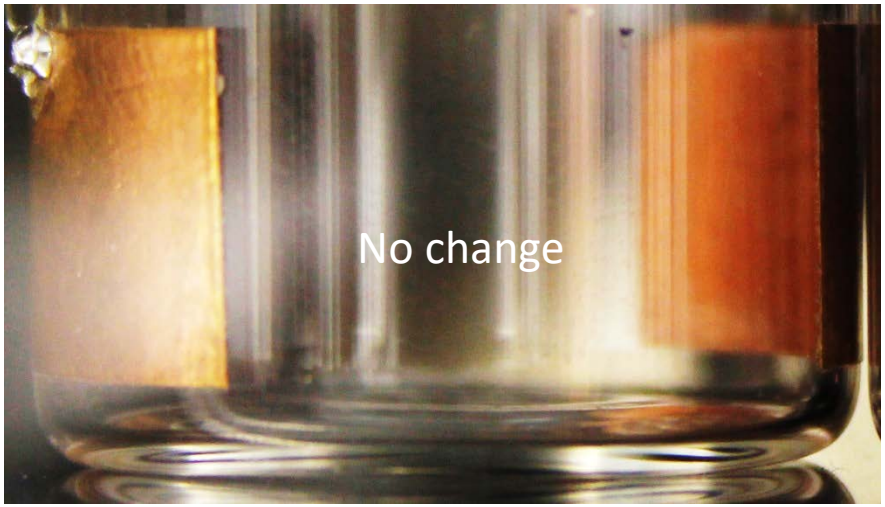

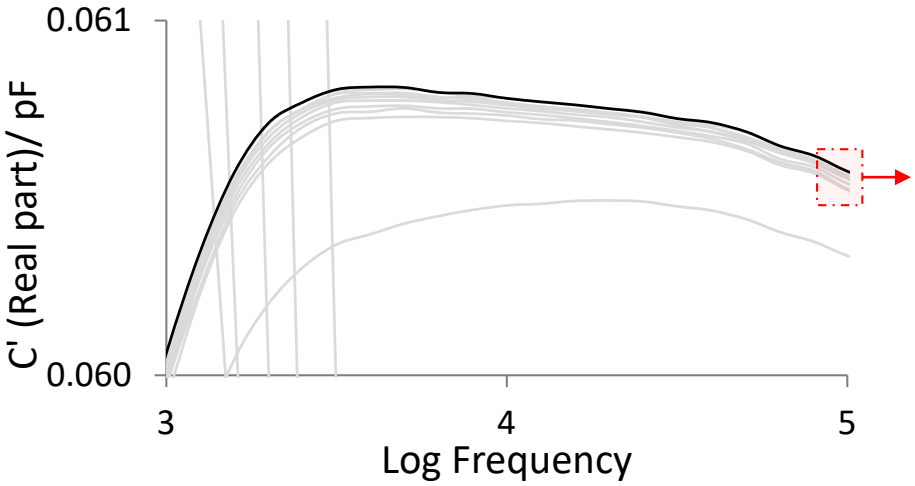

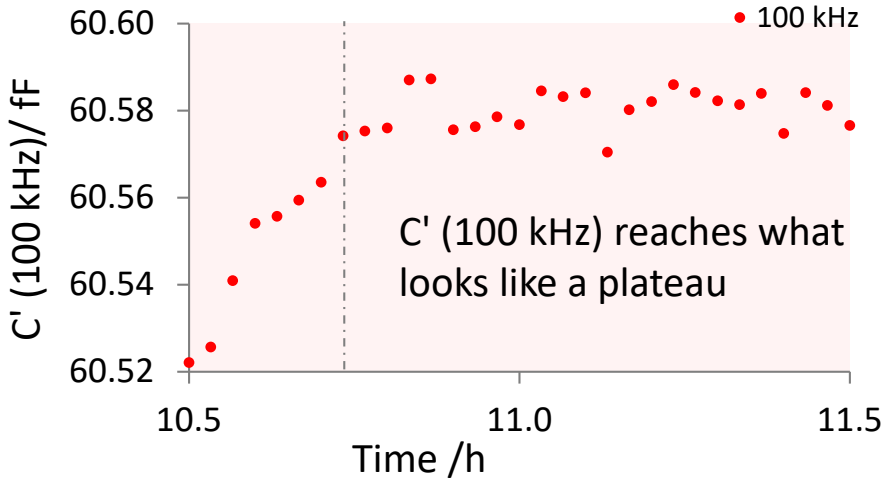

Summary

- End point determine by high frequency (i.e. 100 kHz for ice) real part capacitance (i.e. 100 kHz for ice)

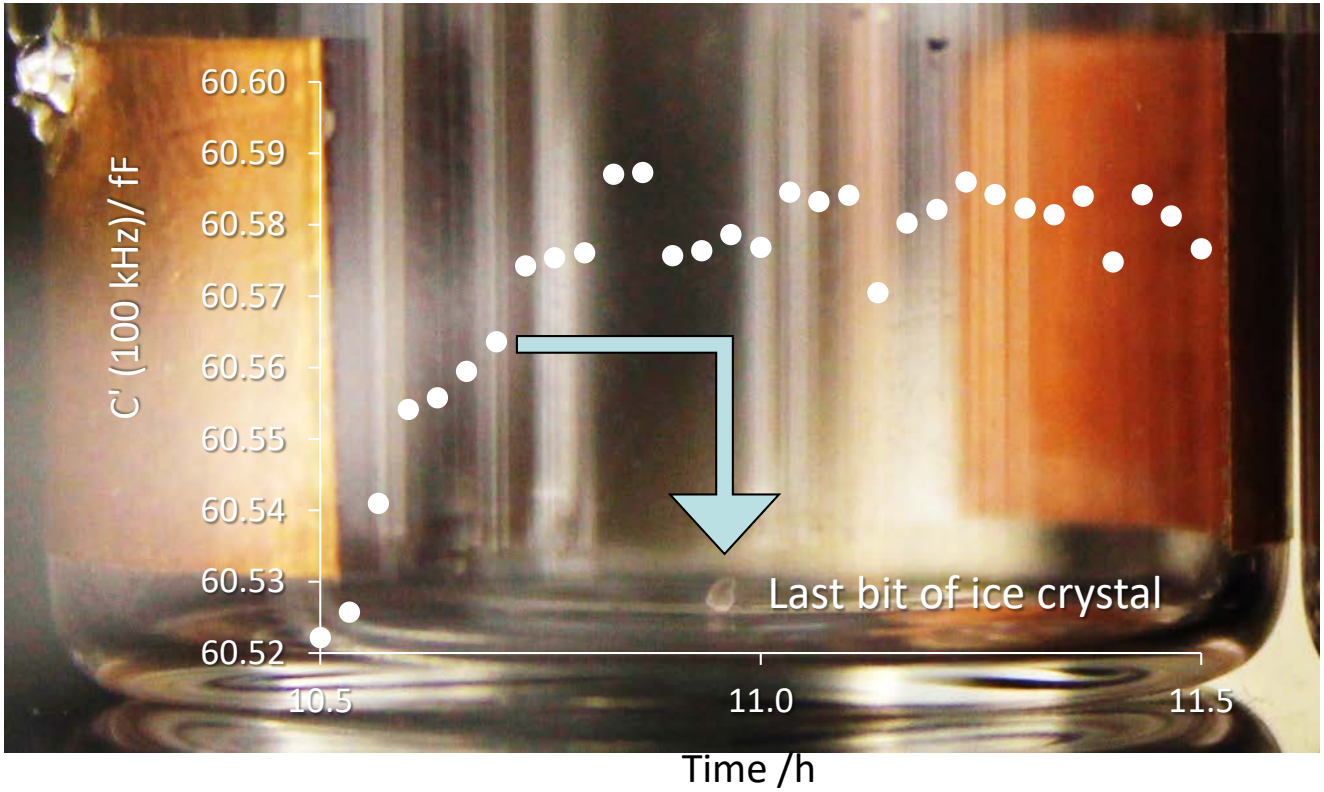

Summary

- End point determine by high frequency (i.e. 100 kHz for ice) real part capacitance (i.e. 100 kHz for ice)

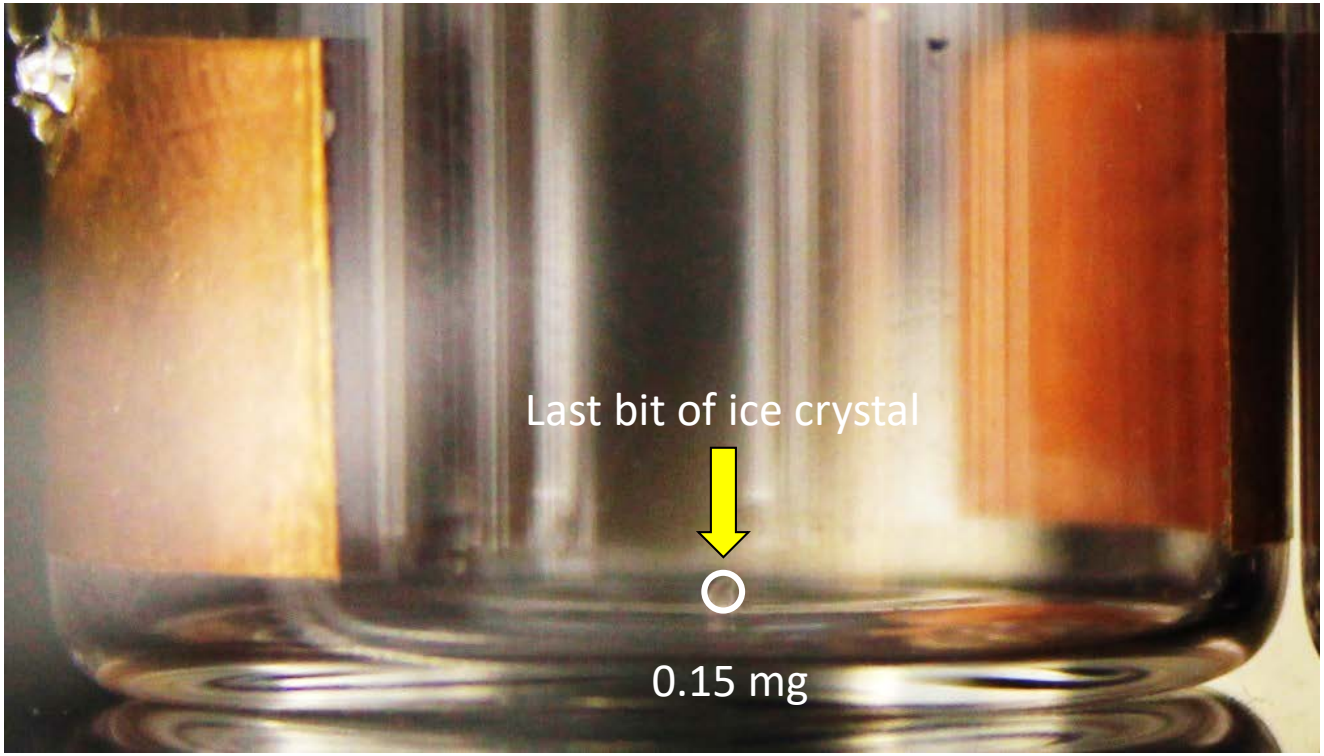

Through Vial Impedance Spectroscopy (TVIS)

Product Resistance Determination

Product Resistance (R_P) Determination

$$\hat{R}p = \left(\frac{P_{ICE} - P_{CHAMBER}}{dm/dt}\right) \cdot A_P$$

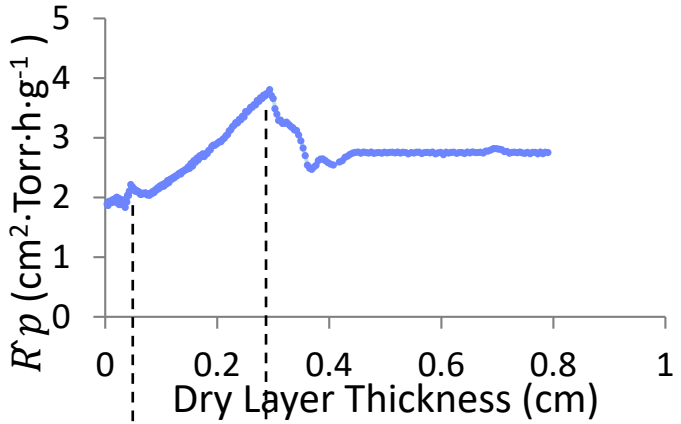

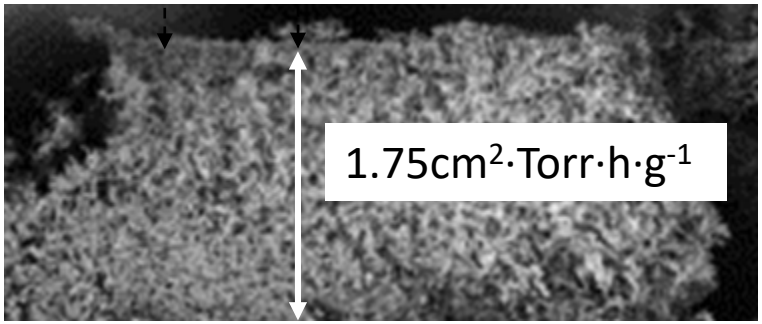

Lactose freeze-dried matrix

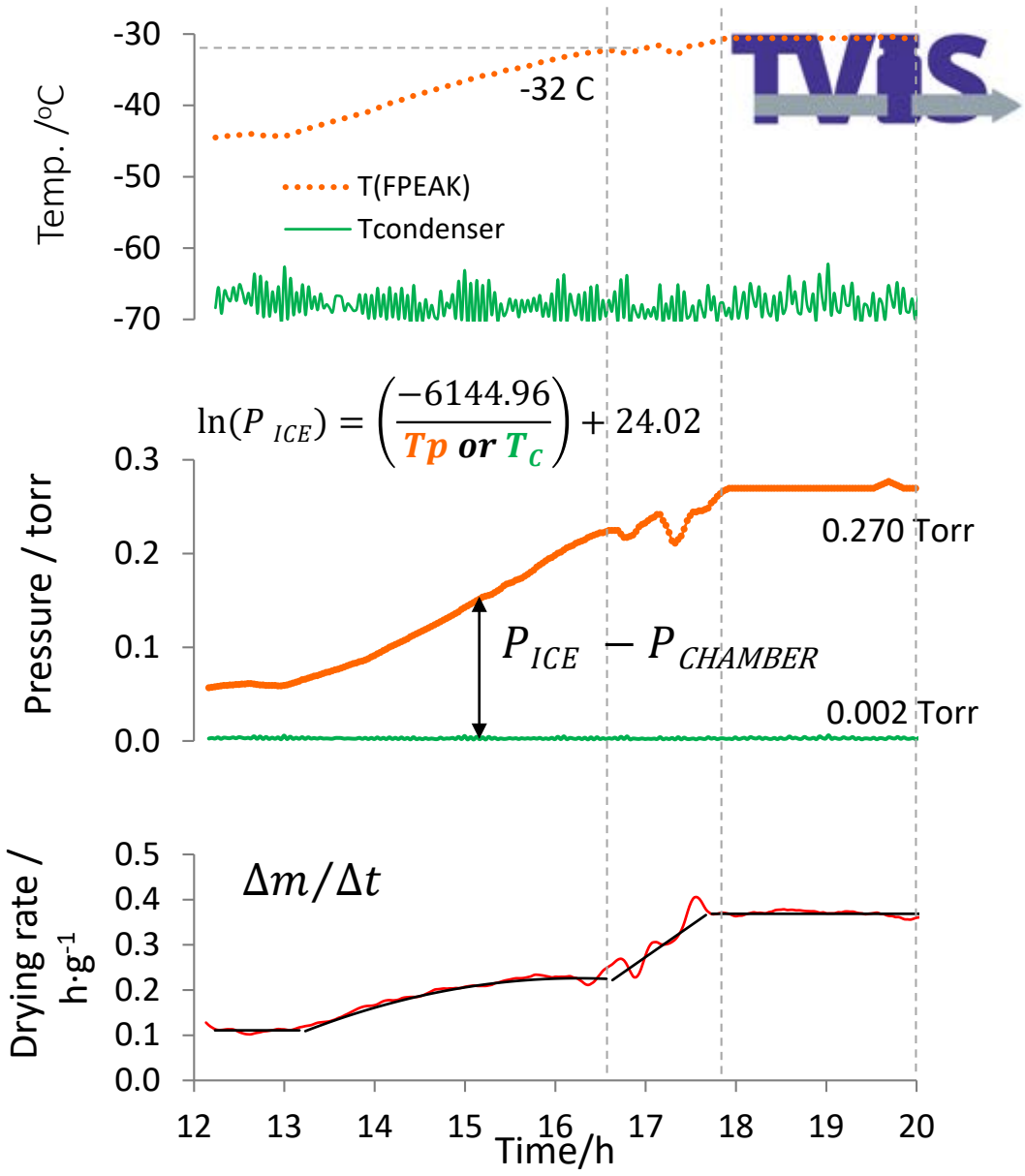

Product Resistance (R_P) Determination

$$\hat{R}p = \left(\frac{P_{ICE} - P_{CHAMBER}}{dm/dt} \right) \cdot A_P$$

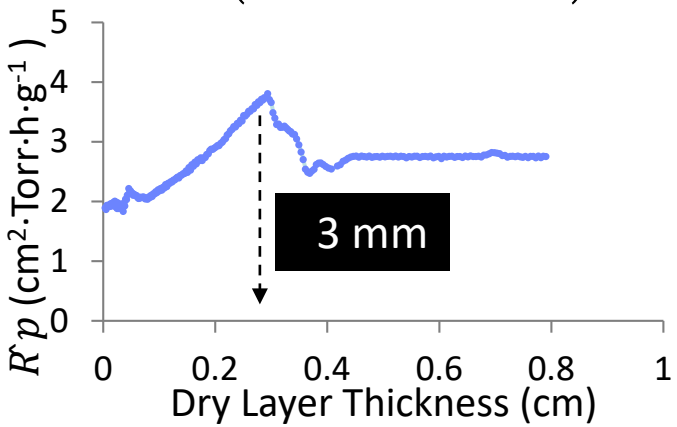

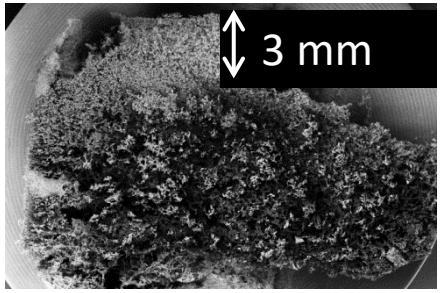

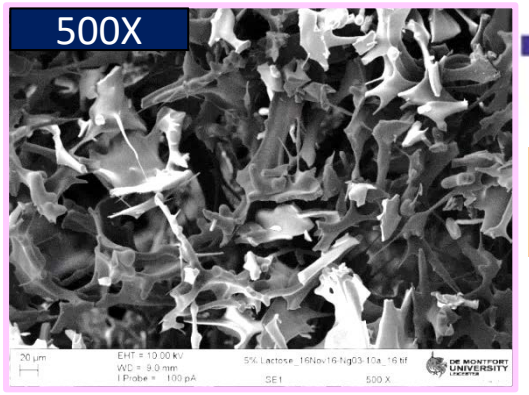

Top layer
Fine pores

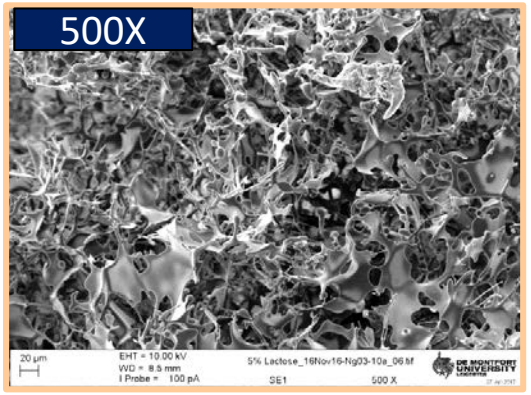

Middle layer
Micro-collapse

500X

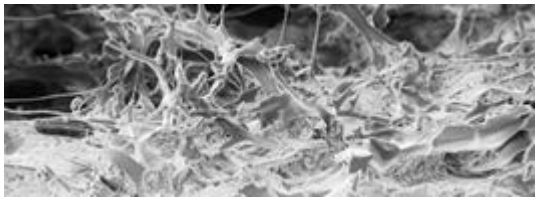

Bottom layer
Full collapse

Through Vial Impedance Spectroscopy (TVIS)

Collapse Phenomena

5% Sucrose

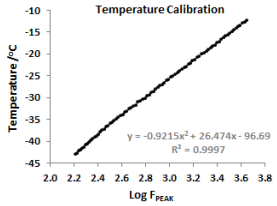
Temperature Calibration
Temperature /°C
Log F_{PEAK}
$y = -0.9215x^2 + 26.474x - 96.69$
$R^2 = 0.9997$

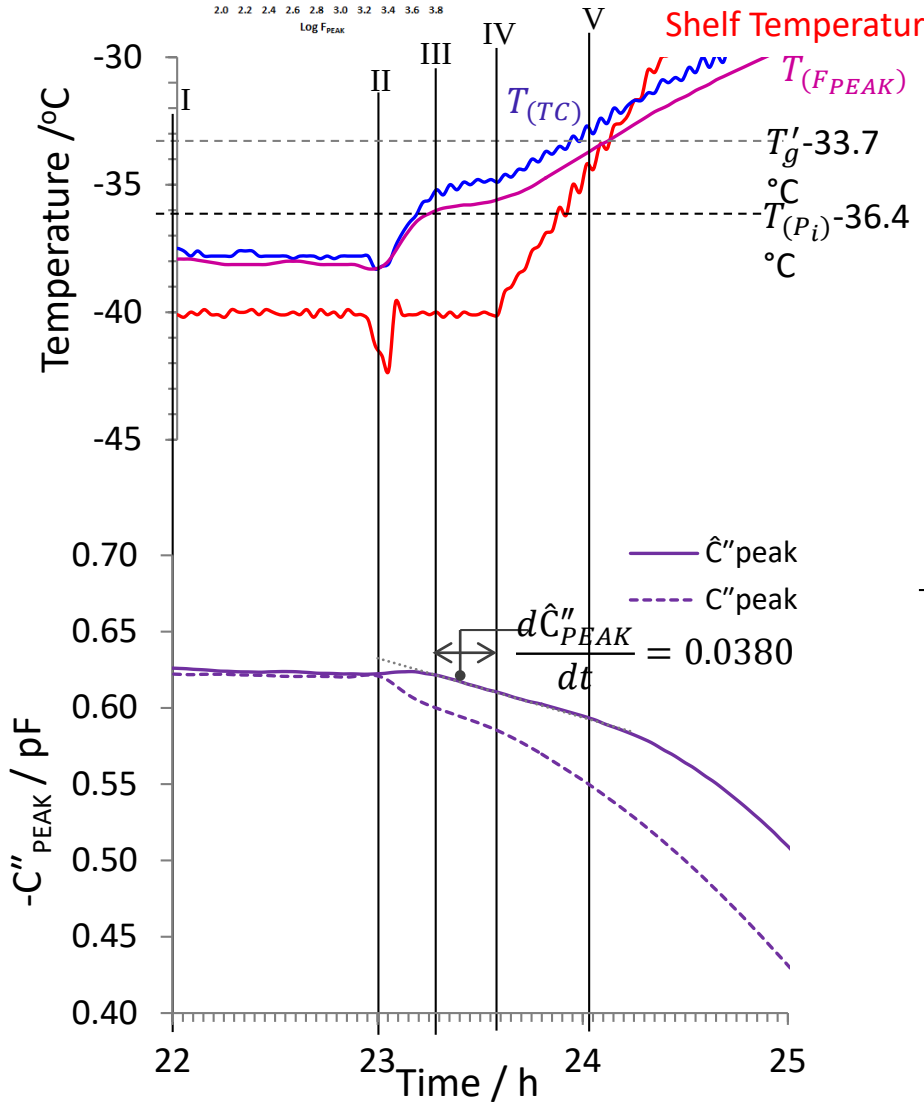
Shelf Temperature
$T_{(F_{PEAK})}$
$T_{(TC)}$
T_g'-33.7 °C
$T_{(P_i)}$-36.4 °C
I
II
III
IV
V
Temperature /°C
-30
-35
-40
-45
Ĉ″peak
C″peak
$\frac{d\hat{C}''_{PEAK}}{dt} = 0.0380$
-C″ PEAK / pF
0.70
0.65
0.60
0.55
0.50
0.45
0.40
22
23
24
25
Time / h

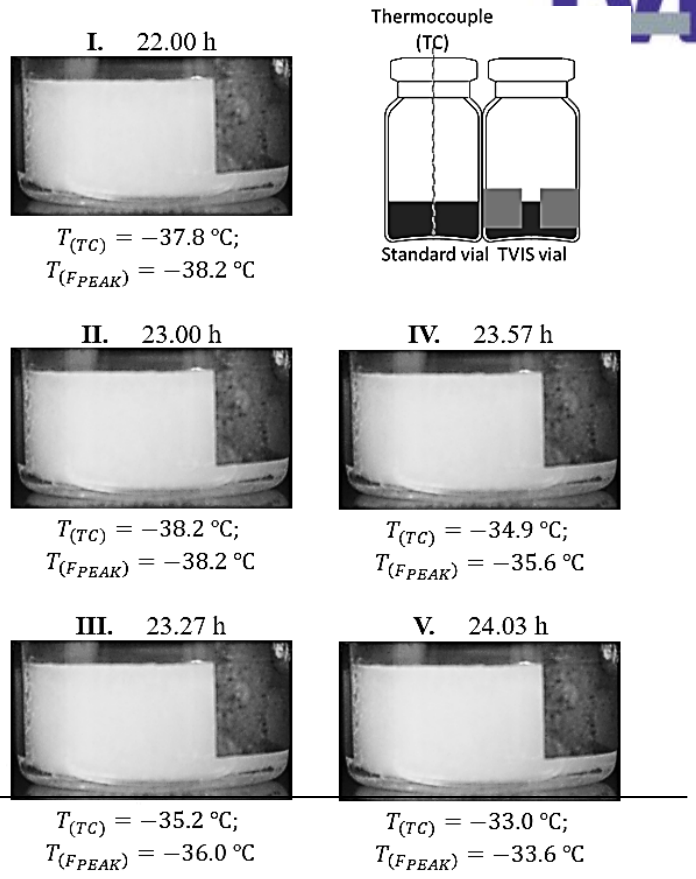
I. 22.00 h
$T_{(TC)} = -37.8$ °C;
$T_{(F_{PEAK})} = -38.2$ °C
Thermocouple (TC)
Standard vial
TVIS vial
II. 23.00 h
$T_{(TC)} = -38.2$ °C;
$T_{(F_{PEAK})} = -38.2$ °C
IV. 23.57 h
$T_{(TC)} = -34.9$ °C;
$T_{(F_{PEAK})} = -35.6$ °C
III. 23.27 h
$T_{(TC)} = -35.2$ °C;
$T_{(F_{PEAK})} = -36.0$ °C
V. 24.03 h
$T_{(TC)} = -33.0$ °C;
$T_{(F_{PEAK})} = -33.6$ °C

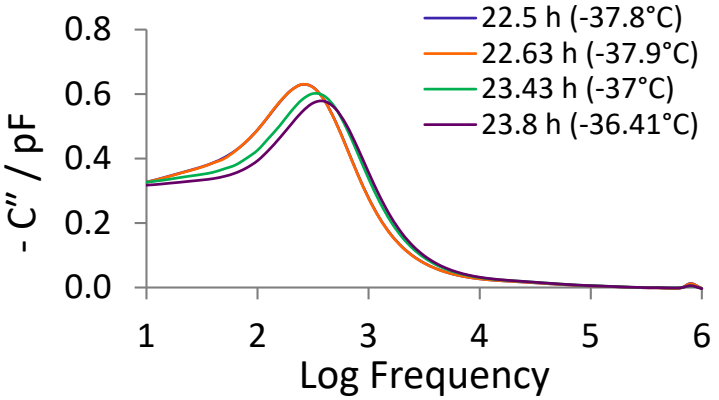
22.5 h (-37.8°C)
22.63 h (-37.9°C)
23.43 h (-37°C)
23.8 h (-36.41°C)
- C″ / pF
0.8
0.6
0.4
0.2
0.0
1
2
3
4
5
6
Log Frequency

5% Sucrose in 0.26% NaCl

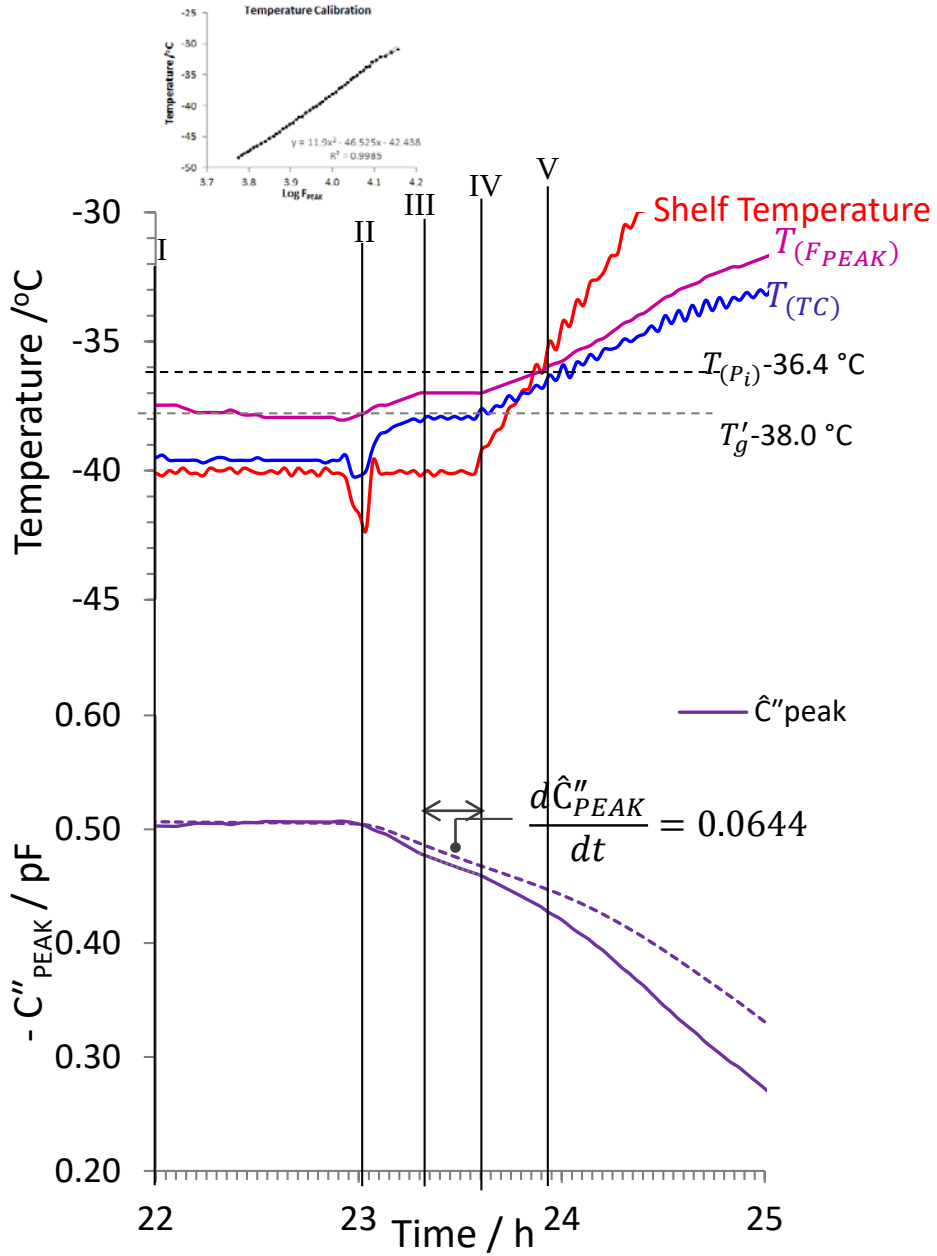

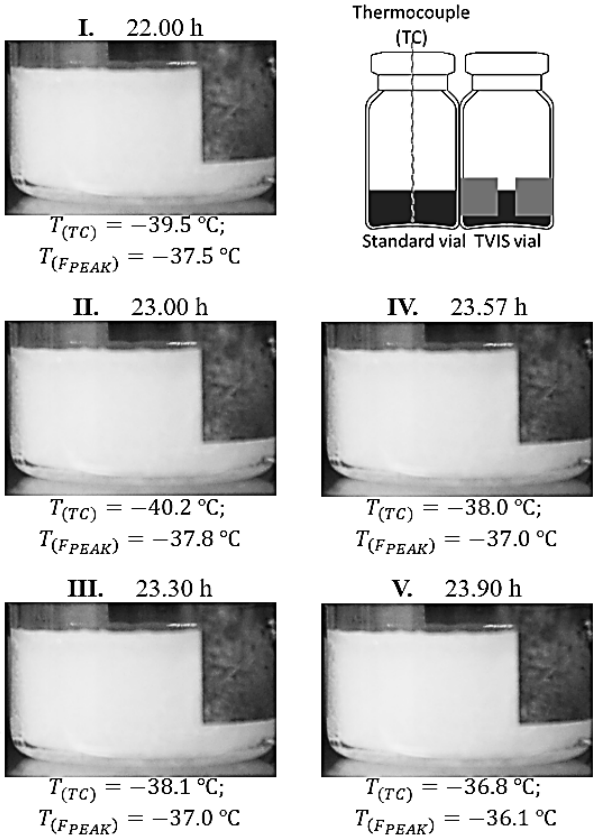

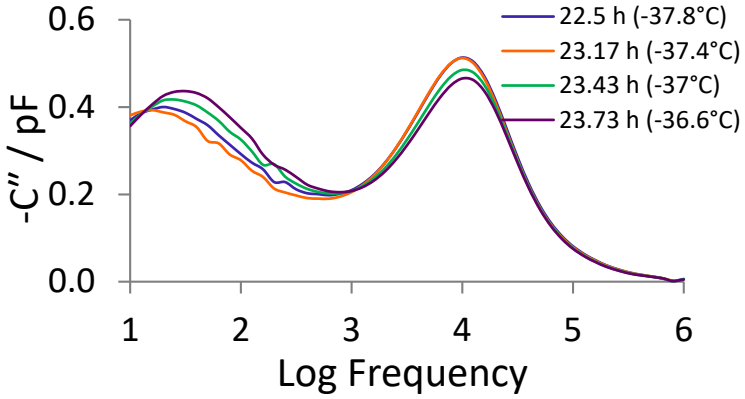

5% Sucrose +0.55% NaCl

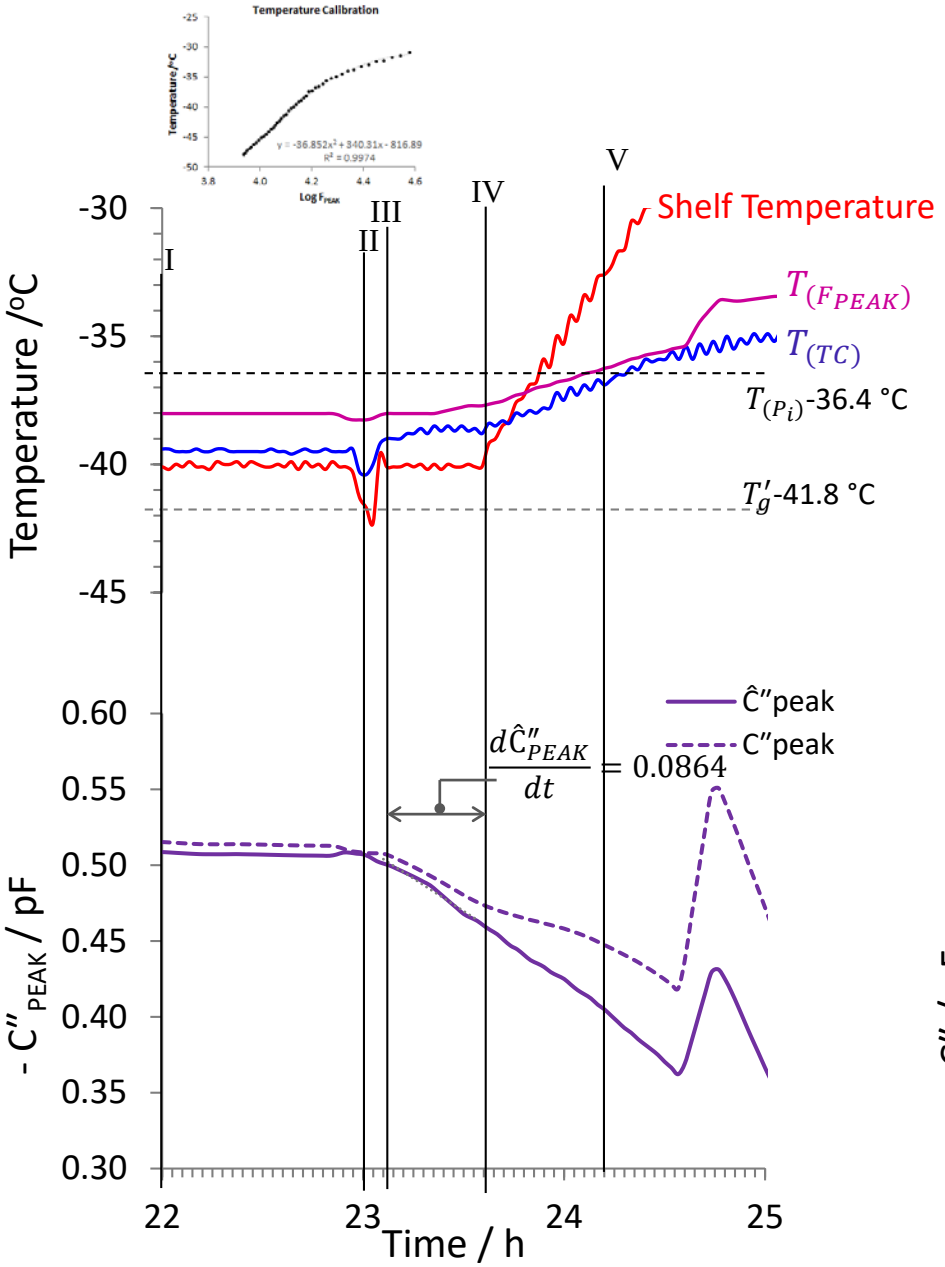

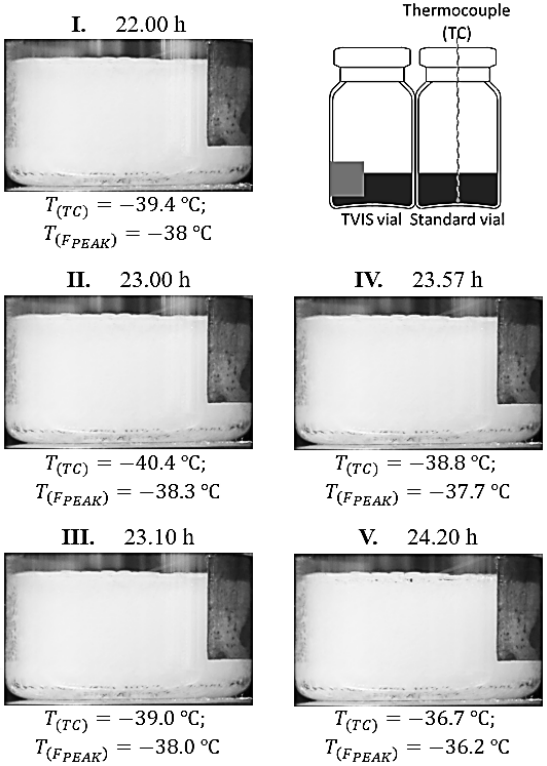

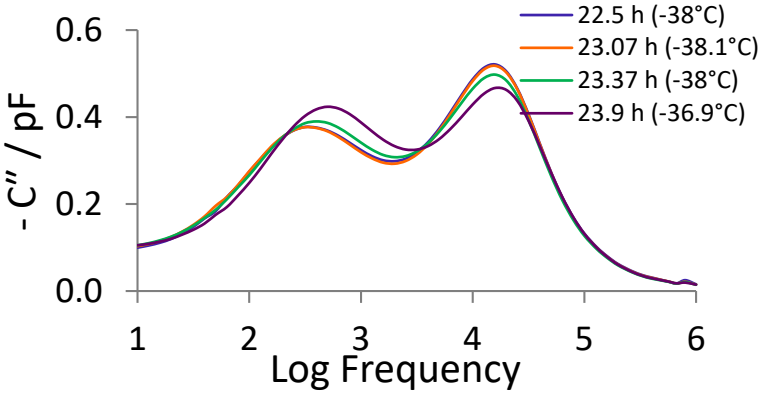

Summary results of sugar- salts solutions

Parameters	Unit	S-1	S-2	S-3
Component				
Sucrose	%w/v	5	5	5
Sodium chloride	%w/v	-	0.26	0.55
T'_g **(DSC)**	°C	**-33.7**	**-38.0**	-41.8
Temperature stabilization period		III to IV	III to IV	III to IV
(Before ramping shelf temperature)	h	23.3 - 23.6	23.3 - 23.6	23.1 - 23.6
$T_{(F_{PEAK})}$	°C	-36.0 to -35.6	**-37.0**	**-38.3 to -37.7**
Surrogate drying rate ($d\hat{C}_{PEAK}/dt$)	pF/h	0.0380	0.0644	0.0864
Structural state		Non-collapse	micro-collapse?	Micro-collapse
		VII to VIII	VII to VIII	VII to VIII
Temperature stabilization period	h	26.0 - 26.8	26.0 – 26.4	26.0 -26.2
(After shelf temperature constant)	°C	-26.4 to -25.6	-30.1 to -30.0	-32.8 to -32.7
Surrogate drying rate ($d\hat{C}_{PEAK}/dt$)	pF/h	0.2243	0.1227	0.1569
Structural State*		Micro-collapse	Collapse	Collapse

5% Sucrose in Salt Solutions

VI. 23.90 h

$T_{(TC)} = -36.8$ °C;
$T_{(F_{PEAK})} = -36.1$ °C

VIII. 26.40 h

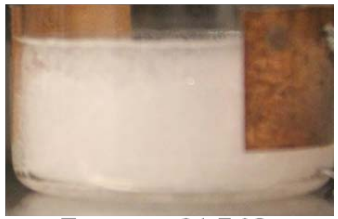

$T_{(TC)} = -31.7$ °C;
$T_{(F_{PEAK})} = -30.0$ °C

VII. 26.03 h

$T_{(TC)} = -31.5$ °C;
$T_{(F_{PEAK})} = -30.1$ °C

IX. 26.67 h

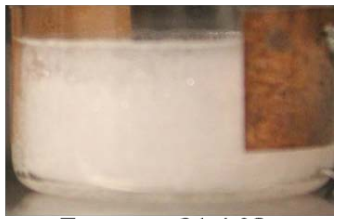

$T_{(TC)} = -31.4$ °C;
$T_{(F_{PEAK})} = -27.9$ °C

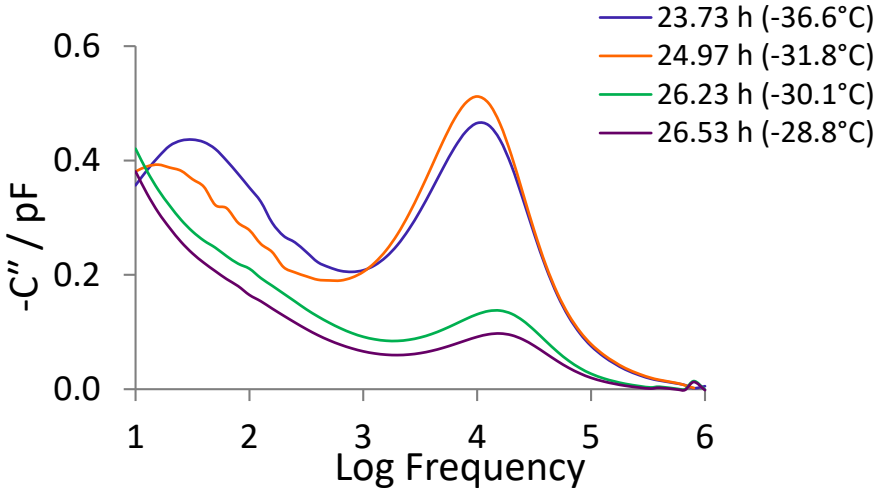

5% sucrose in 0.26% NaCl

VI. 24.20 h

$T_{(TC)} = -36.7$ °C;
$T_{(F_{PEAK})} = -36.2$ °C

VIII. 26.20 h

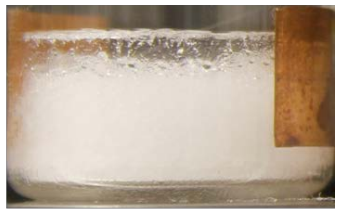

$T_{(TC)} = -34.4$ °C;
$T_{(F_{PEAK})} = -32.7$ °C

VII. 26.03 h

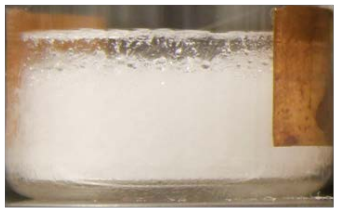

$T_{(TC)} = -34.1$ °C;
$T_{(F_{PEAK})} = -32.8$ °C

IX. 26.90 h

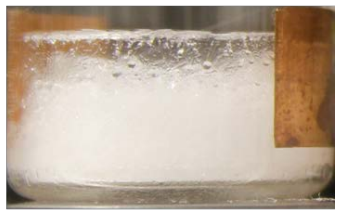

$T_{(TC)} = -34.7$ °C;
$T_{(F_{PEAK})} = -32.5$ °C

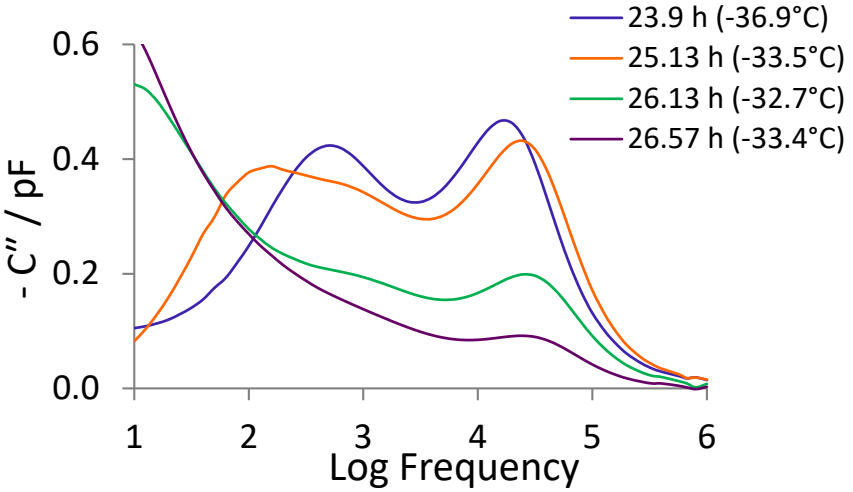

5% sucrose in 0.55% NaCl

Limitations

- C''_{PEAK} and F_{PEAK} parameters rely on intimate contact of ice cylinder with glass wall
- C'(100 kHz) parameter does not dependent on contact and can be used for end point but relationship between C'(100 kHz) ice constant is non-linear
- Cable length limited to 1m at present
- C-TVIS not compatible with front loading system
- Incompatible with TCs in same TVIS vial (use fibre optic sensors – INFAP)

Future Work

- Development mapping a drying characteristics
  - heat transfer coefficients (K_V)
  - dry layer resistance (R_P)

- TVIS vial – Electrode Coating!
  - Electrodeposition
- Instrument Development
  - Commercial C-TVIS (2018)
  - Non-contact TVIS (2018-19)
    - Micro-well screening
    - Vial clusters in batch FD
  - TVIS - Shuttle (2019-20)

Non-invasive real time information for characterising the freeze drying

Acknowledgements, Recent Projects & Collaborators

- De Montfort University, School of Pharmacy
  - Evgeny Polygalov: co-inventor of TVIS instrument
  - Yowwares Jeeraruangrattana. PhD student
  - Bhaskar Pandya. PhD student
  - Irina Ermolina. Senior Lecturer

GEA Pharma Systems

bluefrog design

NIBSC Confidence in Biological Medicines

SANOFI

Innovate UK
Government Support for industry

LyoDEA
Lyophilization process analytics
By dielectric analysis

BIOSTART
Biopharmaceutical Stability at
Room Temperature

AtlasBio
Analytical Technologies for the
Stabilization of Biopharmaceuticals